
Pre-Conference Excursion

Pre-Conference Field Trip: Erzgebirge (Ore Mountains),
Germany and Czech Republic;
August 4–5, 2011

German Part of the Saxonian Erzgebirge

Hans-Joachim MASSONNE

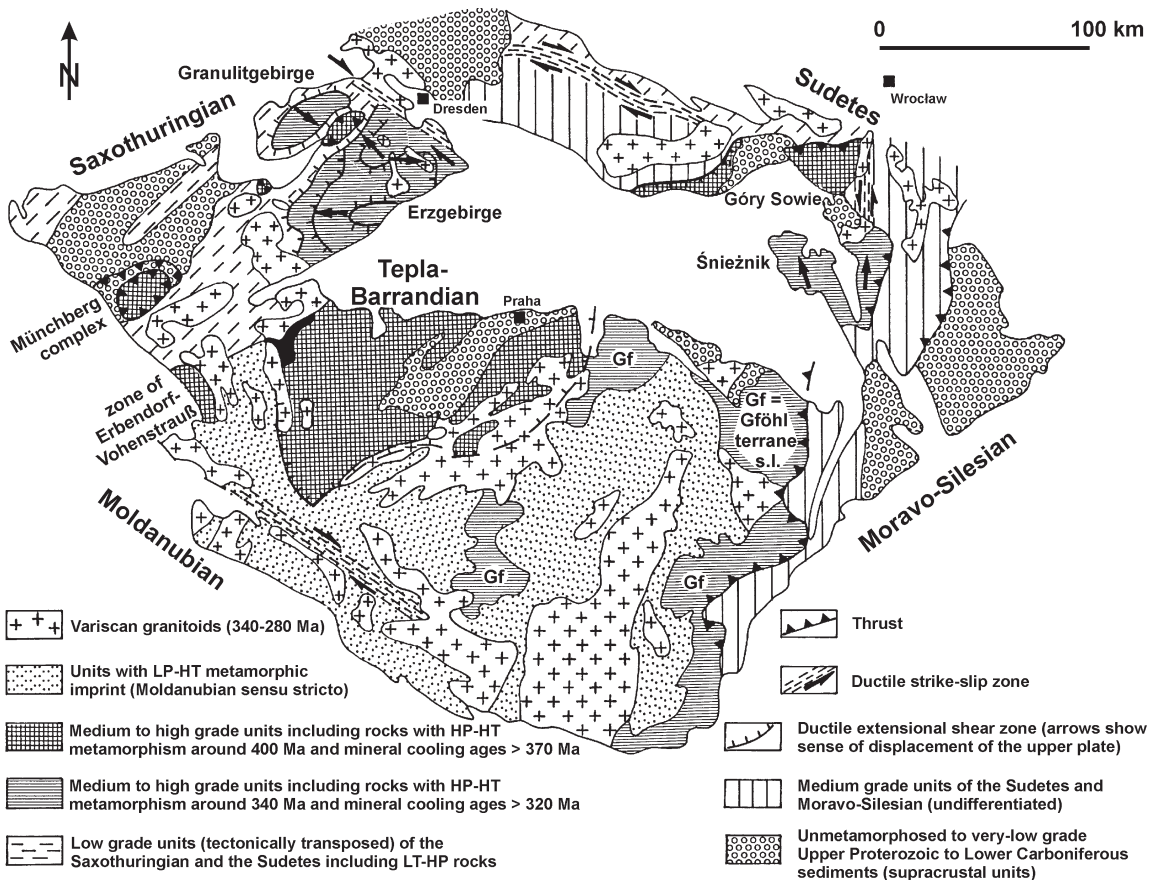
Institut für Mineralogie und Kristallchemie, Universität Stuttgart, Azenbergstr. 18, D-70174 Stuttgart, Germany, e-mail: h-j.massonne@mineralogie.uni-stuttgart.de

The field itinerary for the first part of the pre-conference excursion, related to the 9th International Eclogite Conference, includes 5 stops within the central and western Erzgebirge in Saxony. Stop 1-3 comprises several stops which are visited at or close to the Saldenbach reservoir by walking. High and ultrahigh pressure rocks of different genesis can be studied at the excursion stops. Eclogite south-east of the village of Eppendorf experienced peak pressure conditions of 1.8 GPa at 715 °C and is an example of eclogitization at the base of thickened continental crust due to the Variscan collision of Laurussia and Gondwana. Bodies of eclogite and diamondiferous saidenbachite at the northern and eastern shore of the Saldenbach reservoir, embedded in high-pressure (around 1.8 GPa) gneisses, represent ultrahigh pressure rocks which were heated to more than 1000 °C. During this process saidenbachite was significantly molten at $P \geq 5$ GPa, resulting in its rapid ascent through the mantle and emplacement at the base of thickened Variscan crust. Garnet peridotite at the town of Zöblitz represents another rock type also inserted in this crust. Eclogites of the western Erzgebirge experienced a nearly isobaric (~2.6 GPa) temperature increase from about 500 to 700 °C and subsequent exhumation at decreasing temperatures to finally form bodies in mica-schist and gneiss, which were metamorphosed at a maximum pressure of 1.3 GPa. The metamorphic P-T path of these eclogites is related to mass flow in a subduction channel.

Introduction

The first part of the pre-conference excursion, related to the 9th International Eclogite Conference, is aimed at presenting key occurrences of rocks, formed at ultrahigh pressure (UHP) and near-UHP conditions, in the German part of the crystalline com-

plex of the Erzgebirge (Ore Mountains) in the Saxothuringian zone, which is located at the northwestern margin of the Bohemian Massif (Fig. 1). Krušné Hory is the name which is synonymously used in Czech for this complex. The Saxonian Erzge-

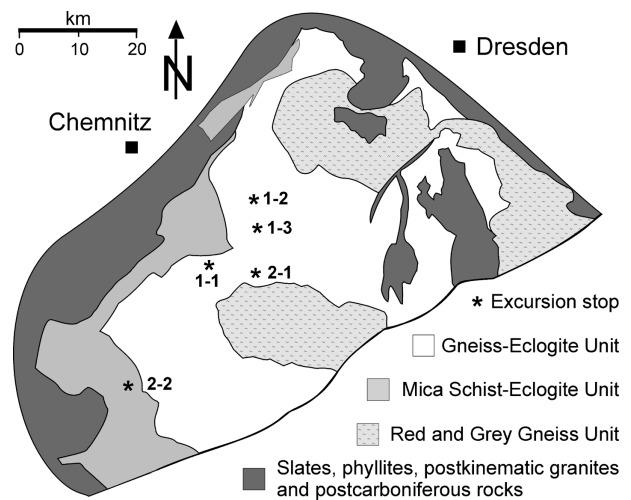


■ Fig. 1. Overview map showing the location of basement complexes within the Bohemian Massif (modified after Willner et al., 2000).

birge is an anticlinal structure with an ellipsoidal shape, extending in a WSW-ENE direction (Fig. 2). It is surrounded by anchimetamorphic to low-grade metamorphic rocks. Towards the south the crystalline complex of the Erzgebirge is limited by the Eger graben (the river Eger is named Ohře in Czech), which is a Late Cretaceous to Tertiary structure. The outcropping rocks in the Erzgebirge are variable in terms of metamorphic degree. Various subdivisions have been proposed for the metamorphic rocks. Here, the proposal by Willner et al. (2000) is preferred, who recognized three major medium to high-grade metamorphic units, which are surrounded by the low-grade Phyllite Unit (Fig. 2). Two of these three units, Mica-schist – Eclogite Unit (MEU) and Gneiss – Eclogite Unit (GEU), contain abundant eclogite lenses, whereas high-pressure (HP) rocks are absent from the Red and Grey Gneiss Unit.

For detailed information on the regional geology, the map series, “Geologische Meßtischblätter”, is recommended. These maps, at a scale of 1:25000, are distributed by “Sächsisches Landesamt für Umwelt, Landwirtschaft und Geologie” at Dresden. In addition, an explanatory text is available for each map. The following sheets cover the areas visited during the first part of the pre-conference excursion: GK25 5245 Lengefeld, GK25 5344 Marienberg-Wolkenstein, GK25 5345 Zöblitz, and

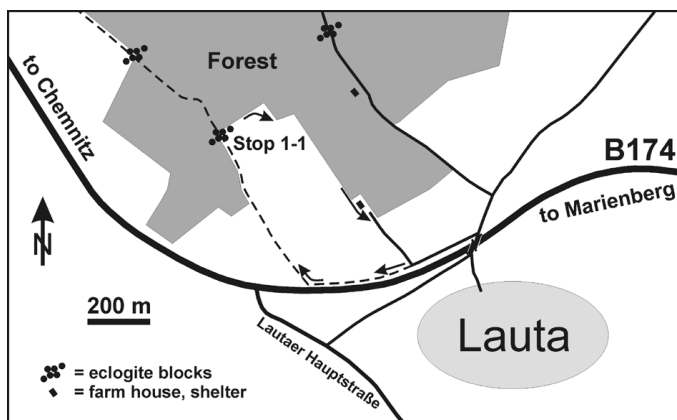
GK25 5543 Oberwiesenthal. An overview map, Geologische Karte Erzgebirge/Vogtland at a scale of 1:100000, is also available.



■ **Fig. 2.** Simplified geological map of the Saxonian Erzgebirge according to Willner et al. (2000). Excursion stops are shown by stars.

Stop 1-1 (Day 1). Eclogite, NW of Lauta

Coordinates: N50°40'26.6" E13°08'08.9"



■ **Fig. 3.** Location map for stop 1-1 north-west of the town of Marienberg. The sites of eclogite boulders refer to eclogite and amphibolite lenses as mapped by Schalch (1879).

This stop is located at the northern border of the GEU with the MEU in the basement of the Saxonian Erzgebirge. In the target area boulders of fresh eclogite occur. In general, the concentration of such boulders at a specific site (see, e.g., Fig. 3) is interpreted as evidence for the existence of an eclogite body in the underground. Normally, such a body is enveloped by gneisses, which is probably the case at stop 1-1, in view of the abundant field stones of mica-schist and gneiss in the vicinity of this stop.

The excursion starts in the town of Marienberg. From the centre of this town go to the north-west. 2.2 km after passing the Zschopauer Tor, the old gate built in the middle of the 16th century, turn to the right, 300 m in front of the entrance of the Lautaer Hauptstraße into the national route 174 (Fig. 3). After some hundred metres, just after passing B174 via a bridge, turn to the left and stop the vehicle after 250 m. From here walk some hundred metres first to the west and then to the north-west following a farm track to the margin of a forest (Fig. 3).

In addition, we will find eclogite boulders by walking along the field margin, suggesting that they were sampled from the field.

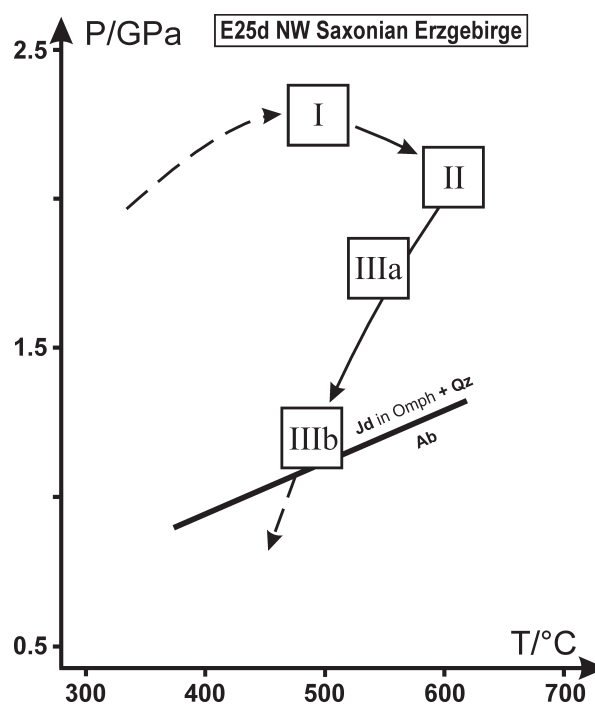
A typical feature of eclogite at stop 1-1 is the homogeneous distribution of black, up to cm-sized amphibole porphyroblasts within a single boulder. These porphyroblasts have overgrown a fine-grained, equigranular matrix of garnet, omphacite, phengite, and quartz, mainly at the expense of omphacite. Massonne (1992) has studied an eclogite sample with mm-sized amphibole

Mineral Stage	Garnet				Omphacite				Phengite				Amphibole		
	I	II	IIIa	IIIb	I	II	IIIa	IIIb	I	II	IIIa	IIIa	II	IIIa	IIIb
Si	5.812	5.846	5.883	5.920	1.981	1.980	1.976	1.983	6.793	6.711	6.515	6.283	6.168	6.751	6.381
Al(IV)					0.019	0.020	0.024	0.017	1.207	1.290	1.485	1.717	1.832	1.249	1.619
Ti	0.038	0.003	0.012	0.008	0.001	0.003	0.003	0.003	0.078	0.083	0.085	0.093	0.046	0.061	0.073
Al(VI)	3.912	3.977	3.971	3.984	0.411	0.448	0.434	0.422	2.983	3.023	3.132	3.280	1.265	0.930	1.060
Cr	0.005	0.007	0.003	0.000	0.000	0.001	0.000	0.000	0.003	0.005	0.009	0.011	0.011	0.006	0.003
Fe ³⁺	0.083	0.017	0.027	0.016	0.025	0.001	0.011	0.034					0.099	0.238	0.281
Fe ²⁺	3.310	3.447	3.415	3.502	0.070	0.137	0.118	0.099	0.178	0.178	0.188	0.174	1.557	0.981	1.199
Mn	0.076	0.062	0.079	0.086	0.001	0.002	0.000	0.002	0.000	0.003	0.000	0.004	0.014	0.003	0.000
Mg	1.096	1.371	1.130	1.092	0.512	0.438	0.453	0.454	0.790	0.755	0.674	0.558	2.008	2.781	2.384
Ca	1.519	1.120	1.376	1.320	0.559	0.536	0.556	0.539	0.000	0.000	0.000	0.000	1.605	1.424	1.461
Na					0.420	0.436	0.426	0.446	0.105	0.114	0.169	0.138	0.935	0.980	1.041
K									1.716	1.729	1.703	1.672	0.214	0.127	0.166
Ba									0.014	0.027	0.021	0.021	0.002	0.000	0.000
F									0.000	0.000	0.020	0.000	0.000	0.086	0.093

■ **Tab. 1.** Representative structural formulae of minerals in eclogite sample E25d taken north-west of the village of Lauta, Erzgebirge in Saxony, according to Massonne (1992). Metamorphic stage I is the earliest (inner core compositions of garnet, omphacite, and phengite), IIIb the latest (outermost rim compositions) eclogite stage recorded by the rock. Structural formulae were calculated on the following basis: garnet: 24 O, 10 six- and eight-fold coordinated cations; omphacite: 6 O, 4 cations; mica: 42 – (Ca+Ba) valencies; amphibole: 46 valencies, 13 cations without Ca, Na, K, Ba.

porphyroblasts from this locality. This author noted a chemical zonation of garnet, omphacite, phengite, and amphibole (Table 1) and correlated the different compositions of these minerals with metamorphic stages I (early: core compositions) to III (late: rim compositions, b = outermost rim). Amphibole growth started at stage II and significantly increased in stages IIIa and IIIb. P-T conditions of the metamorphic stages were thermodynamically calculated by considering equilibria with mineral components of phengite, omphacite, and garnet (Massonne, 1992), resulting in the P-T path shown in Fig. 4. According to this path, peak pressure conditions were 2.3 GPa. Peak temperature conditions reached about 600 °C after the peak pressure event. The exhumation process, accompanied by amphibole growth, is characterized by significant cooling during decompression, a factor that might have prevented the rock from strong retrogression.

Massonne and Czambor (2007) studied the chemical bulk-rock composition of eclogites from the Saxonian Erzgebirge, including a sample from stop 1-1 (Erz02-8, see Table 2). Two groups of eclogites were distinguished: one occurring at and close to the Saldenbach reservoir, examples of which we will see and discuss at stop 1-3, and another distributed from the south-western to the central Erzgebirge, which is characterized by an N-MORB signature with a tendency towards P-MORB, as observed for the eclogite from stop 1-1.



■ **Fig. 4.** P-T path derived for sample E25d (see also Table 1) from stop 1-1 according to Massonne (1992).

Site	Lauta *Epp.				Saldenbach reservoir								Siebensäure – Meluzina				
Stop No.	1-1	1-2	1-3A	1-3A	1-3A	1-3A	1-3A	1-3A	1-3A	1-3C	1-3C	1-3C	1-3D	2-2	2-2		
Sample No.	Erz02-8	E174c	E99-22	E99-23	E99-24	E99-25	E00-6	E00-17	E42-1c	E42-1d	E99-3	E42-3P		E22a	E22c	E96-15c	E95-5.3b
SiO ₂	wt.% 48.00	49.50	55.75	47.53	47.40	50.60	49.12	49.92	58.54	51.17	52.13	54.83		50.84	49.74	49.56	49.91
TiO ₂	wt.% 2.55	1.92	1.66	0.85	1.09	3.37	1.22	3.07	1.78	1.57	2.45	1.75		1.56	1.37	1.58	1.67

■ **Tab. 2.** Chemical compositions of eclogites from the Erzgebirge in the Bohemian Massif. The analytical data were obtained by X-ray fluorescence and, regarding some trace elements as marked in the table, ICP - mass spectrometry (Massonne and Czambor, 2007). * Epp. = 2.5 km southeast of the village of Eppendorf.

Site	Lauta * Epp.		Saidenbach reservoir										Siebensäure – Meluzína				
Stop No.	1-1	1-2	1-3A	1-3A	1-3A	1-3A	1-3A	1-3A	1-3A	1-3C	1-3C	1-3C	1-3D	2-2	2-2		
Sample No.	Erz02 8	E174c	E99 22	E99 23	E99 24	E99 25	E00 6	E00 17	E42 1c	E42 1d	E99 3	E42 3P		E22a	E22c	E96 15c	E95 5.3b
Al ₂ O ₃ wt.%	13.55	14.80	15.80	17.63	17.38	15.28	16.55	16.23	15.88	16.48	16.43	16.13		14.48	13.92	14.19	13.64
FeO wt.%	13.33	11.30	8.13	7.08	8.14	9.19	7.97	12.44	7.48	6.06	10.76	8.13		9.80	10.25	8.29	11.37
Fe ₂ O ₃ wt.%			0.90			3.51				2.42						2.91	
CaO wt.%	11.20	12.30	7.44	10.08	11.96	8.34	12.84	8.28	4.73	8.78	7.91	7.21		11.21	10.68	11.45	11.65
MgO wt.%	5.62	6.33	4.24	8.79	8.73	4.29	8.42	4.03	3.66	5.56	4.45	4.56		7.20	6.92	6.89	6.76
MnO wt.%	0.23	0.20	0.14	0.11	0.13	0.20	0.14	0.20	0.14	0.14	0.19	0.13		0.18	0.16	0.24	0.21
K ₂ O wt.%	0.14	0.23	1.54	0.96	0.39	0.78	0.41	0.51	2.40	1.46	0.74	1.80		0.21	0.25	0.41	0.12
Na ₂ O wt.%	2.53	2.32	3.30	2.28	1.69	3.21	2.33	3.49	3.31	3.43	3.37	3.40		2.89	2.99	3.06	2.84
P ₂ O ₅ wt.%	0.27	0.12	0.15	0.22	0.14	0.79	0.15	0.84	0.16	0.28	0.45	0.24		0.11	0.08	0.09	0.11
H ₂ O _{tot} wt.%	0.45	0.26	0.82	0.36	0.15	0.57	0.25	0.22	0.92	1.42	0.61	0.79		0.26	1.29	0.94	0.34
CO ₂ wt.%	0.21	0.13	0.12	0.34	0.55	0.10	0.25	0.11	0.18	0.30	0.16	0.20		0.11	0.33	0.02	0.15
Sum wt.%	98.08	99.41	99.99	96.23	97.40	100.23	99.65	99.34	99.18	99.07	99.65	99.17		98.85	97.98	99.63	98.77
F wt.%	0.04	0.03	0.04			0.05	0.04	0.04	0.03	0.07	0.06	0.06		0.07	0.05	0.07	0.09
S wt.%	0.15	0.09	0.05			< 0.01	0.04	0.02	< 0.01	0.04	< 0.01	< 0.01		< 0.01	0.01	0.07	< 0.01
Cl wt.%	< 0.01	< 0.01	< 0.01			< 0.01	0.02	0.01	< 0.01	0.02	< 0.01	0.01		< 0.01	< 0.01	< 0.01	< 0.01
Li ppm ICP	53.9	22.4	36.9	32.2	14.4	14.1	11.2	16.1	31.6	21.1	26.8	34.4		35.8	23.3	16.3	14.3
Sc ppm	54	50	27	19	36	34	47	36	26	33	33	26		52	54	52	55
V ppm	420	353	214	138	126	317	227	317	181	207	261	203		350	320	352	361
Cr ppm	307	298	102	263	413	47	213	83	98	204	62	86		288	357	199	181
Ni ppm	70	95	36	150	152	21	93	37	51	47	46	43		87	80	79	81
Cu ppm	74	69	22	72	122	37	81	30	36	48	42	29		17	17	145	122
Zn ppm	147	116	92	63	58	128	60	136	85	83	129	93		128	87	99	106
Ga ppm	23	20	23	16	15	24	19	24	22	19	25	25		19	16	19	19
Rb ppm	8	13	34	13	8	18	14	15	52	41	33	58		13	8	29	12
Sr ppm	191	114	132	474	344	173	192	262	356	164	114	216		102	58	128	78
Y ppm ICP	69.4	39.7	29.8	16.8	9.4	37.1	18.7	55.0	26.4	25.1	53.8	28.8		45.2	44.7	40.8	35.3
Zr ppm	162	111	158	98	79	109	77	87	206	171	139	180		90	74	86	89
Nb ppm ICP	4.86	2.79	12.3	8.49	8.42	47.9	18.2	58.9	30.5	23.7	45.7	26.7		1.89	1.72	1.50	1.52
Sn ppm ICP	1.29	1.27	0.65	1.06	0.66	0.32	0.27	0.00	1.03	1.07	5.85	1.88		23.9	10.7	7.20	1.61
Ba ppm	94	42	306	2823	352	65	164	182	280	110	34	277		22		56	
Hf/Zr ICP	0.053	0.032	0.029	0.025	0.025	0.028	0.032	0.048	0.035	0.030	0.037	0.040		0.048	0.082	0.040	0.033
Ta ppm ICP	0.49	0.34	0.49	0.59	0.46	2.48	1.23	3.53	2.23	1.20	5.29	1.84		0.27	0.19	0.18	0.20
Pb ppm ICP	3.46	1.59	5.05	107	11.9	1.48	3.37	4.85	10.1	1.53	8.33	4.58		0.73	1.36	6.21	10.1
Th ppm ICP	1.59	0.16	3.97	18.2	2.63	0.07	4.48	3.63	0.57	0.31	2.45	1.73		0.33	0.27	0.19	0.08
U ppm ICP	0.33	0.14	0.27	4.41	0.97	0.04	0.89	0.60	3.73	0.17	1.81	0.68		0.06	0.05	0.04	0.03
La ppm ICP	14.7	4.26	14.2	111.2	35.4	11.6	19.8	35.9	9.14	15.2	29.6	15.3		4.14	4.11	2.99	2.89
Ce ppm ICP	45.2	13.0	29.2	222.0	72.3	30.1	46.2	99.4	21.0	36.0	66.3	34.5		16.0	14.9	10.0	8.60
Pr ppm ICP	6.86	2.13	3.99	27.9	8.75	4.97	5.37	12.3	3.11	5.43	10.5	5.12		2.82	2.56	1.83	1.77
Nd ppm ICP	31.9	11.1	16.0	106.3	35.3	22.4	21.0	50.6	13.1	23.0	35.0	20.4		14.2	12.3	12.1	9.48
Sm ppm ICP	9.30	4.23	4.36	23.0	8.19	5.89	4.99	10.74	3.85	6.15	10.55	5.32		4.79	3.96	4.11	3.58
Eu ppm ICP	2.59	1.35	1.24	5.31	2.94	1.66	1.38	2.70	0.96	1.63	1.76	1.28		1.30	1.15	1.56	1.19
Gd ppm ICP	9.26	6.86	5.25	17.9	8.91	6.81	4.28	10.13	4.80	6.32	11.60	6.10		4.85	4.40	5.39	5.36
Tb ppm ICP	1.60	1.26	1.04	2.62	1.12	1.27	0.57	1.51	0.85	1.14	1.94	1.02		0.87	0.78	1.03	0.96
Dy ppm ICP	10.06	6.97	6.33	8.46	4.38	7.83	3.20	9.25	5.18	6.14	10.96	5.79		5.42	4.98	6.96	6.08
Ho ppm ICP	2.24	1.49	1.33	1.31	0.72	1.67	0.66	1.89	1.07	1.20	2.13	1.13		1.21	1.12	1.54	1.36
Er ppm ICP	9.47	4.39	3.98	3.94	2.03	4.86	4.15	10.50	3.11	3.42	5.97	3.20		4.44	4.16	4.60	4.11
Tm ppm ICP	0.94	0.60	0.55	0.38	0.22	0.63	0.23	0.64	0.42	0.45	0.73	0.41		0.51	0.47	0.63	0.57
Yb ppm ICP	6.21	4.04	3.42	2.80	1.52	3.75	1.67	4.59	2.76	2.71	4.54	2.66		3.31	3.08	4.11	3.78
Lu ppm ICP	1.03	0.60	0.51	0.35	0.19	0.56	0.29	0.78	0.40	0.41	0.62	0.38		0.56	0.51	0.76	0.57

■ Tab.2. (continued)

Stop 1-2 (Day 1). Eclogite, SE of Eppendorf

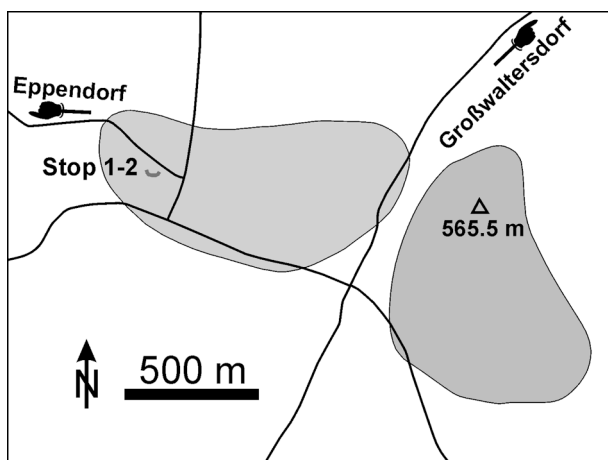
Coordinates: N50°46'36.3" E13°14'49.2"

The route of the excursion continues to Pockau (go first to national route 174 via Lauter Hauptstrasse, then 2 km to the north-west turning to the right; go on B101 for 9 km). Pass Pockau and reach the entrance to the village of Forchheim after going 5 km on B101. Directly on the left hand side there is the manor house of Forchheim. On the opposite side is a parking lot where the vehicle can be entered after the walking tour of stop 1-3. Continue to the exit of Forchheim and turn to the left heading for the village of Lippersdorf. After 3.5 km turn to the right following the main road through this village for 2.5 km. After a left and an immediate right turn proceed for 0.7 km. Then turn to the right. After 200 m park the vehicle in the vicinity of the exit of a road coming from the village of Eppendorf in the north-west.

In the abandoned quarry at stop 1-2 there is a good exposure of massive eclogite which shows the same geochemical signature as eclogite from stop 1-1 (see Table 2). The eclogite of stop 1-2 probably belongs to a large body (Fig. 5) or an assembly of several eclogite lenses. In spite of the two large eclogite bodies of Fig. 5 assumed to be below ground, additional outcrops of eclogite do not exist, although abundant large blocks of eclogite occur along the borders between fields and woods in the vicinity. These blocks and eclogite in the quarry may contain fresh omphacite, although locally this mineral may be completely altered to fine-grained symplectites of amphibole and plagioclase. Occasionally, amphibole porphyroblasts, as in eclogite at stop 1-1, can be found here as well. This amphibole and the rare enrichment of potassic white mica might be a reaction product by infiltrating H₂O during late eclogite facies conditions. Another interpretation of eclogitic layers rich in white mica is that they represent a pelitic protolith originally present as thin strata within the basic rocks.

A fresh phengite-bearing eclogite (sample E174c) from the quarry of stop 1-2 was investigated in detail. Mineral compositions of moderately chemically zoned garnet (64 analyses: X_{Pmp} = 0.211–0.243, X_{Grs} = 0.300–0.359, X_{Sps} ≤ 0.010; see also Fig. 6) and omphacite (36 analyses: Na between 0.371 and 0.403 per formula unit = pfu) are given in Table 3. Phengite of the matrix and enclosed in omphacite (Fig. 7) shows Si contents be-

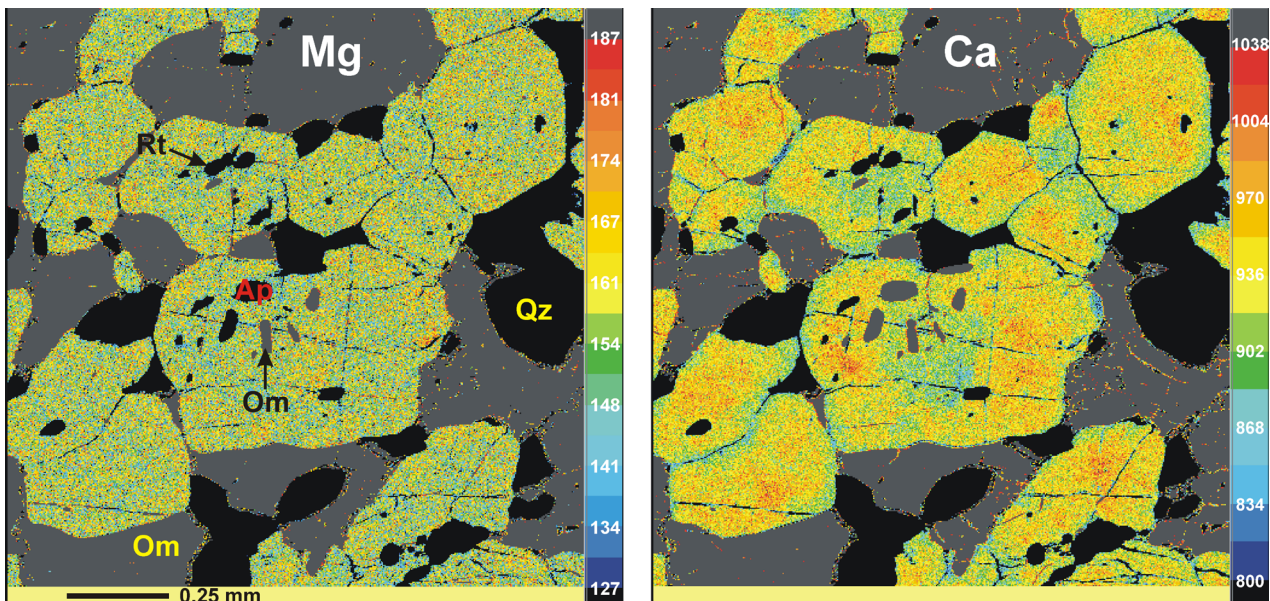
tween 3.30 and 3.35 pfu. Rims of matrix phengite can be lower in Si pfu (Table 3). Zr in rutile (19 analyses) of various textural positions is between 260 and 510 ppm (average 405 ppm). On the basis of a P-T pseudosection (Fig. 8A), which was calculated with the computer software package PERPLE_X (Connolly, 2005) for the bulk-rock composition of eclogite E174c (Table 2) reduced to the NCKFMASH-system with TiO₂, MnO, and O₂, and its contouring by various chemical and modal parameters (Figs. 8B–D, F) was used to derive the P-T conditions



■ Fig. 5. Location map for stop 1-2 south-east of the village of Eppendorf. The large eclogite bodies shown on the map were mapped by Hazard (1886).

Mineral	Garnet		Omphacite		Phengite	
	core	rim	core	rim	core	rim
Anal.-No.	1109/09	1109/91	1109/80	1109/12	1109/33	1109/72
SiO ₂	38.32	38.04	54.87	54.39	50.45	48.25
TiO ₂	0.12	0.10	0.08	0.23	1.55	1.12
Al ₂ O ₃	21.66	21.63	10.19	10.80	26.98	30.60
Cr ₂ O ₃	0.01	0.04	0.00	0.03	0.02	0.01
FeO	21.07	20.96	4.63	4.25	1.28	1.29
MnO	0.38	0.43	0.00	0.07	0.00	0.00
MgO	5.65	6.13	8.81	9.03	4.01	2.71
CaO	13.12	11.85	15.21	15.76	0.00	0.00
BaO					0.18	0.11
Na ₂ O			5.40	5.33	0.47	0.83
K ₂ O					9.57	9.00
Total	100.33	99.19	99.36	99.88	94.51	93.93
Si	5.811	5.830	1.976	1.949	6.705	6.437
AlIV			0.024	0.051	1.295	1.563
Ti	0.013	0.012	0.002	0.006	0.155	0.113
AlVI	3.871	3.907	0.409	0.405	2.932	3.247
Cr	0.001	0.005	0.000	0.001	0.002	0.001
Fe ³⁺	0.128	0.088	0.000	0.003		
Fe ²⁺	2.544	2.598	0.139	0.125	0.142	0.144
Mn	0.049	0.056	0.000	0.002	0.000	0.000
Mg	1.277	1.400	0.473	0.483	0.795	0.539
Ca+Ba	2.131	1.946	0.587	0.605	0.010	0.006
Na			0.389	0.371	0.120	0.216
K					1.623	1.531

■ Tab. 3. Electron microprobe analyses (in wt.%) of minerals from eclogite E174c (stop 1-2) taken from Massonne and Bautsch (2004). Structural formulae were calculated as given in Table 1.



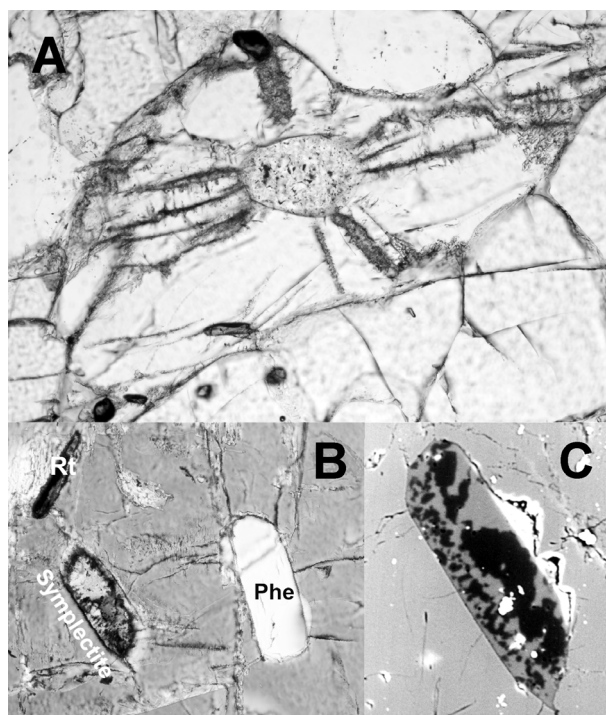
■ **Fig. 6.** Concentration maps of Mg and Ca in moderately zoned garnets of eclogite sample E174c (stop 1-2). Garnets contain inclusions of omphacite (Om), rutile (Rt), quartz (Qz), and apatite (Ap).

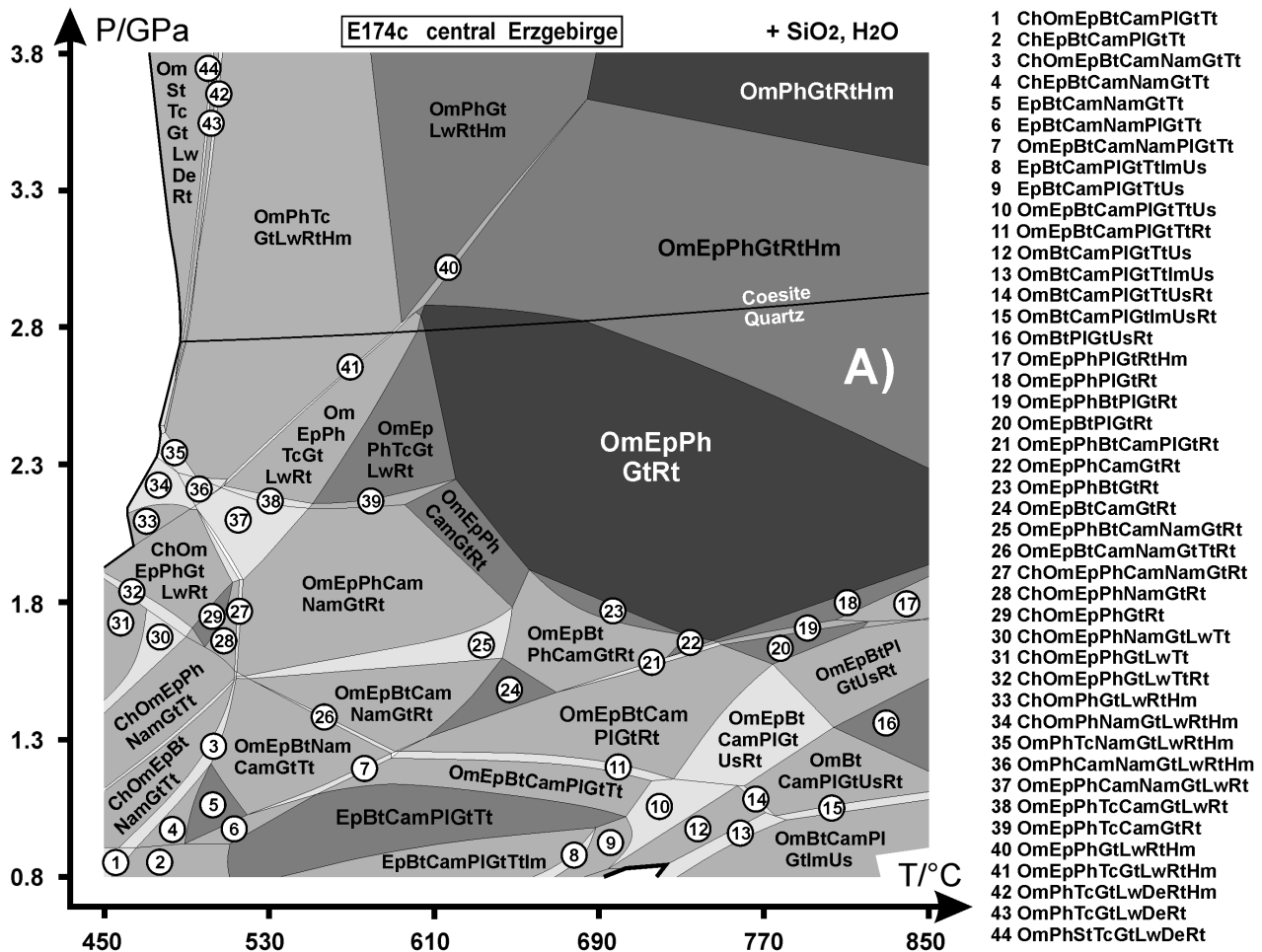
of the eclogite stage. In addition, the Ti-in-muscovite/phengite barometer (Massonne et al., 1993), calculated with the computer program PTGIBBS (Brandelik and Massonne, 2004), and the Zr-in-rutile thermometer (Tomkins et al., 2007) were applied to several potassic white mica compositions and the average Zr concentration in rutile, respectively. Corresponding average P-T curves (Si content of Si-rich potassic white mica, Ti content in potassic white mica, Na content of omphacite, Zr content of rutile, Mg content of garnet), including the calculated boundaries for biotite and amphibole (Fig. 8F), define a P-T datum of about 1.8 GPa and 715 °C (Fig. 8G) which is very close to the estimate of the conditions of the HP event for the surrounding gneisses of the GEU (Willner et al., 1997). The isopleth for the mean Ca content of garnet (Fig. 8G) even suggests lower pressures, but this isopleth can sensitively shift with the O_2 content, that can be related to the Fe^{2+} : Fe^{3+} ratio of the rock, selected for the calculation of the P-T pseudosection. According to this calculation, some epidote should be present in the rock, but as this is not the case, the O_2 might be lower than that selected resulting in a low-

er epidote content and, thus, in a higher grossular content at specific P-T conditions.

A peculiar feature in the eclogite at stop 1-2 are inclusions in omphacite, which consist mainly of intergrown K-feldspar and quartz, resembling a symplectite (Fig. 7). Often, these symplectites are surrounded by cracks in omphacite. This might be the reason why these inclusions were mistaken as pseudomorphs after coesite by Schmädicke et al. (1992), who also

■ **Fig. 7.** Photomicrographs of minerals in eclogite E174c (stop 1-2) taken from Massonne and O'Brien (2003). A) Large inclusion of a symplectite, mainly composed of K-feldspar and quartz, in omphacite under plain polarized light. The inclusion is typically surrounded by cracks. Image width is 0.7 mm. B) A symplectite, somewhat smaller than that of A), rutile (Rt) and phengite (Phe) enclosed in omphacite (crossed nicols). Image width is 0.4 mm. C) Back-scattered electron image of the symplectite in B). Dark: quartz, light grey: K-feldspar and omphacite.

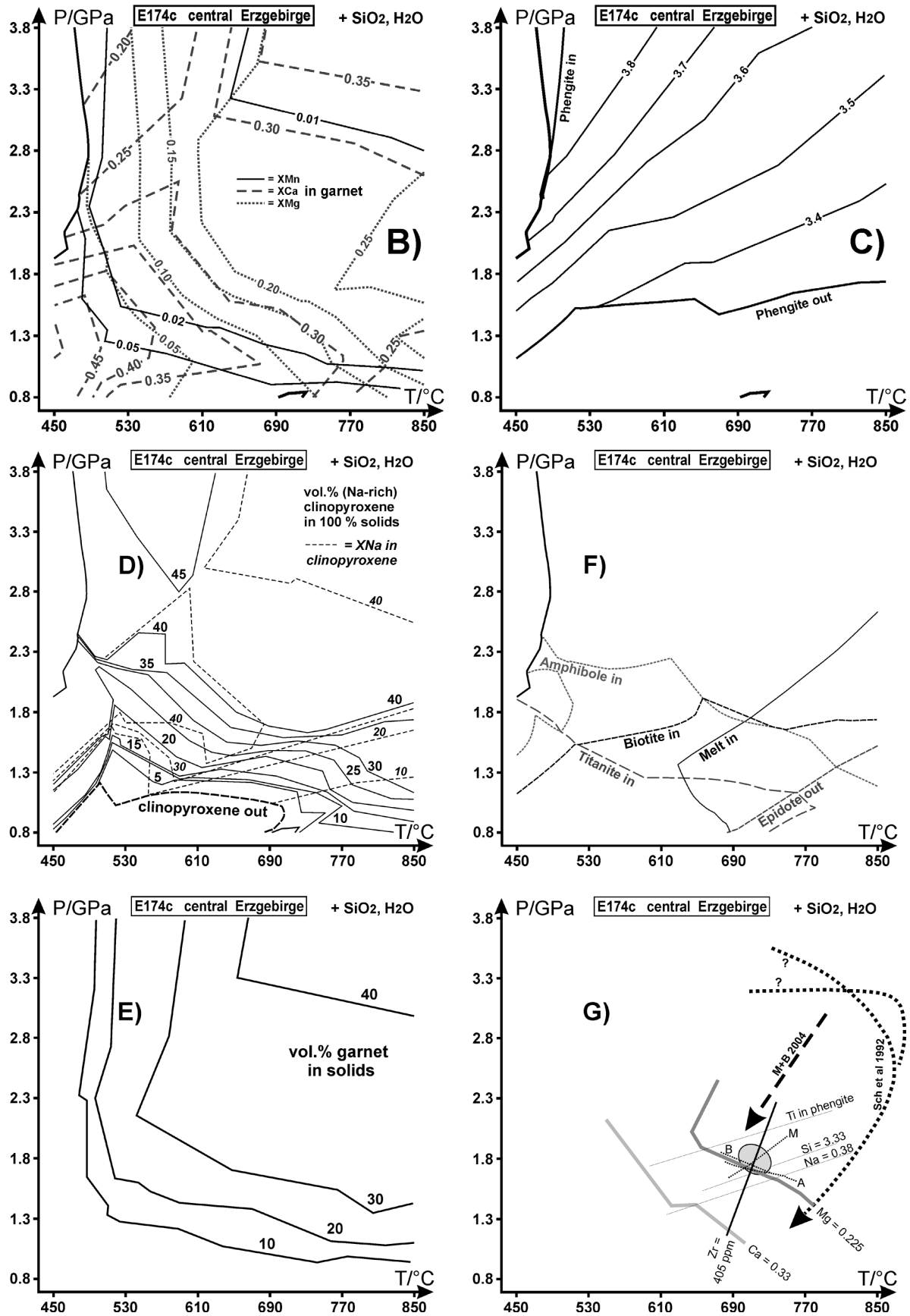




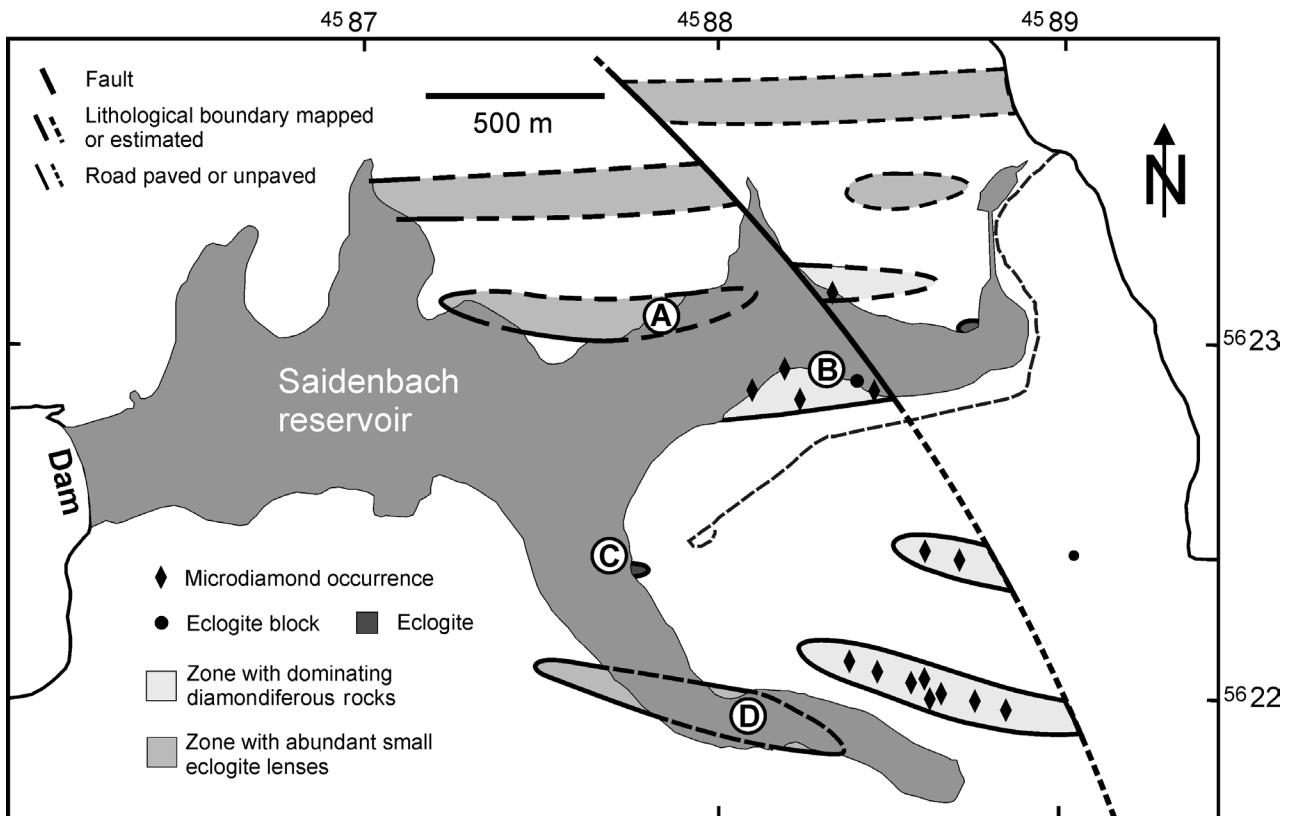
■ **Fig. 8.** (A) P-T pseudosection calculated for the simplified composition of eclogite E174c (SiO₂: 47.82 wt.%, TiO₂: 1.86 wt.%, Al₂O₃: 14.30 wt.%, FeO: 10.92 wt.%, O₂: 0.10 wt.%, MnO: 0.19 wt.%, MgO: 6.12 wt.%, CaO: 11.73 wt.%, Na₂O: 2.24 wt.%, K₂O: 0.22 wt.%, H₂O: 4.5 wt.%) with the computer software package PERPLE_X (Connolly, 2005). This calculation was undertaken as reported by Massonne and Toulkeridis (2010). However, (1) the solid-solution model IIGkPy for ilmenite was additionally selected from the corresponding data-file newest_format_solut.dat and (2) TiBiO(HP) was applied instead of Bio(HP). Furthermore, a model for the magnetite (1)-ulvöspinel (2) solid-solution, Usp(M), was newly introduced with Margules parameters W₁₁₂ = 6600 Joule/mol and W₁₂₂ = 14300 Joule/mol. Abbreviations: Bt = biotite, Cam = Ca-amphibole, Ch = chlorite, De = deerite, Ep = epidote, Gt = garnet, Hm = hematite, Im = ilmenite, Lw = lawsonite, Mt = magnetite, Nam = Na-amphibole, Om = Na-bearing clinopyroxene, Ph = phengite, Pl = plagioclase, Rt = rutile, St = stilpnomelane, Tc = Talc, Tt = titanite, Us = magnetite-ulvöspinel. The P-T pseudosection was contoured by isopleths for (B) molar fractions of Ca, Mg, and Mn in garnet, (C) Si contents pfu in potassic white mica, (D) modal and Na content of clinopyroxene, and (E) modal content of garnet. (F) displays curves limiting the P-T occurrence of specific minerals. The P-T position of the solidus curve “Melt in” was calculated additionally using the haplogranitic melt model “melt(HP)” (see, e.g., White et al., 2001) also stored in Connolly’s file newest_format_solut.dat (see Massonne and Toulkeridis, 2010). This curve demonstrates that the low-pressure, high-temperature portion of the P-T pseudosection shows metastable phase relations with regard to silicate melt. (G) exhibits specific curves (A, B, M = amphibole, biotite, and melt in) shown or related to those in (A)-(F) and average ones referring to the Zr and Ti contents in rutile and phengite (see text), respectively, which are relevant to the derivation of a P-T datum (grey ellipsis) for the studied eclogite E174c. In addition, P-T paths for eclogites from the central Erzgebirge are displayed (Sch et al. 1992 = Schmädicke et al., 1992; M + B 2004 = Massonne and Bausch, 2004).

studied the eclogites SE of Eppendorf. On the basis of this assumption, these authors estimated metamorphic pressures as high as 3.6 GPa (Fig. 8G). In addition, a temperature peak of

850–900 °C, reached at pressures between 2.5 to 3.2 GPa, was proposed by Schmädicke et al. (1992). The symplectites enclosed in omphacite were carefully studied by Massonne et al.



■ Fig 8. – see previous page.



■ **Fig. 9.** Locations of stops 1-3 A to D along the shore of the Saidenbach reservoir. The simplified geological map was taken from Massonne (2001).

(2000), who concluded that they are breakdown products of K-cymrite. On the basis of this assumption and geothermobarometry with garnet, omphacite, and phengite components as applied to eclogite E25d from stop 1-1, Massonne and Bartsch (2004) proposed a P-T path, which started at UHP conditions of somewhat more than 3.0 GPa and ended close to 2.0 GPa and 700 °C (Fig. 8G).

The P-T conditions derived here and by Willner et al. (1997) for the GEU are compatible with a continent-continent collisional scenario in which one continental plate was thrust under the other. This process led to thickened continental crust, which was eclogitized at and close to its base. The eclogites of stop 1-2 provide evidence for this event. During the burial of rocks located

in the lower crust of the lower plate, heating may occur from temperatures of 600–650 °C (0.8 GPa) to around 700 °C, and Ca-amphibole in basic rocks (calculated modal content of E174c at 620 °C and 0.8 GPa in vol.%: 8.9 % epidote, 54.7 % amphibole, 1.9 % biotite, 2.4 % garnet, 25.6 % plagioclase, 3.0 % quartz, 2.8 % titanite, 0.8 % ilmenite) breaks down to form anhydrous phases and H₂O or melt (see “melt in” curve of Fig. 8E). In the latter case and before reaching the peak pressure conditions (1.8 GPa, 715 °C), the solidus curve is crossed again (Fig. 8G). Thus, the symplectite inclusions in omphacite of eclogite E174c could be the result of enclosed melt, the albite component of which was consumed by the overgrowing omphacite. Consequently, mainly K-feldspar and quartz remained in these inclusions.

Stop 1–3 (Day 1). HP and UHP Rocks at the Saidenbach Reservoir

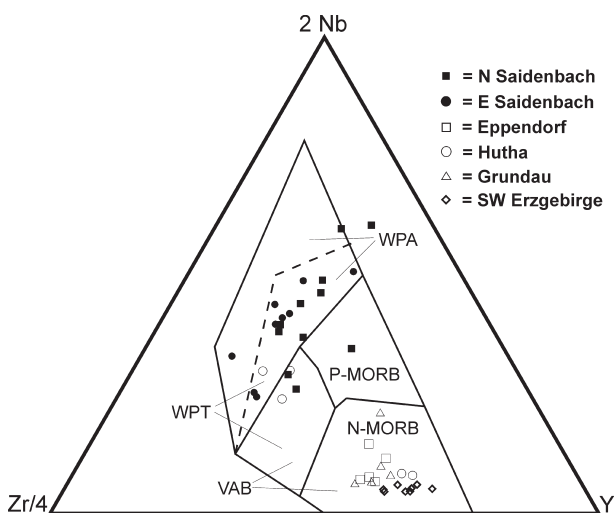
Go the same way back to Forchheim. However, before reaching Forchheim stop at the small bridge crossing Saidenbach brook. From here one has good access to the Saidenbach reservoir by walking on forest roads. To visit the coesite-bearing eclogites at the northern shore of the reservoir (see Fig. 9), take the trail on the north-western side of the brook. Walk for somewhat less than 2 km to reach stop A of the tour along the shore of the reservoir provided that (1) the water level is at least a few metres below maximum and (2) a permit was granted by the responsible person for the reservoir (office directly north of the dam). Chances for (1) are best in the late summer and early autumn. In case the water level is at or close to maximum, alternative stops in the adjacent forests can be considered, especially to see the diamondiferous quartzofeldspathic rocks, which are called saidenbachite (Massonne, 2003) according to the type locality.

Stop 1-3 – A (Day 1). Eclogite at the Northern Shore

Coordinates: N50°44'14.2" E13°14'36.1"

At this site numerous blocks of eclogite are scattered along the strand (Fig. 9) showing a considerable diversity. Massive and foliated types exist, as well as fine and coarser grained varieties. In addition, the chemical variability of the eclogites is remarkable. Samples E99-21 to 24 and E00 (Table 2) demonstrate the significant variation in some minor and trace elements. However, the rare-earth element (REE) patterns of the Saldenbach eclogites are very similar, being characterized by $(La/Sm)_N$ values >1 . In contrast, the aforementioned eclogites with N-MORB to P-MORB signatures have $(La/Sm)_N$ values ≤ 1 . Massonne and Czambor (2007) concluded that the eclogites from the Saldenbach reservoir most likely originated from within-plate basalts to trachyandesites or corresponding plutonic rocks, based on various discrimination diagrams such as that shown in Fig. 10 after Meschede (1986).

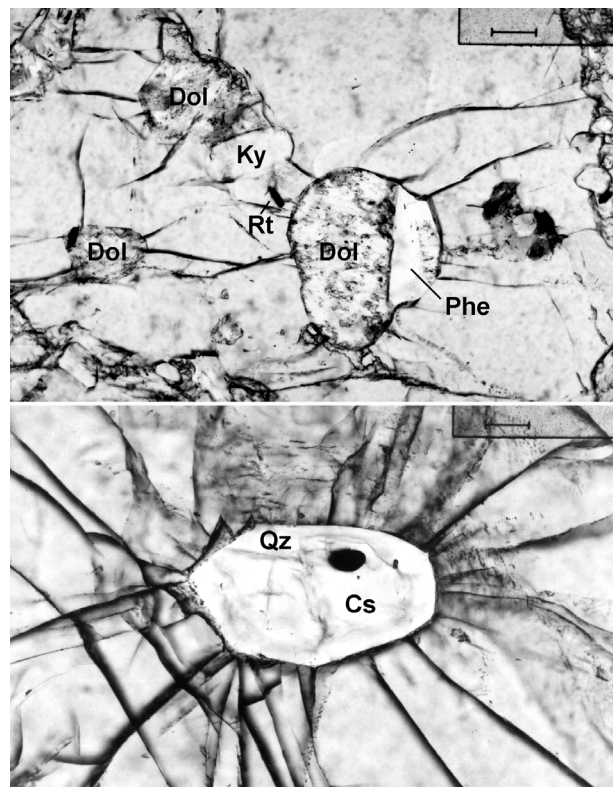
The mineral assemblages of the eclogite blocks at stop 1-3A are also somewhat variable. Most of these blocks contain fresh garnet and omphacite. Rutile and quartz are pervasive. In a few cases, coesite has been detected in eclogite from this locality (Massonne, 2001; O'Brien and Ziemann, 2008). However, coesite is only preserved as rare inclusions in omphacite and garnet (Fig. 11), although partial transformation to quartz is common. Due to the variable chemical bulk rock composition, especially in regard to certain minor and trace elements such as P, Sr, Ba, and Ce (see Table 2), unusual eclogitic minerals occur. For instance, abundant Ba-rich potassic white mica (Table 4) with decreasing Ba contents from core to rim was found in eclogite that also contains cymrite as rare inclusion mineral (Massonne and Bausch, 2004). Cl-rich apatite with relatively high amounts of Sr (>4 wt.% SrO) was reported by Massonne and Burchard (2000) from this locality. Kyanite and dolomite can be constituents in eclogite blocks at stop 1-3A (Fig. 11). Such is the case for sample E99-24, which is used here to illustrate the P-T conditions experienced by the eclogites of this site during



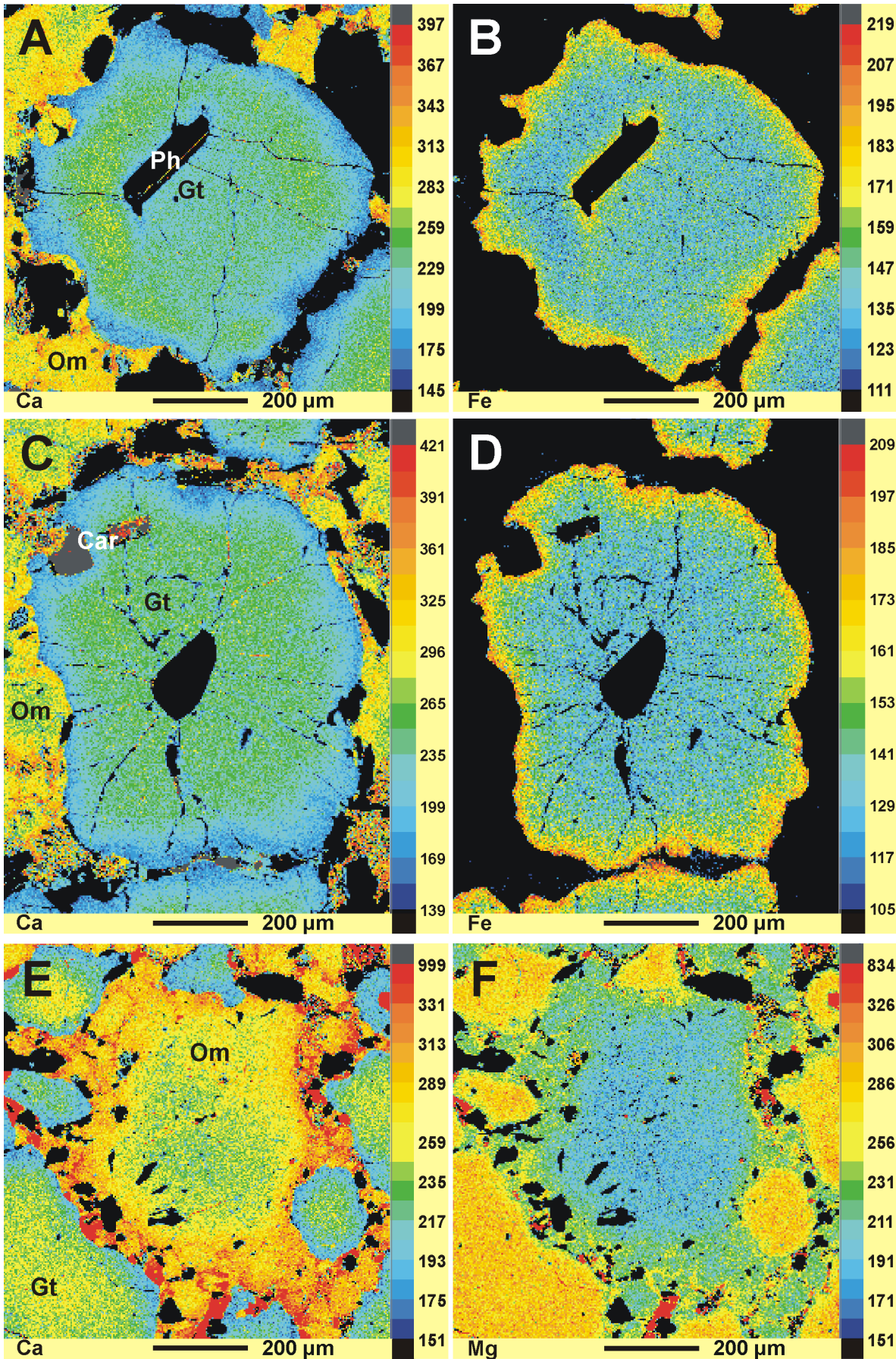
■ **Fig. 10.** Plot of chemical analyses of eclogites from the Saxonian Erzgebirge in the discrimination diagram of Meschede (1986). The graph was taken from Massonne and Czambor (2007).

their metamorphic evolution (chemical compositions of minerals in E99-24 are given in Table 4). Garnet and omphacite in E99-24 are moderately zoned, which is demonstrated by the X-ray maps of Fig. 12. For instance, grossular contents in garnet inner cores are 27 mol% and increase towards the outer core to values between 30–39 mol%. At the outermost garnet rim, grossular contents are between 22 and 26 mol%. Furthermore, relatively large phengite grains enclosed in garnet are richer in Si (close to 3.30 pfu) than moderately zoned potassic white mica (3.19–3.30 pfu) in the matrix. The rims of the latter white mica coexist with biotite (Fig. 12 G+H).

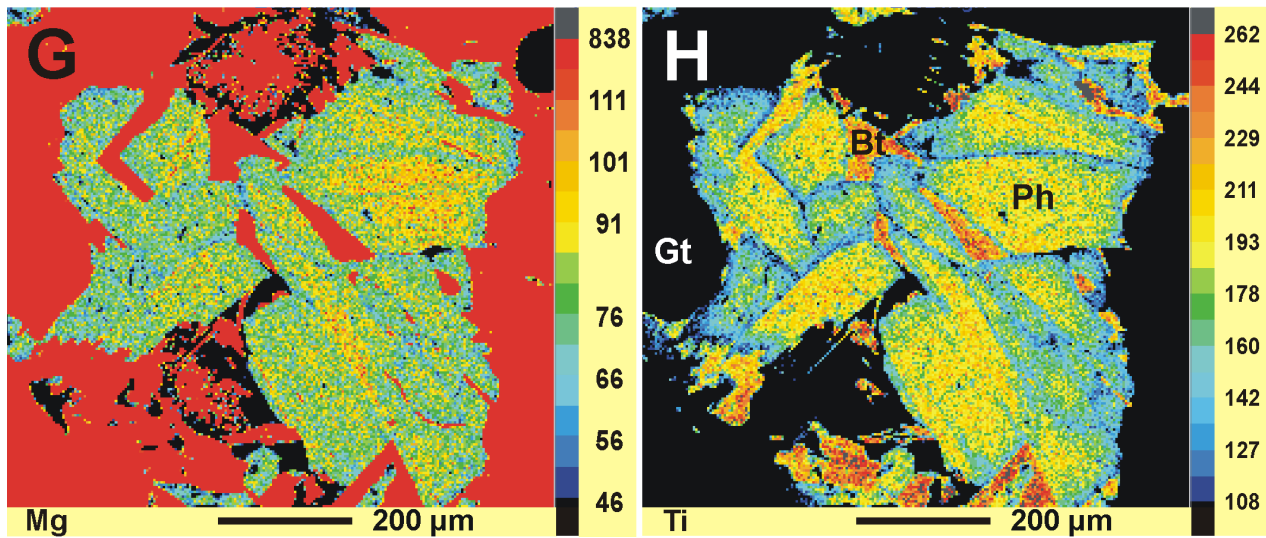
P-T pseudosections were calculated in the NCKFMASH-system with TiO_2 , MnO , CO_2 and O_2 for compositions of E99-24 at different contents of H_2O , CO_2 , and O_2 (see legend of Fig. 13) to account for three different metamorphic stages. The calculation with the computer program PERPLE_X (Connolly, 2005) was performed as outlined in Massonne (2011a). However, the solid-solution models $TiBio(HP)$ and $Omph(HP)$ were used instead of $Bio(HP)$ and $Cpx(HP)$. In addition, the models $Usp(M)$, mentioned in the legend of Fig. 8, and $Ep(HP)$ were applied. The results of the PERPLE_X calculations for sample E99-24 are



■ **Fig. 11.** Photomicrographs of inclusions (Dol = dolomite, Ky = kyanite, Phe = phengite, Rt = rutile) in garnet of eclogite sample E99-24 (stop 1-3A) under plain polarized light (Massonne, 2001). Coesite (Cs) is surrounded by quartz (Qz). Image widths are 1.3 mm (at the top) and 5 mm (at the bottom).



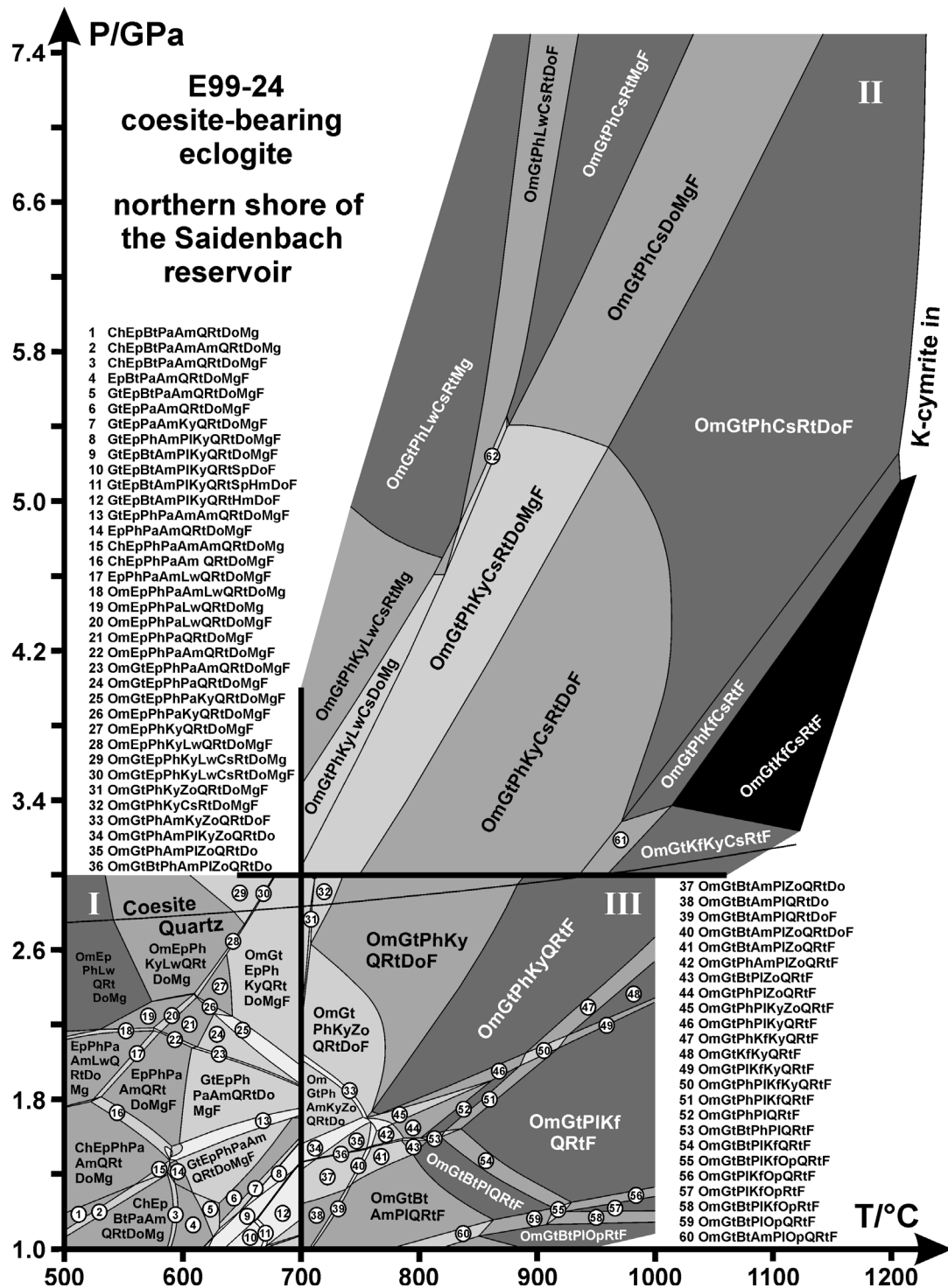
■ Fig. 12. Concentration maps of Ca and Fe of garnet (A-D), Ca and Mg of omphacite (E,F), and Mg and Ti of phengite (G,H) in eclogite sample E99-24 (stop 1-3A). Bt = biotite, Car = carpholite, which is dolomite partially transformed to calcite, Gt = garnet, Om = omphacite, Ph = phengite.



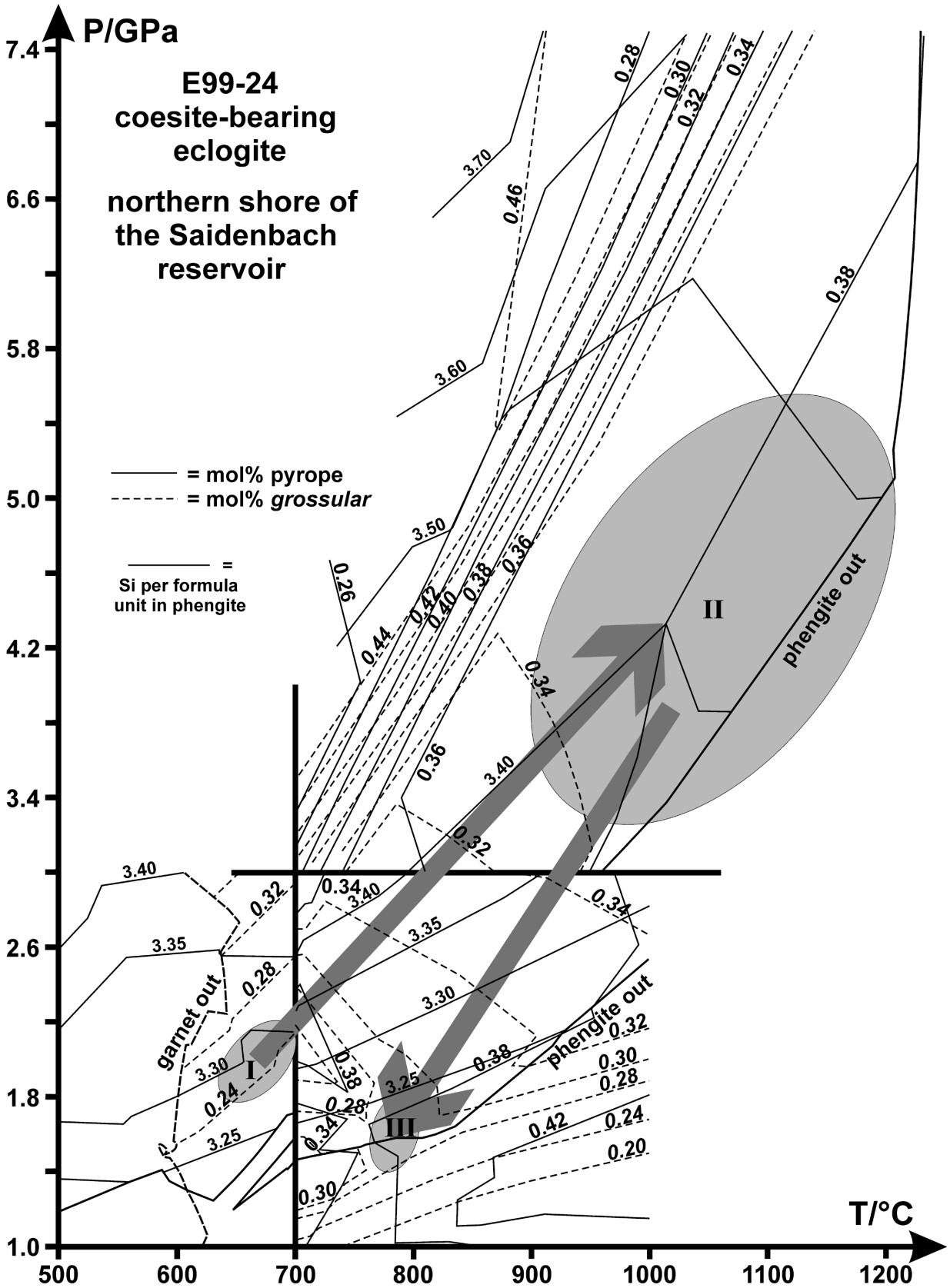
■ Fig. 12. (continued).

Mineral	garnet outer core	garnet outer rim	omphacite core	omphacite outer rim	phengite inclusion	phengite matrix	dolomite inclusion	kyanite inclusion	K,Ba-mica	cymrite
Sample	E99-24	E99-24	E99-24	E99-24	E99-24	E99-24	E99-24	E99-24	E99-23	E99-23
Anal. No.	170558	170560	170523	170528	170519	170516	11617/156	11617/152		
SiO ₂	40.62	40.03	55.67	54.02	49.11	48.27	0.10	35.54	37.40	31.54
TiO ₂	0.18	0.07	0.22	0.35	2.60	2.49	0.04	0.08	4.42	0.17
Al ₂ O ₃	22.87	22.48	14.34	12.14	27.03	28.29	0.03	63.46	30.11	24.62
Cr ₂ O ₃	0.09	0.08	0.20	0.09			0.04	0.08		
FeO _{tot}	11.39	18.46	2.64	2.94	1.34	1.32	3.30	0.34	0.85	0.31
MnO	0.15	0.39	0.00	0.04	0.00	0.00	0.09	0.03		
MgO	11.35	10.39	7.84	9.58	3.82	3.13	19.23	0.05	2.72	0.17
CaO	13.59	9.36	12.29	16.29	0.00	0.00	32.83	0.03	0.06	0.05
Na ₂ O	0.04	0.03	7.42	5.36	0.42	0.45	0.02	0.00	0.61	0.12
K ₂ O			0.00	0.00	10.60	10.82	0.00	0.00	5.06	0.28
BaO					0.74	0.74	0.00	0.01	14.51	39.79
Cl									0.10	0.81
Total	101.29	101.29	100.63	100.81	95.65	95.51	55.68	99.62	95.84	97.86
Si	5.880	5.895	1.947	1.908	6.581	6.495	0.003	0.962	5.632	2.044
Ti	0.020	0.008	0.006	0.009	0.262	0.252	0.001	0.002	0.501	0.008
Al	3.901	3.901	0.591	0.505	4.268	4.486	0.001	2.024	5.344	1.881
Cr	0.011	0.010	0.006	0.002			0.001	0.002		
Fe	1.501	2.275	0.077	0.087	0.150	0.148	0.082	0.008	0.107	0.017
Mn	0.019	0.049	0.000	0.001	0.000	0.000	0.002	0.001		
Mg	2.449	2.280	0.409	0.504	0.762	0.628	0.855	0.002	0.611	0.016
Ca	2.108	1.476	0.461	0.616	0.000	0.000	1.049	0.001	0.010	0.004
Na	0.012	0.010	0.503	0.367	0.109	0.118	0.001	0.000	0.178	0.015
K			0.000	0.000	1.812	1.857	0.000		0.972	0.023
Ba					0.039	0.039	0.000		0.856	1.010
Cl									0.026	0.089

■ **Tab. 4.** Analyses with the wave-length dispersive systems of CAMECA SX50 and SX100 electron microprobes (in wt.%) of minerals in coesite-bearing eclogites from the northern shore of the Saldenbach reservoir (stop 1-2A). The analyses of minerals in E99-23 were taken from Massonne and Burchard (2000). Structural formulae were calculated as given in Table 1 and as follows: dolomite–2 cations without C, kyanite–3 cations, cymrite–16 valencies. Contents of F were below the detection limit.



■ **Fig. 13.** P-T pseudosections calculated for the composition (simplified compared to that given in Table 2) of dolomite-bearing eclogite E99-24 (stop 1-3A) in the system KNCFMASH-Mn-Ti-O-C. The three selected metamorphic stages I (early = mineral assemblage enclosed in garnet), II (peak temperature related to the rim composition of extended garnet cores, which is Mg-richer), and III (late = matrix assemblage including the garnet outermost rim) were related to different H₂O, O₂, and CO₂ contents (after normalization to a total of 100 wt%: I = 2, 0.2, 12 wt%, II = 0.5, 0, 4 wt%, and III = 0.5, 0, 1 wt%) guided by the idea that the growth of the majority of garnet after stage I was caused by decarbonation reactions. Abbreviations: Am = amphibole, Bt = biotite, Ch = chlorite, Cs = coesite, Do = dolomite, Ep = epidote, F = mixed H₂O-CO₂ fluid, Gt = garnet, Kf = alkali feldspar, Ky = kyanite, Lw = lawsonite, Mg = magnesite, Om = Na-rich clinopyroxene, Op = orthopyroxene, Pa = paragonite, Ph = phengite, Pl = plagioclase, Q = quartz, Rt = rutile, Zo = zoisite. P-T fields labelled with two times Am refer to coexisting Na- and Ca-amphibole. The latter amphibole appears at higher temperatures and lower pressures relative to the occurrence of Na-amphibole.



■ Fig. 14. Pseudosection of Fig. 13 contoured by the following sets of isopleths: (1) Si per formula unit in phengite, (2) grossular and (3) pyrope contents in garnet. Grey ellipses mark likely P-T conditions for the three stages I to III (see legend of Fig. 13), and are connected by arrows defining a P-T path for eclogite E99-24.

shown in Figures 13 and 14. For the early metamorphic stage I, characterized by the inclusion assemblage of kyanite, dolomite, phengite, (clino)zoisite and omphacite in garnet (Fig. 13), P-T conditions around 2.0 GPa and 660 °C were estimated (Fig. 14). At this stage there should be little garnet present, according to the calculation results (see Table 5). Garnet grew during further burial mainly at the expense of carbonate minerals (dolomite and inferred magnesite), quartz/coesite and zoisite-epidote. Peak P-T conditions (stage II) cannot be precisely assessed as the garnet composition is not very sensitive at the inferred P-T conditions around 4.5 GPa and 1050 °C (see Fig. 14). Zr in rutile geothermometry yielded ca. 900 °C (at 4.5 GPa) based on the calibration by Tomkins et al. (2007) and 19 of 20 rutile analyses with a mean value close to 1300 ppm Zr. Application of the garnet-omphacite Fe²⁺-Mg exchange thermometry gave temperatures around 1200 °C at 4.5 GPa, using the calibration by Ellis and Green (1979). However, this temperature estimate is rather uncertain, due to the difficulty in determining the amounts of Fe²⁺ and Fe³⁺ in omphacite. The retrograde stage III, which is characterized by micas and kyanite of the matrix and the garnet and omphacite outermost rims (see Table 3), was defined at P-T conditions around 1.6 GPa and 770–800 °C (Fig. 14).

Eclogite E99-24 yielded a δ¹³C(PDB) value of -9.2 (analytical method as reported by Massonne and Tu, 2007). Such a result for δ¹³C does not exclude freshwater carbonates as a possible source of carbon in the protolith of this eclogite. On the other hand, the δ¹³C value would still be compatible with mantle carbon (usually around δ¹³C(PDB) = -5).

Stage	I	II	III
P/GPa	2.1	4.5	1.8
T/°C	670	1050	780
Om	15.3	20.4	42.3
Gt	2.9	55.7	40.4
Zo/Ep	21.3		
Ph	2.8	4.0	4.2
Pa	4.0		
Ky	6.0		6.0
Q/Cs	21.1	12.1	6.1
Rt	0.7	0.9	0.9
Do	9.4	6.8	
Mg	16.4		
XNa(Om)	0.54	0.59	0.30
XCa(Gt)	0.255	0.355	0.29
XFe(Gt)	0.47	0.26	0.345
XMg(Gt)	0.24	0.38	0.36
Si(Ph) pfu	3.30	3.42	3.25

Stages and mineral abbreviations as in Fig. 13.

■ **Tab. 5.** Modal content (in vol%) and compositional characteristics of minerals calculated with the PERPLE_X software for the simplified eclogite composition of E99-24.

Stop 1-3 – B (Day 1). Saidenbachite at the Eastern Shore

Coordinates: N50°44'10.0" E13°15'08.6"

Walk back along the shore, cross the Saidenbach creek, turn to the south, and continue to walk along the shore until the forest road changes to a westerly direction. Then, continue walking for about 400 metres to some large boulders that, however, would be partially submerged when the reservoir is at its maximum level.

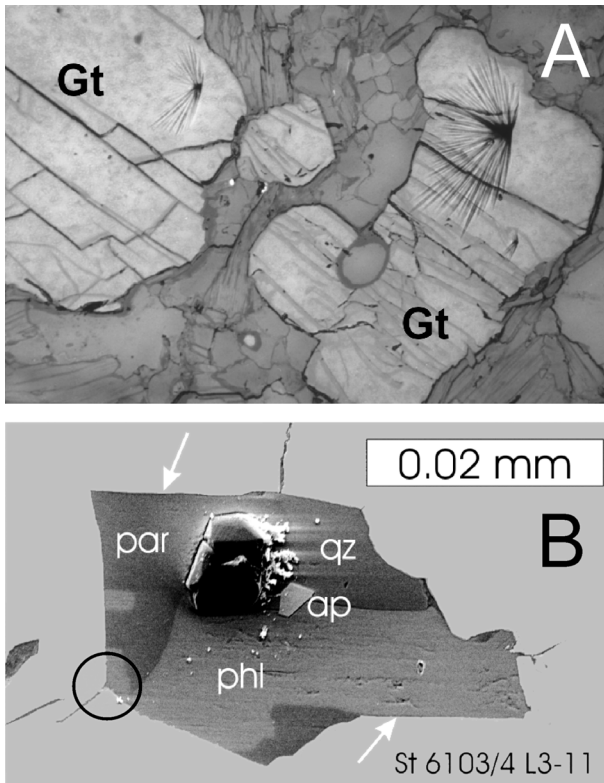
Boulders of saidenbachite differ from those of migmatitic gneisses ("Flammengneise") that occur abundantly as field stones and blocks along the strand and in the adjacent forest. Saidenbachite is a non- or slightly foliated quartzofeldspathic rock with a homogeneous distribution of abundant mm-sized garnets in a muscovite-rich matrix. Boulders of saidenbachite, which are distributed for 500 metres to the west, occur only very locally and are likely related to (lensoid?) bodies underground surrounded by migmatitic gneisses (see map of Fig. 9).

Microdiamonds up to 30 µm, but generally between 5 to 10 µm, in diameter occur as inclusions in garnet and other phases (Fig. 15) of the saidenbachite and were first reported by Massonne (1999). Nasdala and Massonne (2000) confirmed the existence of these microdiamonds by Raman-spectroscopy. Hwang et al. (2001) and Stöckhert et al. (2001) reported the association of quartz, feldspars, various micas, and occasionally apatite and rutile with diamond within a single inclusion in garnet (Fig. 15). These authors interpreted such polyphase inclusions as trapped siliceous fluid or melt. The microdiamonds themselves contain nanometre-sized inclusions, the minerals of

which can hardly be identified and related to the larger inclusion minerals (Dobrzhinetskaya et al., 2003).

Detailed studies of saidenbachite demonstrate that the microdiamonds are enclosed in an intermediate compositional zone of garnet (Massonne, 2003) characterized by relatively low Ca concentrations (Table 6, Fig. 16). Microdiamond inclusions also occur in an intermediate zone of mm-sized kyanite grains, which are relicts corroded by potassic white mica (Fig. 17). Occasionally, abundant small idiomorphic garnets are enclosed in the cores of kyanite.

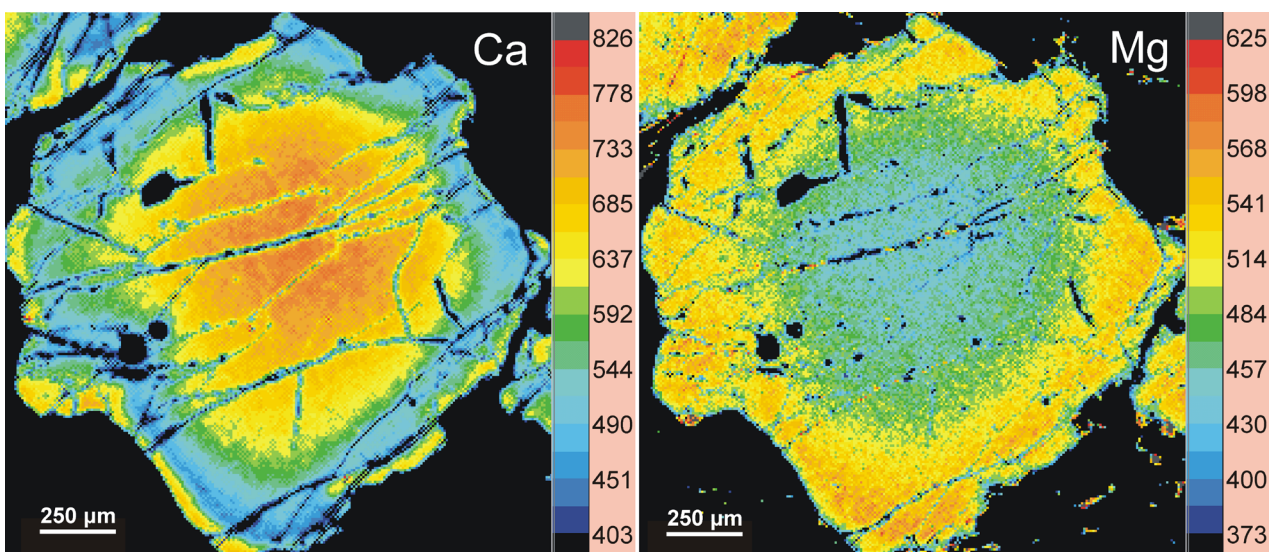
Microdiamonds also occur in an intermediate growth zone in zircon (Fig. 18). Rare inclusions of graphite, garnet and jadeite were found in zircon cores (Nasdala and Massonne, 2000; Massonne and Tu, 2007). In addition, inclusions of phengite, quartz, and rutile occur in garnet cores. From the assemblage of these inclusions, P-T conditions of 1.8 GPa and 650 °C were derived by geothermobarometry (Massonne and Nasdala, 2003) a result which is the same as the peak pressure estimated for gneisses in the vicinity of the saidenbachites (Willner et al., 1997) and for eclogite of stop 1-2 (see Fig. 8). This coincidence



■ **Fig. 15.** (A) Photomicrograph of microdiamonds enclosed in garnet (Gt) from quartzofeldspathic rock E97-3 (alternative stop 1-3E) seen under reflected light. Striations around the diamonds, due to the preparation method applied (Massonne et al., 1998), allow their detection. Image width is 3 mm. (B) SEM image of a polyphase diamond-bearing inclusion in garnet from saidenbachite (Stöckhert et al., 2001). Arrows point to rational mica garnet interfaces. The circle marks an offshoot that typically originated at the edges of such inclusions by decrepitation due to internal overpressure. qz = quartz, par = paragonite, phl = phlogopite, ap = apatite.

was interpreted by Massonne and Nasdala (2003) as evidence for the location of the saidenbachite protolith at the base of a continental crust thickened to 60 km, or more, during the Variscan orogeny. Subsequently, this protolith was deeply buried into the mantle to be heated to about 1200 °C (Massonne, 2003) resulting in extensive anatexis. Corresponding melts, containing residual garnet and zircon (cores), ascended from depths of more than 150 km (the diamond-graphite transition occurs in depths of 150 km at 1100 °C). If TiO₂ with α -PbO₂ structure, found by Hwang et al. (2000) in saidenbachite, would have been a stable phase, this depth could have been 200 km or more. During ascent, still at high pressures, garnet and kyanite, but also rutile, zircon, and diamond, crystallized from the magma (Massonne, 2003). Finally, the magma was emplaced in deep portions of still thickened continental crust at P-T conditions of 1.5 to 1.8 GPa (55–60 km) and temperatures close to 750 °C, as determined by phengite geothermobarometry (Massonne, 1999; 2003). At this stage considerable muscovite formed by a peritectic reaction from the remaining melt (Massonne, 2003) and during subsequent retrogression, some biotite grew at the expense of muscovite. It is noteworthy that several microstructural features indicate the early formation (or existence) of coesite, jadeitic pyroxene, and possibly K-cymrite during the ascent of the saidenbachitic magma (Massonne, 2003; Massonne and Nasdala, 2003).

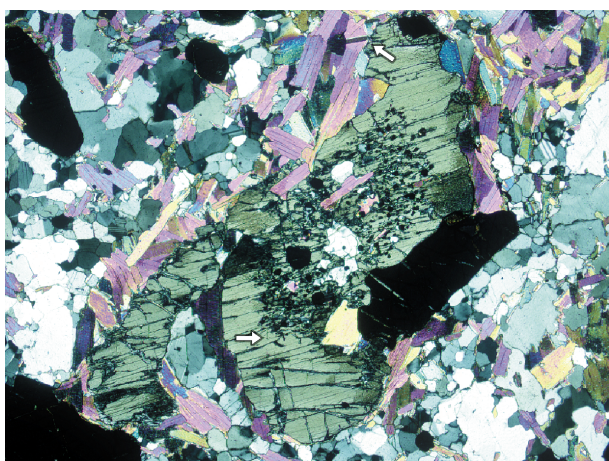
In contrast to the magmatic interpretation for the genesis of saidenbachite, Hwang et al. (2006) suggested that microdiamonds were generated by infiltration of ultrapotassic fluids. However, the enclosure of abundant small garnet crystals in kyanite (Fig. 17) cannot be explained by such fluid infiltration. On the contrary, crystallization of a saidenbachitic melt can account for this texture by undercooling accompanied by formation of many garnet nuclei (Massonne, 2003). In addition, the concentration of phosphorus in saidenbachite is so low (Tab. 7) that the amounts of the putative “P/K-rich melts”, penetrating and reacting with gneissic rocks as suggested by Hwang et al. (2006), must also be very low. Thus, it would be surprising that such



■ **Fig. 16.** Concentration maps of Ca and Mg of garnet in saidenbachite sample E97-2 (alternative stop 1-3E) taken from Massonne and O’Brien (2003).

Mineral	kyanite	garnet core	garnet intermediate zone	garnet rim	garnet core	garnet incl. in zircon	jadeite incl. in zircon	phengite incl. in garnet	phengite core	phengite rim
Sample	E97-2	E97-2	E97-2	E97-2	St6100	St6100	St6100	St6100	E97-1	E97-1
SiO ₂	36.66	38.57	38.66	39.00	38.80	39.07	58.54	49.67	47.90	47.15
TiO ₂	0.067	0.203	0.133	0.053	0.075	0.018	0.284	3.32	2.11	2.32
Al ₂ O ₃	63.19	22.20	22.32	22.34	22.59	22.44	22.80	28.25	28.64	29.70
Cr ₂ O ₃	0.037	0.02	0.02	0.06	0.01	0.04	0.02	0.05	0.05	0.05
FeO _{tot}	0.084	26.06	26.11	25.32	26.02	24.93	1.72	1.11	1.48	1.54
MnO		0.34	0.34	0.295	0.39	0.25	0.00	0.06	0.00	0.03
MgO	0.046	7.57	8.26	8.33	9.59	10.18	2.28	3.51	2.97	2.59
CaO		5.50	4.40	5.22	3.57	3.44	3.04	0.01	0.02	0.01
Na ₂ O					0.13	0.08	11.95	0.72	0.27	0.23
K ₂ O					0.00	0.00	0.00	9.77	9.91	9.91
BaO								0.28	0.32	0.21
F								0.21	0.11	0.10
Total	100.08	100.46	100.24	100.62	101.17	100.44	100.63	96.97	93.79	93.83
Si	0.988	5.906	5.918	5.936	5.785	5.871	2.003	6.497	6.476	6.367
Ti	0.0014	0.024	0.016	0.006	0.008	0.002	0.007	0.327	0.215	0.235
Al	2.007	4.006	4.026	4.006	3.970	3.974	0.920	4.354	4.564	4.727
Cr	0.0008	0.002	0.002	0.006	0.001	0.004	0.001	0.005	0.005	0.005
Fe	0.0019	3.338	3.342	3.220	3.245	3.133	0.049	0.122	0.167	0.174
Mn		0.044	0.044	0.038	0.049	0.032		0.006	0.000	0.004
Mg	0.0019	1.728	1.884	1.890	2.131	2.280	0.116	0.685	0.598	0.521
Ca		0.902	0.720	0.850	0.570	0.554	0.111	0.001	0.000	0.000
Na					0.035	0.022	0.793	0.184	0.070	0.060
K									1.710	1.706
Ba									0.017	0.011
F								1.645	0.048	0.044

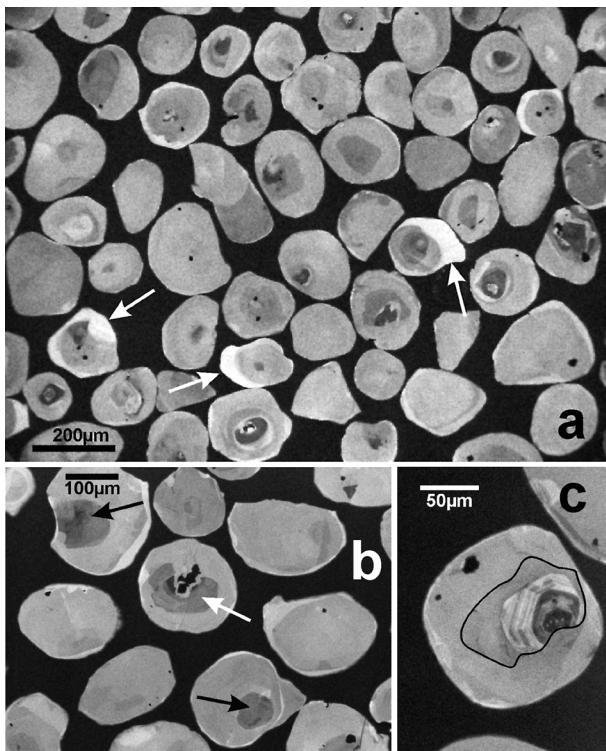
■ **Tab. 6.** Electron microprobe analyses (in wt.%) of minerals in diamondiferous quartzofeldspathic rocks from the Saidenbach reservoir taken from Massonne (1999) and Massonne and Nasdala (2003). Structural formulae were calculated as given in Table 4.



■ **Fig. 17.** Photomicrograph of a large kyanite from sample E97-3 (alternative stop 1-3E), viewed under crossed nicols (Massonne, 2003). The colour image was taken from Massonne and O'Brien (2003). Kyanite is partly replaced mainly by micas. Abundant small garnets are enclosed in the core of the crystal. Arrows point to enclosed microdiamonds. Image width is 4 mm.

small amounts of penetrating fluids could produce abundant polyphase inclusions in mm-scale garnet sometimes throughout a nearly entire garnet grain (Stöckhert et al., 2009).

The various metamorphic-magmatic stages were dated by SHRIMP analysis of Pb, U, and Th isotopes in zircon (Massonne et al., 2007). The determined ages were around 337 Ma (Fig. 19) for core and intermediate domains of zircon (see Fig. 18). Zircon rims yielded a mean age of 330 Ma. In addition, monazite ages from SHRIMP and electron microprobe analyses were about 332 Ma and 325 Ma, respectively (Massonne et al., 2007). Monazite appears exclusively in the matrix of the saidenbachites and is a relatively late-stage mineral. Based on such U-Th-Pb dating results and the above described P-T path, Massonne et al. (2007) estimated that burial rates for the saidenbachites and their protoliths were on the order of several cm per year, and that exhumation rates were »10 cm per year (Fig. 19). This very high exhumation rate was explained by ascent of the saidenbachitic magma, from which the intermediate zircon domain crystallized. This view is supported by Stöckhert et al. (2009), who deduced a minimum exhumation rate on the order of 100 m per year, based on decrepitation of fluid inclusions in garnet (see Fig. 15B), rather than plastic deformation of the enclosing garnet.



■ **Fig. 18.** Cathodoluminescence (CL) images of zircon grains (fraction 125–250 μm) separated from saidenbachite sample St6100 (alternative stop 1–3E). These images were taken from Massonne et al. (2007). (a) Overview. White arrows show relatively extended zircon rims with light CL. Less than half of the grains show cores with minor CL. Black spots in the zircons are due to mineral inclusions, among which microdiamonds dominate. (b) Enlarged area of the zircon population. Arrows show zircon cores which are typically corroded. This is shown best in the middle zircon (white arrow), where relatively large microdiamonds (black spots) appear. In addition, the diamond-bearing intermediate zone in zircons often shows a relatively homogeneous CL. (c) Zircon with core (tentatively outlined by the black line) showing rare alternating zones typical of magmatic zircons.

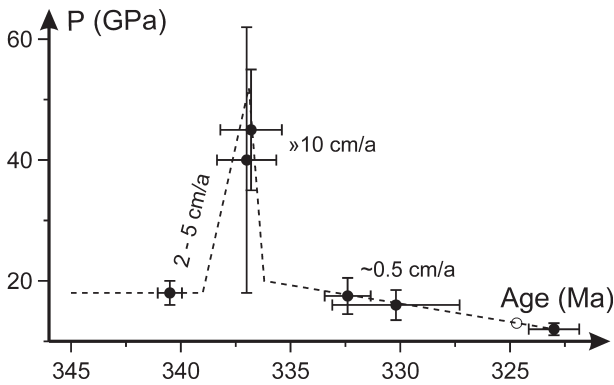
The bulk composition of saidenbachite is typical for that of psammopelite (i.e., low P and relatively high Ti, V, Cr, and Ni contents; Table 7), whereas the surrounding migmatitic gneisses were once granitic rocks (Düffels and Massonne, 2001). According to the study by Tichomirowa (2003), the orthogneisses belong to the red-gneiss family (especially Tichomirowa's type A) which is characterized by elongated zircons. These zircons yield ages in the range, 470–500 Ma, which are interpreted as crystallization ages of S-type granitoids. However, zircon rims around older cores crystallized around 340 Ma during the migmatite-forming event (Tichomirowa et al., 2005). Another difference between saidenbachite and surrounding orthogneiss is shown by their REE patterns, in which a significant Eu anomaly occurs in orthogneisses, but is only moderately developed in saidenbachite (Fig. 20). From the above geochemical differences it is concluded that the saidenbachites do not represent

	1	2	3	4	5	6
	E99-2a	E00-4	E98-7b	KD54	KD55	KD63
SiO ₂ in wt.%	64.33	69.77	59.58	74.26	71.12	74.19
TiO ₂	0.76	0.61	1.04	0.29	0.42	0.30
Al ₂ O ₃	18.03	15.04	21.56	14.19	14.84	13.29
FeO _{tot}	5.29	4.71	6.29	2.53	2.73	1.94
CaO	0.95	1.46	0.28	1.59	1.33	0.90
MgO	2.46	2.00	1.52	0.89	0.82	0.47
MnO	0.05	0.06	0.05	0.04	0.03	0.02
K ₂ O	3.39	2.41	5.65	1.77	4.85	5.02
Na ₂ O	2.51	3.23	0.37	4.28	2.92	2.51
P ₂ O ₅	0.05	0.04	0.07	0.07	0.16	0.18
H ₂ O _{tot}	1.30	0.58	2.86	0.52	0.56	0.92
CO ₂	0.09	0.08	0.04	0.03	0.04	0.05
Sum	99.21	99.99	99.31	100.46	99.82	99.79
Li in ppm	<i>100.6</i>	<i>100.1</i>	<i>65.4</i>	<i>120.0</i>	<i>42.3</i>	<i>76.0</i>
Sc	<i>20.6</i>	<i>15.6</i>	<i>6.0</i>	<i>9</i>	<i>7.2</i>	<i>4.9</i>
V	<i>117</i>	<i>89</i>	<i>139</i>	<i>32</i>	<i>40</i>	<i>25</i>
Cr	<i>77</i>	<i>64</i>	<i>114</i>	<i>1</i>	<i>11</i>	<i>0</i>
Ni	<i>45.4</i>	<i>26.1</i>	<i>23.1</i>	<i>3.85</i>	<i>8.45</i>	<i>5.01</i>
Cu	<i>17</i>	<i>0</i>	<i>19</i>	<i>10</i>	<i>0</i>	<i>5</i>
Zn	<i>104</i>	<i>67</i>	<i>22</i>	<i>31</i>	<i>41</i>	<i>36</i>
Ga	<i>23</i>	<i>19</i>	<i>33</i>	<i>19</i>	<i>18</i>	<i>19</i>
Rb	<i>135</i>	<i>103</i>	<i>338</i>	<i>73</i>	<i>170</i>	<i>252</i>
Sr	<i>112</i>	<i>102.4</i>	<i>12.8</i>	<i>27</i>	<i>112.5</i>	<i>94.2</i>
Y	<i>13.8</i>	<i>14.9</i>	<i>10.2</i>	<i>65.8</i>	<i>45.1</i>	<i>49.0</i>
Zr	<i>167</i>	<i>166</i>	<i>103</i>	<i>83</i>	<i>190</i>	<i>172</i>
Nb	<i>13.7</i>	<i>12.7</i>	<i>19.8</i>	<i>6.57</i>	<i>11.1</i>	<i>14.8</i>
Sn	<i>1.84</i>	<i>2.17</i>	<i>34.8</i>	<i>8.95</i>	<i>2.8</i>	<i>4.6</i>
Ba	<i>415</i>	<i>297</i>	<i>699</i>	<i>142</i>	<i>657</i>	<i>430</i>
Hf/Zr	<i>0.053</i>	<i>0.032</i>	<i>0.030</i>	<i>0.025</i>	<i>0.032</i>	<i>0.034</i>
Ta	<i>0.92</i>	<i>0.92</i>	<i>1.92</i>	<i>0.25</i>	<i>0.61</i>	<i>1.44</i>
Pb	<i>2.12</i>	<i>1.83</i>	<i>3.25</i>	<i>1.14</i>	<i>14.41</i>	<i>32.12</i>
Th	<i>2.44</i>	<i>6.38</i>	<i>4.58</i>	<i>0.54</i>	<i>12.89</i>	<i>16.84</i>
U	<i>1.23</i>	<i>1.82</i>	<i>4.30</i>	<i>0.10</i>	<i>0.77</i>	<i>5.42</i>

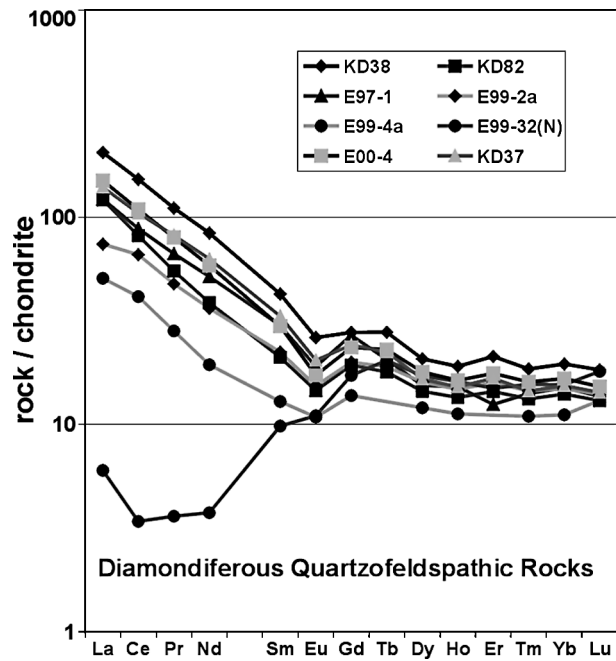
■ **Tab. 7.** XRF and ICP-MS (numbers in italics) analyses of quartzofeldspathic rocks from the GEU of the Saxonian Erzgebirge taken from Massonne and Bausch (2004). 1,2 = saidenbachite from the Saidenbach reservoir, 3 = rock without diamonds, but with aspect similar to saidenbachite, taken northeast of the serpentinite body at Zöblitz, 4 = gneiss unusually rich in Na sampled SW of the village of Forchheim, 5,6 = ordinary gneisses taken close to diamondiferous rocks SW of Forchheim.

country rocks, which were transformed by later metamorphism and deformation.

Microdiamonds from saidenbachite near Forchheim have a high nitrogen aggregation state (Dobrzynetskiy et al., 2006) and $\delta^{13}\text{C}$ (PDB) values around -30‰ (Massonne and Tu, 2007). A similar $\delta^{13}\text{C}$ signature was found for graphite, both that enclosed in zircon cores and that occurring as relatively large flakes in the rock matrix (Massonne and Tu, 2007). Such $\delta^{13}\text{C}$ (PDB) values were taken to indicate an organic source for the carbon. Combining the ^{13}C signature with concordant U-Pb ages of ca. 400 Ma for rare oscillatory zoned (magmatic) zircon cores (Fig. 18; Massonne et al., 2007) and a psammopelitic bulk-rock composition, Massonne and Tu (2007) hypothesized that the saidenbachites were sediments deposited no earlier than Mid-Devonian time. In addition, it is conceivable that these sediments were turbidites (see bulk-rock compositions of Table 7)



■ **Fig. 19.** Pressure-time diagram displaying a likely burial and exhumation course for saidenbachites from the Saxonian Erzgebirge during an episode of the Variscan orogeny (Massonne et al., 2007). Error bars for time are related to 1σ . The open circle represents the mean age acquired via EMP dating of monazite from saidenbachite by Massonne et al. (2007). The U-Pb zircon age at 340.5 Ma was dated by Kröner and Willner (1998) for sample E42x (at or close to stop 1-3D). The age at 323 Ma is a Rb-Sr biotite (cooling) age determined for a granulite from the nearby Granulitgebirge (see Fig. 1) by Romer and Rötzler (2001). The other ages are SHRIMP U-Pb ages of zircon and monazite from saidenbachite (Massonne et al., 2007).



■ **Fig. 20.** REE patterns of saidenbachites from the GEU of the Saxonian Erzgebirge taken from Massonne and Bautsch (2004). The data were obtained by ICP-MS analyses and subsequently normalized to chondrite according to Boynton (1984). The light REE depletion of sample E99-32(N) may be explained by the escape of a melt fraction before complete crystallization. For this reason, monazite is absent from saidenbachite E99-32(N), but present in all other saidenbachites plotted here.

deposited in the shrinking ocean basin before collision of the Laurussia and Gondwana continental plates (or microcontinents derived from Gondwana, e.g., Linnemann et al., 2000)

Subsequently, the protolith of the saidenbachite was likely deeply buried by a subduction event. In this context, Behn et al. (2011) suggested that pelitic material at the top of deeply subducted crust can form buoyant diapirs that ascend into the hot, overlying mantle wedge, where partial melting begins. This scenario may be applicable to the saidenbachites. Alternatively, the saidenbachite characteristics might be related to lithospheric delamination below the thickened Variscan crust, possibly tens of million years after the continent-continent collision (Willner et al., 2002; Massonne, 2005). If crustal material from the base

of this thickened crust were already partially (?) eclogitized (see eclogite E174c from stop 1-2 and stage I of eclogite E99-24 from stop 1-3A, and see Leech, 2001), it could have foundered into the hot mantle to be melted there. In either case, buoyant diapirism or crustal delamination, melting of the saidenbachite protolith occurred in the mantle although no interaction with mantle material is discernible in the chemical composition of saidenbachite.

Stop 1-3 – C (Day 1). Eclogite at the Eastern Shore

Coordinates: N50°43'52.5" E13°14'35.5"

From the western end of the saidenbachite body (stop 1-3B) at the shore of the reservoir, continue walking in a south-westerly direction for 500 metres to a natural outcrop on the shore, which would be still discernible if the water level of the reservoir is at its maximum.

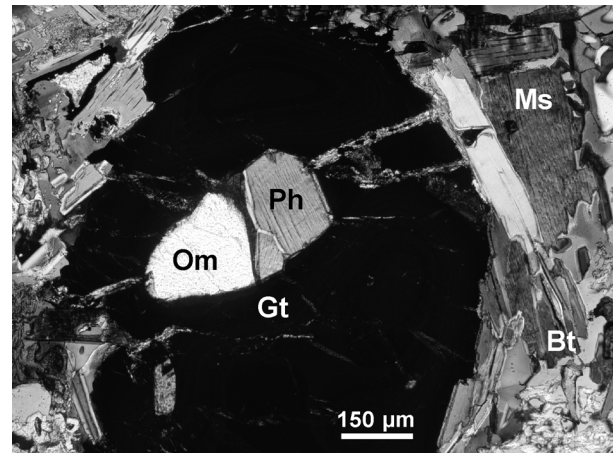
Exposed at this stop (Fig. 9) in the south-eastern portion of the reservoir is a homogeneous eclogite, which is partially penetrated by whitish schlieren and pegmatoid dykes. Thick, up to cm-sized white mica flakes occur in the pegmatoid and such mica also appears in eclogite directly adjacent to the pegmatoid.

The eclogite is characterized by abundant mm-sized garnet grains, which are homogeneously distributed in the rock as in the nearby saidenbachite. The eclogite matrix consists of

a greenish-greyish material, which is mainly composed of relatively coarse-grained symplectite of plagioclase, Ca-amphibole and Na-poor clinopyroxene after former omphacite. Although matrix omphacite has been completely altered to symplectite, fresh omphacite has been preserved as relatively large inclusions in garnet (Fig. 21, Table 8) of samples E42-1d and E03-14 from stop 1-3C. This is also true for other natural exposures of this type of homogeneous eclogite along the shore of the Said-

enbach reservoir. This type of eclogite also occurs as blocks and field stones in the forests and along field boundaries north of the Saidenbach reservoir (see also Fig. 9). Another important inclusion mineral is phengite, the composition (Table 8) of which is nearly identical to that of phengite enclosed in garnet of eclogite E99-24 at stop 1-3A. The same is true for potassic white mica in the matrix, with respect to the lower Si contents of this mica compared with that of the inclusion. Although Massonne and Bautsch (2004) determined P-T conditions somewhat above 30 kbar and 1000 °C by phengite geothermobarometry (as applied to eclogite from stop 1-1) based on the compositions of inclusion minerals and the core of the garnet host, it appears from the relations in the P-T pseudosection of Fig. 13 that these minerals did not necessarily coexist at an early metamorphic stage. It seems to be more likely that the homogeneous eclogites from stop 1-3C and elsewhere have experienced P-T conditions similar to those derived for eclogite E99-24. Unfortunately, no carbonate presently occurs in this homogeneous type of eclogite.

Polished, centre-cut zircon grains from eclogite sample E03-14 usually show an extended blurry core in cathodoluminescence images. In contrast, the rim zone of zircon is homogeneous with a cathodoluminescence significantly higher than



■ **Fig. 21.** Photomicrograph of a garnet (Gt) with inclusions of phengite (Ph) and omphacite (Om) in eclogite sample E42-1d (stop 1-3C) viewed under crossed nicols (Massonne and Bautsch, 2004). Muscovite (Ms), often surrounded by biotite (Bt), occurs outside garnet. Scale bar represents 150 μm.

Mineral	Omphacite	Phengite	Garnet		Phengite	Phengite	
	inclusion	inclusion	core	rim	rim	core	rim
Anal.-No.	1868/4	1868/38	1868/18	1868/24	1868/12	1771/13	1771/8
Sample	E42-1d	E42-1d	E42-1d	E42-1d	E42-1d	E42-1e	E42-1e
SiO ₂	54.70	51.70	38.80	38.66	48.06	50.21	50.56
TiO ₂	0.34	3.74	0.21	0.08	2.62	2.77	2.30
Al ₂ O ₃	14.05	27.17	21.86	21.90	28.61	29.01	29.76
Cr ₂ O ₃	0.00	0.08	0.00	0.06	0.05	0.00	0.01
FeO	4.06	1.72	18.80	21.96	2.36	3.10	2.60
MnO	0.02	0.04	0.37	0.53	0.00	0.01	0.01
MgO	6.95	4.09	6.93	7.84	2.74	3.35	3.21
CaO	12.57	0.01	12.63	8.50	0.00	0.00	0.00
BaO		0.36			0.18	0.20	0.20
Na ₂ O	6.92	0.24			0.29	0.23	0.18
K ₂ O		10.42			10.70	9.25	8.90
Total	99.62	99.57	99.60	99.53	95.61	98.13	97.72
Si	1.945	6.591	5.909	5.906	6.438	6.451	6.468
Al ^{IV}	0.055	1.409			1.562	1.549	1.532
Ti	0.009	0.358	0.025	0.010	0.264	0.267	0.221
Al ^{VI}	0.534	2.674	3.924	3.942	2.955	2.843	2.955
Cr	0.000	0.008	0.000	0.007	0.005	0.000	0.001
Fe ³⁺	0.000		0.076	0.051			
Fe ²⁺	0.121	0.184	2.319	2.754	0.264	0.333	0.278
Mn	0.001	0.005	0.047	0.069	0.000	0.001	0.001
Mg	0.368	0.777	1.573	1.785	0.548	0.641	0.611
Ca+Ba	0.479	0.019	2.061	1.392	0.010	0.010	0.010
Na	0.477	0.060			0.076	0.057	0.044
K		1.694			1.829	1.516	1.453

■ **Tab. 8.** Electron microprobe analyses (in wt.%) of minerals from eclogite E42-1d and pegmatoid E42-1e taken from stop 1-3 C (Massonne and Bautsch, 2004). The two inclusion minerals were found in garnet of the eclogite. Structural formulae were calculated as given in Table 1.

the core. SHRIMP II analyses of both zircon domains at Curtin University, Perth WA, (for analytical conditions see Massonne et al., 2007) yielded the following results: A) mean of 12 core analyses: 278 ppm U, 187 ppm Th, 342.0 ± 2.4 (95% confidence level) Ma and B) mean of 12 rim analyses: 71 ppm U, 24 ppm Th, 337.1 ± 4.8 (95% confidence level) Ma. Thus, zircon from sample E03-14 is as old as that from saidenbachite (see above). Interestingly, the occurrence of former K-cymrite from inclusions of K-feldspar-quartz intergrowths in garnet of eclogite from stop 1-3C was reported by Massonne et al. (2000), but perhaps this feature points instead to melt inclusions, as deduced for similar inclusions in omphacite of eclogite exposed a few kilometres north of the Saidenbach reservoir (stop 1-2).

The composition of phengite in the pegmatoid from stop 1-3C indicates crystallization pressures between 1.5 and 1.8 GPa at temperatures between 700 °C and 750 °C (Massonne and Bautsch, 2004). This pressure interval also applies to the late matrix stage of the eclogite, at which potassic white mica and biotite coexist (see Fig. 21). Again, the P-T conditions of this late metamorphic stage are very similar to that derived for stage III in eclogite E99-24. In addition, the composition of the extended garnet core in sample E42-1d is as rich in Ca (Table 8) as that of eclogite E99-24. In fact, the Mg content of the garnet core (Table 8) is lower than that of E99-24 but the Mg content (as well as the Mg/Fe ratio) of the bulk rock of E42-1d is also significantly lower than that of E99-24. It is thus conceivable that eclogites from stops 1-3A and 1-3C and, consequently, from the entire northern and eastern portion of the Saidenbach reservoir and its vicinity have experienced a similar P-T evolution, as shown in Fig. 14. Furthermore, the P-T evolution of saidenbachite is similar. Thus, it is conceivable that the eclogite exposed at stop 1-3C was also partially molten, as was the protolith of saidenbachite. This idea arises from the homogeneous and similar distribution of garnet in both eclogite and saidenbachite from several bodies at and near the Saidenbach reservoir. Possibly, the granitic melts appearing in schlieren and pegmatoid dykes at stop 1-3C represent remaining melts of the postulated melting (and crystalliza-

tion) at UHP conditions. However, external melts, derived from the adjacent migmatitic country rocks, could have produced the whitish schlieren, as well. Contrary to the invoked melting of basic material at UHP, the carbonate (-rich?) eclogite(s) at stop 1-3A might not have been molten at UHP, either due to high CO₂ partial pressures or maximum temperatures lower than those experienced by the eclogite type from stop 1-3C.

In addition to the different bulk-rock compositions of eclogites at the Saidenbach reservoir compared to those from elsewhere in the Saxonian Erzgebirge, the peak temperatures of the Saidenbach eclogites were significantly higher (at least 1000 °C), compared to those of other areas in the central Erzgebirge. For the latter eclogite group, peak temperatures between 730 °C and 840 °C and around 850 °C (see Fig. 8G) were reported by Massonne (1994) and Schmädicke et al. (1992), respectively. In addition, Zack and Luvizottow (2006) estimated peak temperatures of 850 °C at 3.5 GPa for an eclogite occurrence a few kilometres north of the Saidenbach reservoir. However, these temperature estimates are very likely too high, because the pressures were significantly overestimated, as demonstrated by the new determination of metamorphic P-T conditions for eclogite E174c from stop 1-2 (see Fig. 8G).

The chemical bulk rock compositions of eclogites at stop 1-3C are somewhat variable (see the three analyses in Table 2), despite their similar aspect in the field. Massonne and Czambor (2007) concluded on the basis of trace-element signatures that the protoliths of these eclogites were possibly within-plate igneous rocks, similar to the eclogites at stop 1-3A (see above). These authors previously suggested that these rocks were formed by melting of crustal material in the deep mantle. However, if the protoliths of eclogites from the northern and eastern portion of the Saidenbach reservoir were once (marly) sediments, the relatively high bulk-rock contents of V, Cr, and Ni (see Table 2) would be unexpected. On the other hand, such relatively high contents of the transition metals could be due to minor interaction with mantle material during the melting and crystallization processes in the deep mantle.

Stop 1-3 – D (Day 1). Layered Granulitic Gneiss, Former Small Quarry

Coordinates: N50°43'41.4" E13°14'49.0"

Continue to walk along the shore of the Saidenbach reservoir in a south-easterly direction. After walking ca. 400 metre another natural exposure of rocks appears (actually a former small quarry before the Saidenbach dam was constructed), which is well recognizable even if the level of the Saidenbach reservoir is at its maximum.

Layered granulitic gneisses crop out at this stop (Fig. 9). Greenish and reddish layers represent more basic vs. more acidic rock compositions, respectively. All different rock types at this stop contain abundant up to mm-sized garnet, potassic white mica and biotite. Biotite tends to be a late stage phase, replacing potassic white mica (Fig. 22). Kyanite occurs in some layers, but is commonly replaced by potassic white mica (Fig. 22).

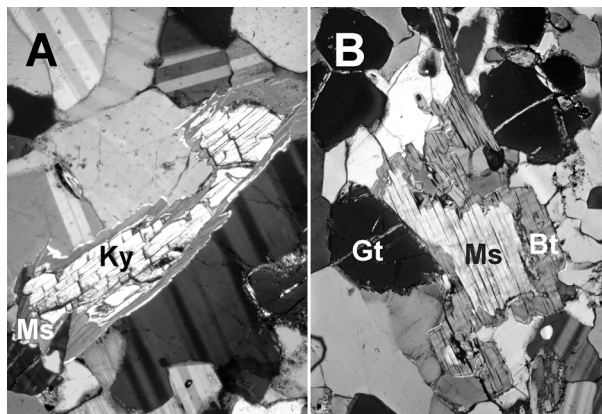
Omphacite was formerly present in the greenish layers, but is now entirely transformed to symplectites of plagioclase, amphibole, and Na-poor clinopyroxene. The same feature is also discernible in some reddish layers although the ratio of amphibole + Na-poor clinopyroxene to plagioclase is significantly

lower compared to that in the greenish layers. This contrast is explained by a higher jadeite content in former clinopyroxene in the reddish layers compared to that in the greenish layers. Locally, in these gneisses a few, mm-thick garnet-rich layers alternate with layers consisting almost exclusively of quartz, plagioclase and subordinate K-feldspar.

Peak P-T conditions for the granulitic gneisses were reported by Willner et al. (1997) to be as high as 2.0 GPa and 800 °C with no indications of higher pressure. The rocks at stop 1-3D might again represent eclogitized crustal material formed at the base of crust thickened by the Variscan orogeny. Whether this thickening event happened 340 Ma ago, indicated by U-Pb

dating of zircon (Kröner and Willner, 1998), or earlier, is still unclear. In spite of the observed eclogitization, the rocks from stop 1-3D do not seem to have been more deeply buried than 70 km (2.0 GPa), whereas other rocks in the area (see stop 1-3A and B) have experienced UHP conditions, explained by the aforementioned delamination process.

- **Fig. 22.** Photomicrographs of metapelitic sample E42/1b (stop 1-3D) under crossed nicols, taken from Massonne and Bartsch (2004). A) Kyanite (Ky) relic marginally replaced by potassic white mica (Ms). Image width is 650 μm . B) Phenogitic muscovite (Ms) marginally replaced by biotite (Bt). Gt = garnet. Image width is 850 μm .



Alternative Stop 1-3 – E (Day 1). Saidenbachite in the Forest

Coordinates: N50 43'41.8" E13 15'15.0"

Continue to walk to the east for somewhat more than 1 km along the shore of the reservoir and the pre-reservoirs until reaching the village of Forchheim and subsequently the national road B 101 and turn to the south-west to see immediately the parked vehicle and/or the manor house of Forchheim. Alternatively, walk towards the hill top and find blocks of saidenbachite, occurring along the slope in the forest, after ca. 400 to 500 m of walking (see Fig. 9). These saidenbachite blocks at alternative stop 1-3E are virtually identical to those at stop 1-3B. From stop 1-3E walk downhill to return to the forest road along the shore of the Saidenbach reservoir to continue to the parked vehicle as described above. Afterwards, go back to Marienberg and stay overnight, for instance, in Hotel Weisses Ross.

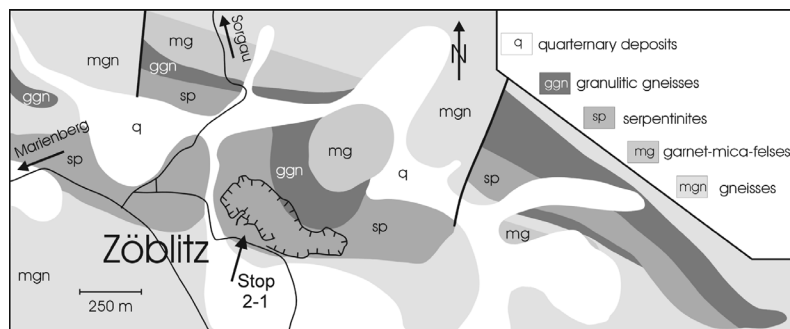
This hotel is located at the margin of the historical town of Marienberg, which was founded by Duke Henry IV, the Pious, of Saxony in 1521 due to the discovery of silver-bearing ores in the vicinity. The old town emerged from the planning stage as a unique Renaissance town north of the Alps, following a rectangular plan. The portal of the town hall from the year 1539 is a relic from this time.

Stop 2-1 (Day 2). Garnet Peridotite at Zöblitz

Coordinates at the gate: N50°39'26.9" E13°14'25.5"

Go on B171 from Marienberg to the east to reach the village of Rittersberg in a few kilometres and cross the river Schwarze Pockau. In Rittersberg, continue heading on B171 for the town of Zöblitz, which is reached after 1.5 km. In the town centre, just after passing the town church on the right hand side, turn to the left heading for the village of Sorgau. After 100 m turn into a small road (Angergasse, later Serpentinstrasse) to the right, go

for ca. 600 m, and stop at the main gate to a large quarry (see Fig. 23), which is operated by Steinbruch Zöblitz GmbH (Tel. +49-37363-7256). The gate is on the left hand side; parking lots are on the right hand side of the road.



■ **Fig. 23.** Simplified geological map of the serpentinite body at the town of Zöblitz, GEU of the Saxonian Erzgebirge. This map is based on mapping by Hazard (1884).

In past centuries serpentinite was quarried at Zöblitz as facing stone, for instance, in the interior of churches and palaces. In addition, drinking vessels and dinnerware were produced from the soft but tough serpentinite by turnery from the time of the late Renaissance. Today, the main purpose of the active quarry at the margin of Zöblitz is to produce macadam. Meanwhile, the serpentinite body at Zöblitz, which extends for ca. 3 km in an E-W direction (Fig. 23), is exploited near the town and for this reason, the quarry was extended to the east. Because of the active quarrying operations, it is uncertain as to which rock types will be visible in the active mining area. For this reason, two stops will be made in the old portion of the quarry near the margin of the serpentinite body. After passing through the gate turn to the left and walk to the low level of the quarry to reach the first stop. Close to the gravel dumps, there is relatively fresh garnet lherzolite in the quarry wall. The second stop will be on the opposite side of the quarry, where layers of garnet pyroxenite are exposed. This site is reached by walking to the NNE across the lower quarry level.

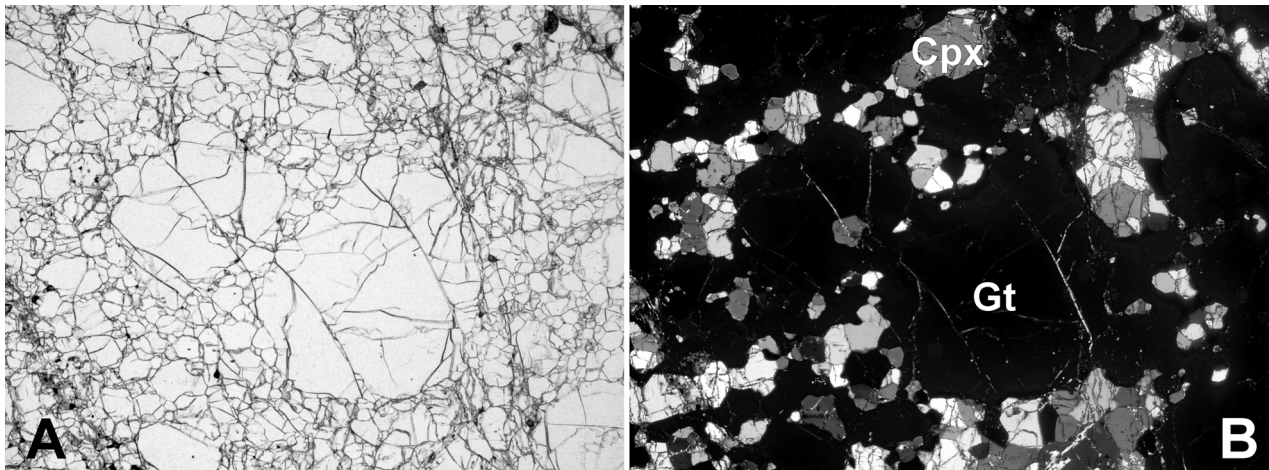
The serpentinite itself consists mainly of lizardite and subordinate clinochrysotile and antigorite. In addition, mm-size aggregates of chlorite occur, which are pseudomorphs after garnet. Occasionally, preserved portions of the original garnet lherzolite can be found as large remnant blocks in the old part of the quarry. The lherzolite consists of cm-size garnet with thin kelyphitic rims in a matrix of mm-size equigranular olivine, clinopyroxene, orthopyroxene, and minor amphibole. The rock fabric is interpreted to be the result of recrystallization after deformation associated with exhumation.

Representative analyses of the minerals in the garnet lherzolite are given in Table 9. Garnet has chemically homogeneous cores and thin rims with slightly lower pyrope contents compared to the cores. Massonne and Bartsch (2004) assumed that the chemical composition of the matrix minerals and the garnet rim were in equilibrium and estimated P-T conditions of about 2.6 GPa and 1000 °C. Schmädicke and Evans (1997) estimated higher pressures up to 3.3 GPa at temperatures somewhat below 1000 °C for the garnet peridotite at Zöblitz.

Pyroxenite layers within the peridotite body consist mainly of clinopyroxene and garnet and accessory rutile. Some pyroxenites contain up to cm-sized garnets that have been marginally transformed to smaller garnet crystals and equigranular clinopyroxene (Fig. 24). Garnet palaeocrysts and neocrysts are chemically zoned as shown in Figure 25. P-T conditions for garnet

rims and matrix phases (Table 9; Massonne and Bartsch, 2004) are 1.66 GPa and 865 °C. Garnet core compositions gave much higher pressures of 3.9 GPa at 1100 °C (Massonne and Bartsch, 2004). Similar P-T conditions of 3.7 GPa and close to 1100 °C were reported by Massonne and Grosch (1995) for another garnet peridotite body situated about 10 km to the east of the serpentinite at Zöblitz. Another possible indication for such high pressures are abundant, tiny oriented ilmenite rods in the cores of some olivine grains in garnet lherzolite at Zöblitz (Massonne and Neuser, 2005). Although no quantifiable pressure significance can be assigned to these rods, a similar exsolution feature reported from the Alpe Arami peridotite massif in the central Alps has been cited as evidence for UHP conditions (Green et al., 1997). Summarizing the petrological information, the exhumation history of the Zöblitz ultrabasic body is similar to that for other ultrabasic rocks from the Saxonian Erzgebirge and the nearby Granulitgebirge (Fig. 1) as outlined by Massonne and Bartsch (2004).

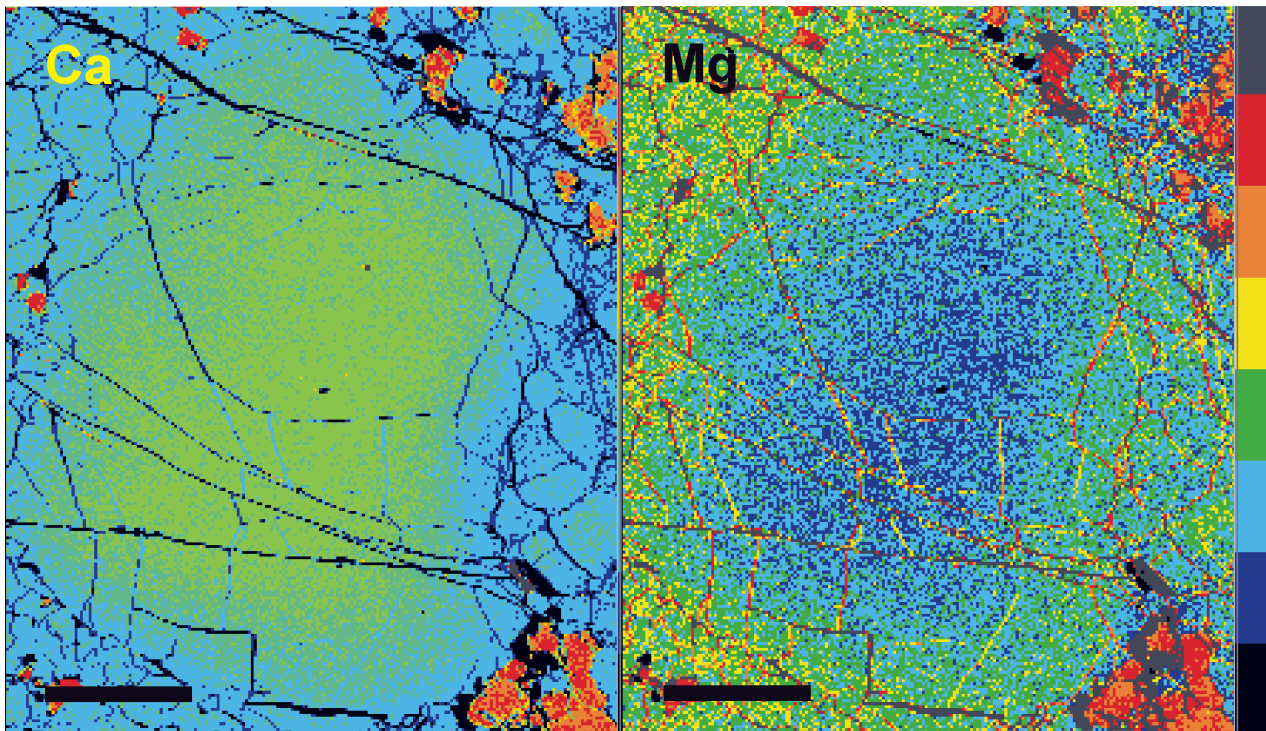
Garnet lherzolite from Zöblitz is slightly depleted in light REE (Table 10). Garnet pyroxenites vary significantly in composition (Table 10). Zircon grains separated from the Zöblitz garnet peridotite yielded U-Pb SHRIMP ages of $332 \pm 5(2\sigma)$ Ma (Liati and Gebauer, 2009). The inclusion mineralogy and the REE pattern of this zircon indicate a crustal origin. Liati and Gebauer (2009) concluded that during exhumation the Zöblitz



■ **Fig. 24.** Photomicrograph of garnet (Gt) in clinopyroxenite sample 18270 from stop 2-1 under plain polarized light (A) and crossed polarizers (B), taken from Massonne and Bautsch (2004). The matrix minerals probably recrystallized after deformation, associated with exhumation, but large garnet palaeocrysts remained. Image width is 4 mm. Cpx = clinopyroxene.

	Erz03-6d						18270			
	Garnet		Orthopyroxene	Clinopyroxene		Olivine	Garnet		Clinopyroxene	
	core 1	rim 6	15	20	rim 36	40	core 14	rim 140	core 35	rim 136
SiO ₂	42.31	42.26	57.90	54.77	54.39	40.91	39.91	40.35	53.64	51.10
TiO ₂	0.66	0.63	0.14	0.41	0.44	0.02	0.57	0.25	0.48	1.03
Al ₂ O ₃	21.92	21.83	0.98	3.72	3.47	0.00	21.97	22.72	5.45	8.61
V ₂ O ₃	0.03	0.03	0.00	0.05	0.07	0.00	0.08	0.05	0.10	0.12
Cr ₂ O ₃	1.60	1.67	0.14	0.92	0.85	0.00	0.01	0.05	0.32	0.04
FeO _{tot}	9.00	10.06	6.49	2.81	2.58	10.15	14.72	15.91	4.79	3.50
MnO	0.33	0.41	0.11	0.07	0.06	0.09	0.27	0.30	0.02	0.00
MgO	21.31	20.47	34.96	15.62	15.69	49.14	9.19	10.35	13.25	12.93
NiO	0.00	0.00	0.06	0.01	0.02	0.37	0.00	0.00	0.00	0.00
CaO	4.26	4.47	0.39	19.61	20.49	0.00	14.81	11.48	20.16	20.40
Na ₂ O	0.08	0.08	0.08	2.53	2.19		0.05	0.05	2.74	2.39
K ₂ O				0.01	0.00		0.00	0.00	0.01	0.01
Total	101.52	101.91	101.27	100.53	100.24	100.70	101.61	101.50	100.97	100.13
Si	5.925	5.928	3.941	3.918	3.908	0.9975	5.855	5.918	3.851	3.704
Al ^{IV}			0.059	0.082	0.092				0.149	0.296
Ti	0.070	0.066	0.007	0.022	0.024	0.0003	0.063	0.028	0.026	0.056
Al ^{VI}	3.618	3.609	0.020	0.231	0.202	0.0000	3.799	3.927	0.312	0.440
Cr	0.177	0.186	0.008	0.052	0.048	0.0001	0.001	0.006	0.018	0.002
V	0.003	0.004	0.000	0.003	0.004	0.0001	0.009	0.006	0.006	0.007
Fe ³⁺	0.202	0.202				0.0044	0.191	0.061		
Mg	4.447	4.000	3.547	1.665	1.680	1.7859	2.009	2.262	1.418	1.397
Mn	0.039	0.048	0.006	0.004	0.004	0.0019	0.033	0.038	0.001	0.000
Fe ²⁺	0.853	0.979	0.370	0.168	0.155	0.2027	1.616	1.891	0.288	0.212
Ni	0.000	0.000	0.004	0.001	0.001	0.0072	0.000	0.000	0.000	0.000
Ca	0.640	0.672	0.028	0.001	0.001	0.0000	2.328	1.804	1.550	1.584
Na	0.022	0.021	0.011	0.350	0.305		0.014	0.006	0.382	0.335
K				0.001	0.000		0.000	0.000	0.001	0.001

■ **Tab. 9.** Electron microprobe analyses (in wt.%) of minerals from serpentized garnet lherzolite, Erz03-6d, and garnet-rich clinopyroxenite, 18270, of the serpentinite body at the town of Zöblitz (stop 2-1) taken from Massonne and Bautsch (2004). Structural formulae were calculated as follows: garnet: O = 12, six- and eightfold coordinated cations = 10; orthopyroxene and clinopyroxene: O = 12, Fe = Fe²⁺; olivine: O = 4



■ **Fig. 25.** Concentration maps of Ca and Mg in garnet, marginally recrystallized to garnet + clinopyroxene, in sample 18270 from stop 2-1. The colour scale shows increasing element concentrations towards the top. Scale bars represent 500 μm .

Sample	Garnet clinopyroxenite			Serpentinite
	E2b	18270	E00-7B	E3b
SiO ₂ in wt. %	46.17	40.70	42.20	39.26
TiO ₂	0.45	1.00	1.30	0.08
Al ₂ O ₃	14.76	18.10	17.88	2.04
FeO	8.11	12.51	12.64	7.04
CaO	9.16	12.40	13.60	0.68
MgO	17.72	10.70	8.26	37.96
MnO	0.21	0.23	0.21	0.11
K ₂ O	0.06	0.01	0.46	0.00
Na ₂ O	0.85	0.17	1.08	0.00
P ₂ O ₅	0.02	0.04	0.08	0.00
H ₂ O _{tot}	1.41	1.52	1.37	11.63
CO ₂	0.08	0.16	0.15	0.31
Sum	99.00	97.54	99.23	99.11
Li in ppm	20.3	90.4	68.3	0.35
Sc	40.9	76.6	71.4	11.1
V	220	402	465	51
Cr	683	112	261	2501
Ni	576	119	128	2350
Cu	86.2	12.5	50.5	18.6
Zn	21	80	92	50
Ga	12.2	15.2	17.2	1.69
Rb	3.79	0.86	13.3	0.00
Sr	74.4	54.3	213	4.00

Sample	Garnet clinopyroxenite			Serpentinite
	E2b	18270	E00-7B	E3b
Y	13.1	22.7	25.8	1.77
Zr	33	49	42	6
Nb	0.43	17.5	1.42	0.02
Sn	0.39	2.88	1.14	0.00
Ba	15.6	12.3	118	2.58
La	1.40	3.95	1.44	0.18
Ce	4.54	10.27	5.63	0.55
Pr	0.77	1.77	1.38	0.10
Nd	3.71	11.07	10.20	0.49
Sm	1.11	5.59	4.84	0.18
Eu	0.46	1.53	1.38	0.06
Gd	1.53	6.13	4.65	0.24
Tb	0.33	0.74	0.66	0.05
Dy	2.31	3.98	4.69	0.31
Ho	0.54	0.80	0.91	0.07
Er	1.71	2.57	2.02	0.21
Tm	0.25	0.31	0.33	0.03
Yb	1.57	2.31	2.42	0.20
Lu	0.25	0.31	0.34	0.03
Hf/Zr	0.033	0.032	0.050	0.026
Ta	1.26	1.33	0.10	0.00
Pb	0.42	2.96	37.1	1.71
Th	0.29	1.23	0.00	0.00
U	0.06	0.72	0.16	0.03

■ **Tab. 10.** XRF and ICP-MS (numbers in italics) analyses of ultrabasic rocks from the serpentinite body at Zöblitz, GEU of the Saxonian Erzgebirge, given by Massonne and Bautsch (2004).

ultrabasic body interacted with melts, which originated in the adjacent felsic gneisses. Perhaps the aforementioned delamination process, which involved crustal material and produced the

saidenbachitic melts, could also be responsible for the crustal zircons found by Liati and Gebauer (2009) in the Zöblitz ultrabasic body.

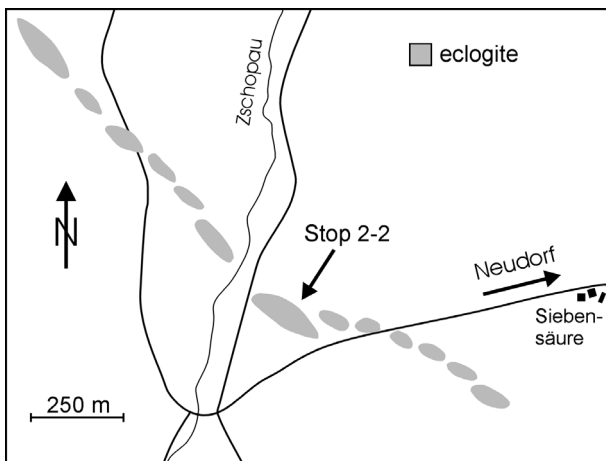
Stop 2-2 (Day 2). Eclogite at Siebensäure

Coordinates: N50°28'37.1" E12°56'18.7"

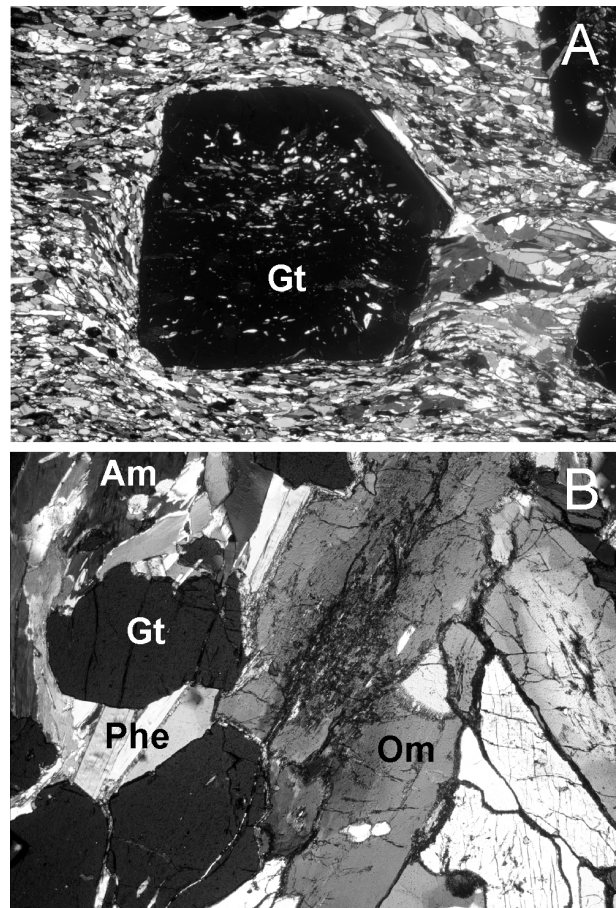
From the serpentinite quarry go back to Marienberg and continue via federal road B171 to the town of Wolkenstein to meet with federal road B101. Follow this road to the town of Annaberg-Buchholz. At the southern town exit leave B101 heading for the villages of Cranzahl and Neudorf. In the centre of Neudorf turn to the right into a small paved road, just before crossing the railroad tracks of the operating museum train, heading for the Forsthaus (forester's house) at the site Siebensäure. Pass the Forsthaus and stop on a parking lot for hikers. Walk for about 500 m in westerly direction and then move into the forest where cliffs expose eclogite and country rock (see Fig. 26).

The cliffs in the forest nearest to the road are orthogneisses, whereas those further north consist of eclogite, which is either a single, elongated lens or, as shown on the map (Fig. 26), a number of smaller lenses. These lenses are situated in the MEU only a few kilometres west of the boundary with the GEU (Fig. 2). The eclogite here is foliated and fine-grained. Strongly deformed portions contain mm-sized garnet embedded in a matrix of small oriented crystals, mainly of epidote and amphibole (Fig. 27A). In coarser-grained portions, cm-scale portions an earlier fabric is preserved, in which mm-sized garnet and omphacite occur with relatively large phengite grains (Fig. 27B). Epidote and amphibole are also present in the coarser-grained portions, where amphibole appears to replace omphacite.

Omphacite and garnet in the non-foliated rock portions of eclogite 18342 are strongly chemically zoned (Fig. 28, Table 11). The latter mineral, independent of its occurrence in deformed and non-deformed domains, shows prograde zoning with significantly decreasing Mn and increasing Mg contents from core to



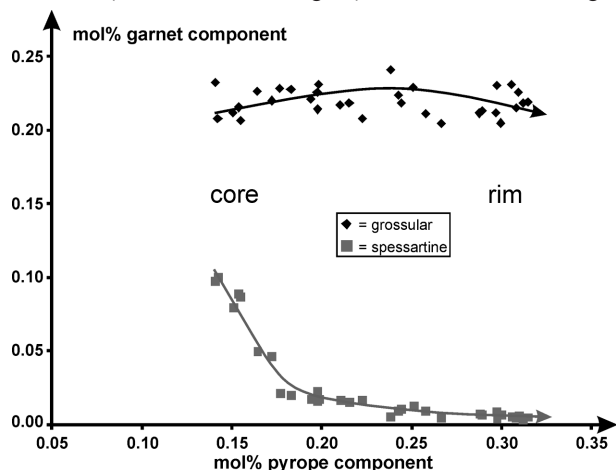
■ **Fig. 26.** Simplified geological map showing the occurrence of eclogite bodies in an area of the MEU in the Saxonian Erzgebirge a few kilometres west of the village of Neudorf, which is located south of the town of Annaberg-Buchholz. These bodies are shown as mapped by Sauer (1884).



■ **Fig. 27.** Photomicrographs of eclogite sample 18342, taken from a cliff west of the forester's house at the Siebensäure site (stop 2-2). Image widths are 4 mm each. (A) Large garnet, seen under crossed polarizers, in a foliated matrix consisting mainly of amphibole and clinzoisite. The many inclusions in garnet are mainly quartz and rutile. (B) A preserved portion of palaeocrysts, especially of omphacite, under crossed polarizers. The dirty rims of omphacite are due to a late replacement by fine-grained symplectites of amphibole + plagioclase.

rim. Phengite in non-foliated domains has Si contents between 3.3 and 3.5 pfu (see Table 11) and exhibits gradational zoning.

On the basis of a calculated P-T pseudosection for eclogite 18342, a P-T path was deduced for the prograde metamorphic evolution (Massonne, 2011b; Fig. 29) that is similar to that sug-



■ Fig. 28. Analyses of garnet in eclogite sample 18342 (stop 2-2) in terms of molar fractions of pyrope, grossular and spessartine components, taken from Massonne (2011b). Trend lines show the compositional change from core to rim of garnet.

gested by Massonne and Bausch (2004). These authors estimated 2.4 GPa and 500 °C for an early metamorphic stage and 2.6 GPa and 650 °C for the peak stage. In a similar way, Massonne and Kopp (2005) derived a nearly identical P-T path for an eclogite from the cliffs of the Stümpelfelsen, ca. 5 km SE of stop 2-2. All three prograde P-T paths typically show nearly isobaric heating at 2.6 ± 0.2 GPa, reaching maximum temperatures between 650 °C and 720 °C. Such P-T conditions are slightly higher than those proposed by Schmädicke et al. (2002) for eclogites from the western Erzgebirge.

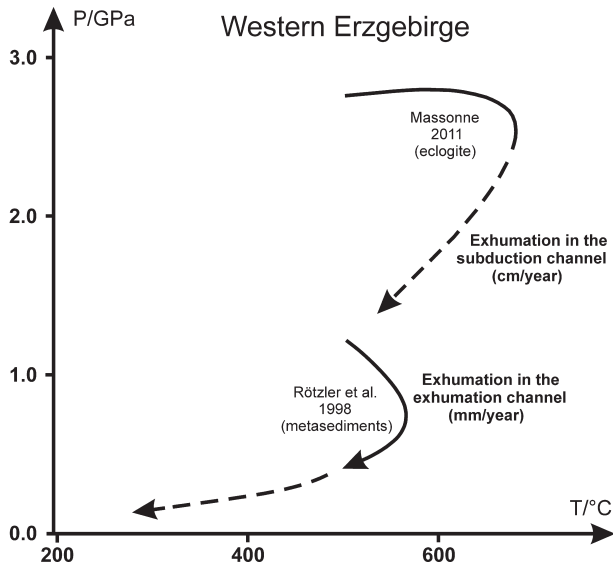
The retrograde path is characterized by cooling within the eclogite facies P-T field (see Fig. 29). During the retrograde evolution and possible beginning at peak temperature conditions either porphyroblasts (Stümpelfelsen eclogite; Massonne and Kopp, 2005) or fine-grained, oriented epidote and barroisitic amphibole (Table 11) formed. Paragonite (Table 11) is a late phase (Massonne and Kopp, 2005) that possibly grew at the expense of amphibole. Eclogite of stop 2-2 has a MORB-type chemical composition (Table 2) virtually identical to that of the Stümpelfelsen eclogite, where Massonne and Kopp (2005) found talc. Although this phase was likely present in the early prograde evolution stage of eclogite of stop 2-2, the absence of talc may be due to pervasive deformation during the retrograde evolution.

The mineralogical evolution of eclogite during its prograde and retrograde P-T path is the result of (1) a subduction of oce-

Mineral	garnet inner core	garnet outer rim	omphacite core	omphacite rim	phengite core	phengite rim	paragonite	amphibole	epidote early	epidote blast
Anal. No.	230402	230414	230429	230435	2304112	2304102	2304114	230437	230440	230420
SiO ₂	37.93	39.32	55.93	56.65	52.97	51.04	47.61	51.36	38.71	39.21
TiO ₂	0.13	0.02	0.02	0.03	0.22	0.24	0.09	0.10	0.12	0.04
Al ₂ O ₃	20.86	22.12	9.29	10.37	25.86	27.85	38.92	9.59	28.89	31.63
Cr ₂ O ₃	0.04	0.04	0.02	0.01	0.00	0.00	0.00	0.01	0.06	0.05
FeO _{tot}	26.08	22.88	6.09	3.253	1.38	1.72	0.37	11.15	5.72	1.87
MnO	4.46	0.25	0.00	0.00	0.00	0.00	0.00	0.11	0.00	0.03
MgO	3.66	8.24	8.57	9.62	4.66	3.77	0.33	13.57	0.12	0.04
CaO	8.42	8.67	13.63	14.36	0.01	0.03	0.21	7.66	23.88	24.42
Na ₂ O	0.03	0.00	7.15	6.69	0.53	0.88	6.93	4.36	0.02	0.00
K ₂ O			0.00	0.01	10.73	10.40	1.17	0.13		
BaO					0.16	0.12	0.02	0.00		
Total	101.63	101.53	100.69	100.99	96.52	96.05	95.63	98.04	97.52	97.30
Si	5.857	5.868	1.976	1.982	6.949	6.752	6.061	7.227	2.993	3.005
Ti	0.015	0.002	0.000	0.001	0.022	0.024	0.008	0.010	0.007	0.002
Al	3.797	3.890	0.387	0.428	3.998	4.342	5.839	1.590	2.632	2.858
Cr	0.004	0.004	0.001	0.000	0.000	0.000	0.000	0.002	0.004	0.003
Fe	3.368	2.855	0.180	0.095	0.151	0.190	0.039	1.312	0.370	0.120
Mn	0.584	0.031	0.000	0.000	0.000	0.000	0.000	0.013	0.000	0.002
Mg	0.844	1.834	0.451	0.502	0.910	0.744	0.062	2.846	0.014	0.005
Ca	1.394	1.386	0.516	0.538	0.002	0.004	0.028	1.155	1.978	2.006
Na	0.010	0.000	0.490	0.454	0.136	0.227	1.710	1.189	0.003	0.000
K			0.000	0.001	1.796	1.755	0.190	0.023		
Ba					0.008	0.006	0.001	0.000		

■ Tab. 11. Analyses with the wave-length dispersive systems of a CAMECA SX100 electron microprobe (in wt.%) of minerals in eclogite sample 18342 (previously called E22h) from stop 2-2. Structural formulae were calculated as given in Table 1 and as follows: epidote - 25 valencies. Contents of F were below the detection limit.

anic crust (see MORB signature of eclogites from the MEU; Massonne and Czambor, 2007), (2) lateral mass flow towards the hot wall of the subduction channel (isobaric heating), and (3) exhumation within the subduction channel. The hydrous fluid necessary to transform omphacite to clinozoisite and amphibole during exhumation could have originated by dehydration of



■ **Fig. 29.** P-T evolution of HP rocks from the MEU of the western Erzgebirge. The P-T conditions of the solid paths were derived from eclogite (Massonne, 2011b; see also text) and surrounding metasediments (Rötzler et al., 1998). Broken lines refer to not well-constrained exhumation paths. According to Massonne (2011b), exhumation either occurred in a subduction channel or was mainly due to surface erosion of a rather mountainous area, after continent-continent collision. The latter process led to exhumation rates in the mm-range.

the oceanic crust (garnet formation) in the downgoing portion of this crust close to the subduction channel (Massonne, 2011b).

The above P-T path and scenario for eclogite of the western Erzgebirge (Massonne and Kopp, 2005; Massonne, 2011b) and associated lenses of marbles (Gross et al., 2008) are clearly different from those of the Saidenbach eclogites, as outlined above. As previously recognized by Massonne (2004), rocks from two different (near)UHP environments exist, which are also exposed in the Saxonian Erzgebirge.

The country rocks, in which the eclogite of stop 2-2 is embedded, can be seen by walking to the nearby Zschopau creek (see map of Fig. 26), where pebbles mainly of mica-schist with mm-sized garnets occur. This phengite-rich rock commonly contains chloritoid. Rötzler et al. (1998) estimated for the mica-schist pressures of 12 kbar and more and temperatures around 525°C for the pressure climax, and 8 kbar and 560°C for the subsequent temperature peak (Fig. 29). These P-T results differ significantly from those derived for the adjacent eclogites. Willner et al. (2000, 2002) explained this pressure contrast by a model involving rapid exhumation of high-pressure rocks from the root zone of a collisional orogen. It remains unknown whether the low-temperature eclogites of the western Erzgebirge were metamorphosed at the same time as those of the central Erzgebirge. Schmädicke et al. (1995) determined ages as old as 355 Ma for eclogites from the western Erzgebirge and $^{40}\text{Ar}/^{39}\text{Ar}$ ages older than 340 Ma were reported by Werner and Lippolt (2000).

Granite-like segregations at the contact between eclogite and country rock are another interesting feature in the outcrop of stop 2-2. The composition of this granitoid is characterized by high Na_2O (>10 wt.%, see Massonne and Bausch, 2004) and, thus, high plagioclase contents. The reason for the formation of these melts remains unclear. One possibility is shear-heating when eclogite and metapelite were tectonically juxtaposed (see also Fig. 29).

Walk back to the parking lot near the forester's house and go back to Neudorf. Turn to the right when meeting with the main road. After 5 km turn to the right and follow national route B95 to the ski resort of Oberwiesenthal. South of this village, cross the border to the Czech Republic.

Acknowledgements

Allen Kennedy (Perth, Western Australia) and Thomas Theye (Stuttgart) are thanked for their support of SHRIMP and EMP work resulting in new data included in this guidebook. Gordon Medaris (Madison, Wisconsin) reviewed the manuscript. His suggestions and comments were highly appreciated.

References

- BEHN M.D., KELEMEN P.B., HIRTH G., HACKER B.R. and MASSONNE H.-J., 2011. Diapirs as the source of the sediment signature in arc lavas. *Nature Geosc.*, in press.
- BOYNTON W.V., 1984. Geochemistry of the rare earth elements: meteorite studies. In: P. HENDERSEN (Editor), Rare earth element geochemistry. Elsevier, Amsterdam, pp. 63-114.
- BRANDELIK A. and MASSONNE H.-J., 2004. PTGIBBS - an EXCEL™ Visual Basic program for computing and visualizing thermodynamic functions and equilibria of rock-forming minerals. *Comp. Geosci.*, 30: 909-923.
- CONNOLLY J.A.D., 2005. Computation of phase equilibria by linear programming: a tool for geodynamic modeling and its application to subduction zone decarbonation. *Earth Planet. Sci. Lett.*, 236: 524-541.
- DOBRZHINETSKAYA L.F., GREEN H.W., WESCHLER M., DARUS M., WANG Y.-C., MASSONNE H.-J. and STÖCKHERT B., 2003. Focused ion beam and transmission electron microscope study of microdiamonds from the

- Saxonian Erzgebirge, Germany. *Earth Planet. Sci. Lett.*, 210: 399-410.
- DOBZHINETSAYA L.F., LIU Z., CARTIGNY P., ZHANG J., TCHKHETIA N.N., GREEN H.W.II and HEMLEY R.J., 2006. Synchrotron infrared and Raman spectroscopy of microdiamonds from Erzgebirge, Germany. *Earth Planet. Sci. Lett.*, 248: 340-349.
- DÜFFELS K. and MASSONNE H.-J., 2001. Geochemical signatures of diamondiferous gneisses and their adjacent rocks from the Erzgebirge, Germany. *Terra Nostra*, 5/2001: 24-26.
- ELLIS D.J. and GREEN D.H., 1979. An experimental study of the effect of Ca upon garnet-clinopyroxene Fe-Mg exchange equilibria. *Contrib. Mineral. Petrol.*, 71: 13-22.
- GREEN H.W.II, DOBZHINETSAYA L., RIGGS E.M. and JIN Z.-M., 1997. Alpe Arami: a peridotite massif from the mantle transition zone? *Tectonophys.*, 279:1-21.
- GROSS J., BURCHARD M., SCHERTL H.-P. and MARESCH W.V., 2008. Common high-pressure metamorphic history of eclogite lenses and surrounding metasediments: a case study of calc-silicate reaction zones (Erzgebirge, Germany). *Eur. J. Mineral.*, 20:757-775.
- HAZARD J., 1884. Geologische Spezialkarte des Königreichs Sachsen No. 129. Section Zöblitz. Königliches Finanz-Ministerium (ed.) under the supervision of Credner, H.
- HAZARD J., 1886. Geologische Spezialkarte des Königreichs Sachsen No. 116. Section Pockau-Lengefeld. Königliches Finanz-Ministerium (ed.) under the supervision of Credner, H.
- HWANG S.-L., SHEN P., CHU H.-T. and YUI T.-F., 2000. Nanometer-size α -PbO₂-type TiO₂ in garnet: a thermobarometer for ultrahigh-pressure metamorphism. *Science*, 288: 321-324.
- HWANG S.-L., SHEN P., CHU H.-T., YUI T.-F. and LIN C.-C., 2001. Genesis of microdiamonds from melt and associated multiphase inclusions in garnet of ultrahigh-pressure gneiss from Erzgebirge, Germany. *Earth Planet. Sci. Lett.*, 188: 9-15.
- HWANG S.-L., CHU H.-T., YUI T.-F., SHEN P., SCHERTL H.-P., LIOU J.G. and SOBOLEV N.V., 2006. Nanometer-size P/K-rich silica glass (former melt) inclusions in microdiamond from the gneisses of Kokchetav and Erzgebirge massifs: Diversified characteristics of the formation media of metamorphic microdiamond in UHP rocks due to host-rock buffering. *Earth Planet. Sci. Lett.*, 243: 94-106.
- KRÖNER A. and WILLNER A.P., 1998. Time of formation and peak of Variscan HP-HT metamorphism of quartz-feldspar rocks in the central Erzgebirge, Saxony, Germany. *Contrib. Mineral. Petrol.*, 132:1-20.
- LEECH M.L., 2001. Arrested orogenic development: eclogitization, delamination, and tectonic collapse. *Earth Planet. Sci. Lett.*, 185: 149-159.
- LIATI A. and GEBAUER D., 2009. Crustal origin of zircon in a garnet peridotite: a study of U-Pb SHRIMP dating, mineral inclusions and REE geochemistry (Erzgebirge, Bohemian Massif). *Eur. J. Mineral.*, 21:737-750.
- LINNEMANN U., GEHMLICH M., TICHOMIROVA M., BUSCHMANN B., NASDALA L., JONAS P., LÜTZNER H. and BOMBACH K., 2000. From Cadomian subduction to Early Palaeozoic rifting: the evolution of Saxo-Thuringia at the margin of Gondwana in the light of single zircon geochronology and basin development (Central European Variscides, Germany). In: W. FRANKE, V. HAAK, O. ONCKEN, O. and D. TANNER (Editors), *Orogenic Processes: Quantification and Modelling in the Variscan Belt*. Geol. Soc. London, Spec. Publ., 179, pp. 131-153.
- MASSONNE H.-J., 1992. Thermochemical determination of water activities relevant to eclogitic rocks. In: Y.K. KHARAKA and A.S. MAEST (Editors), *Water-Rock Interaction. Proc. 7th Int. Symp.*, Park City, Utah: Rotterdam, Balkema, pp. 1523-1526.
- MASSONNE H.-J., 1994. P-T evolution of eclogite lenses in the crystalline complex of the Erzgebirge, Middle Europe: An example for high-pressure to ultrahigh-pressure metabasites incorporated into continental crust. 1st Workshop UHP metamorphism and tectonics, Abstr. Vol.: 29-32.
- MASSONNE H.-J., 1999. A new occurrence of microdiamonds in quartzofeldspathic rocks of the Saxonian Erzgebirge, Germany, and their metamorphic evolution. Proc. 7th Int. Kimberlite Conf., Cape Town 1998, P.H. Nixon Vol., pp. 533-539.
- MASSONNE H.-J., 2001. First find of coesite in the ultrahigh-pressure metamorphic region of the Central Erzgebirge, Germany. *Eur. J. Mineral.*, 13: 565-570.
- MASSONNE H.-J., 2003. A comparison of the evolution of diamondiferous quartz-rich rocks from the Saxonian Erzgebirge and the Kokchetav Massif: are so-called diamondiferous gneisses magmatic rocks? *Earth Planet. Sci. Lett.*, 216: 345-362.
- MASSONNE H.-J., 2004. Ultra high pressure metamorphism. In: R.C. SELLEY, L.R.M. COCKS and I.R. PLIMER (Editors), *Encyclopedia of Geology*, 5, pp. 533-540.
- MASSONNE H.-J., 2005. Involvement of crustal material in delamination of the lithosphere after continent-continent collision. *Int. Geol. Rev.*, 47: 792-804.
- MASSONNE H.-J., 2011a. Phase relations of siliceous marbles at ultrahigh pressure based on thermodynamic calculations: Examples from the Kokchetav massif, Kazakhstan, and the Sulu terrane, China. *Geol. J.*, Special Issue: "Extreme Metamorphism and Continental Dynamics" (Guest editors: M. Santosh, K. Sajeev and T. Tsunogae), 64: 114-125.
- MASSONNE H.-J., 2011b. Formation of amphibole and clinozoisite-epidote during exhumation of eclogite in a subduction channel. *J. Petrol.*, submitted.
- MASSONNE H.-J., GROSCH U. and WILLNER A., 1993. Geothermobarometrie mittels Ti-Gehalten in Kalihellglimmern. *Ber. Dt. Mineral. Ges., Beih. Eur. J. Mineral.*, 5: No. 1, 85.
- MASSONNE H.-J. and GROSCH U., 1995. P-T evolution of Palaeozoic garnet peridotites from the Saxonian Erzgebirge and the Åheim region, Norway. 6th Int. Kimberlite Conf., Novosibirsk, Abstr. Vol., 353-355.
- MASSONNE H.-J., BERNHARDT H.J., DETTMAR D., KESSLER E., MEDENBACH O. and WESTPHAL T., 1998. Simple identification and quantification of microdiamonds in rock thin-sections. *Eur. J. Mineral.*, 10: 497-504.
- MASSONNE H.-J. and BURCHARD M. 2000. Exotic minerals in eclogites from the Central Erzgebirge—evidence for fluid-

- rock interaction at UH metamorphic pressures. *Ber. Dt. Mineral. Ges., Beih. Eur. J. Mineral.*, 12: No. 1, 122.
- MASSONNE H.-J., DOBRZHINETSKAYA L. and GREEN H.W.II, 2000. Quartz - K-feldspar intergrowths enclosed in eclogitic garnet and omphacite. Are they pseudomorphs after coesite? Ext. Abstract, 31st Int. Geol. Congr. Rio de Janeiro, Brazil, 4 pp. (on CD, search for Massone).
- MASSONNE H.-J. and NASDALA L., 2003. Characterization of an early metamorphic stage through inclusions in zircon of a diamondiferous quartzofeldspathic rock from the Erzgebirge, Germany. *Am. Mineral.*, 88: 883-889.
- MASSONNE H.-J. and O'BRIEN P.J., 2003. The Bohemian Massif and the NW Himalaya. In: D.A. CARSWELL and R. COMPAGNONI (Editors), *Ultrahigh Pressure Metamorphism*. EMU Notes in Mineralogy 5, pp. 145-187.
- MASSONNE H.-J. and BAUTSCH H.-J., 2004. Ultrahigh and high pressure rocks of Saxony. *Field Trip Guide Books*, 32nd Int. Geol. Congress, Florence, Italy, Vol. 2, B21, 36 pp.
- MASSONNE H.-J. and KOPP J., 2005. A low-variance mineral assemblage with talc and phengite in an eclogite from the Saxonian Erzgebirge, central Europe, and its P-T evolution. *J. Petrol.*, 46:355-375.
- MASSONNE H.-J. and NEUSER R.D., 2005. Ilmenite exsolution in olivine from the serpentinite body at Zöblitz, Saxonian Erzgebirge - microstructural evidence using EBSD. *Min. Mag.*, 69: 119-124.
- MASSONNE H.-J. and CZAMBOR A., 2007. Geochemical signatures of Variscan eclogites from the Saxonian Erzgebirge, central Europe. *Geochem. (Chem. Erde)*, 67: 69-83.
- MASSONNE H.-J., KENNEDY A., NASDALA L. and THEYE T., 2007. Dating of zircon and monazite from diamondiferous quartzofeldspathic rocks of the Saxonian Erzgebirge. *Min. Mag.*, 71: 407-425.
- MASSONNE H.-J. and TU W., 2007. $\delta^{13}\text{C}$ -signature of early graphite and subsequently formed microdiamond from the Saxonian Erzgebirge, Germany. *Terra Nova*, 19: 476-480.
- MASSONNE H.-J. and TOULKERIDIS T., 2010. Widespread relics of high-pressure metamorphism confirm major terrane accretion in Ecuador: a new example from the Northern Andes. *Int. Geol. Rev.*, in press.
- MESCHEDÉ M., 1986. A method of discriminating between different types of mid-ocean ridge basalts and continental tholeiites with the Nb-Zr-Y diagram. *Chem. Geol.*, 56: 207-218.
- NASDALA L. and MASSONNE H.-J., 2000. Microdiamonds from the Saxonian Erzgebirge, Germany: *in situ* micro-Raman characterisation. *Eur. J. Mineral.*, 12: 495-498.
- O'BRIEN P.J. and ZIEMANN M.A., 2008. Preservation of coesite in exhumed eclogite: insights from Raman mapping. *Eur. J. Mineral.*, 20: 827-834.
- RÖTZLER K., SCHUMACHER R., MARESCH W.V. and WILLNER A.P., 1998. Characterization and geodynamic implications of contrasting metamorphic evolution in juxtaposed high-pressure units of the Western Erzgebirge (Saxony, Germany). *Eur. J. Mineral.*, 10: 261-280.
- ROMER R.L. and RÖTZLER J., 2001. P-T-t evolution of ultrahigh-temperature granulites from the Saxon Granulite Massif, Germany. Part II: Geochronology. *J. Petrol.*, 42:2015-2032.
- SAUER A., 1884. Geologische Specialkarte des Königreichs Sachsen No. 147. Section Wiesenthal. Königliches Finanz-Ministerium (Ed.) under the supervision of CREDNER, H.
- SCHALCH F., 1879. Geologische Specialkarte des Königreichs Sachsen No. 128. Section Marienberg-Wolkenstein. Königliches Finanz-Ministerium (ed.) under the supervision of CREDNER, H.
- SCHMÄDICKE E., OKRUSCH M. and SCHMIDT W., 1992. Eclogite-facies rocks in the Saxonian Erzgebirge, Germany: high pressure metamorphism under contrasting P-T-conditions. *Contrib. Mineral. Petrol.*, 110: 226-241.
- SCHMÄDICKE E., COSCA M.A. and OKRUSCH M., 1995. Variscan Sm-Nd and Ar-Ar ages of eclogite facies rocks from the Erzgebirge, Bohemian Massif. *J. Metam. Geol.*, 13: 537-552.
- SCHMÄDICKE E. and EVANS B.W., 1997. Garnet-bearing ultramafic rocks from the Erzgebirge, and their relation to other settings in the Bohemian Massif. *Contrib. Mineral. Petrol.*, 127: 57-74.
- STÖCKHERT B., DUYSSTER J., TREPMANN C. and MASSONNE H.-J., 2001. Microdiamond daughter crystals precipitated from supercritical COH silicate fluids included in garnet, Erzgebirge, Germany. *Geology*, 29: 391-394.
- STÖCKHERT B., TREPMANN C. and MASSONNE H.-J., 2009. Decrepitated UHP fluid inclusions: About diverse phase assemblages and extreme decompression rates (Erzgebirge, Germany). *J. Metam. Geol.*, 27: 673-684.
- TICHOMIROVA M., 2003. Die Gneise des Erzgebirges – hochmetamorphe Äquivalente von neoproterozoisch – frühpaläozoischen Grauwacken und Granitoiden der Cadomiden. *Freiberger Forschungshefte*, C495, 222 pp.
- TICHOMIROVA M., WHITEHOUSE M.J. and NASDALA L., 2005. Resorption, growth, solid state recrystallisation, and annealing of granulite facies zircon – a case study from the Central Erzgebirge, Bohemian Massif. *Lithos*, 82: 25-50.
- TOMKINS H.S., POWELL R. and ELLIS D.J., 2007. The pressure dependence of the zirconium-in-rutile thermometer. *J. Metam. Geol.*, 25: 703-713.
- WERNER O. and LIPPOLT H.J., 2000. White mica $^{40}\text{Ar}/^{39}\text{Ar}$ ages of Erzgebirge metamorphic rocks: simulating the chronological results by a model of Variscan crustal imbrication. In: W. FRANKE, V. HAAK, O. ONCKEN and D. TANNER (Editors), *Orogenic Processes: Quantification and Modelling in the Variscan Belt*. Geol. Soc. London Spec. Publ. 179, pp. 323-336.
- WHITE R.W., POWELL R. and HOLLAND T.J.B., 2001. Calculation of partial melting equilibria in the system $\text{Na}_2\text{O}-\text{CaO}-\text{K}_2\text{O}-\text{FeO}-\text{MgO}-\text{Al}_2\text{O}_3-\text{SiO}_2-\text{H}_2\text{O}$ (NCKFMASH). *J. Metam. Geol.*, 19: 139-153.
- WILLNER A.P., RÖTZLER K. and MARESCH W.V., 1997. Pressure-temperature and fluid evolution of quartzofeldspathic metamorphic rocks with a relic high-pressure, granulite-facies history from the Central Erzgebirge (Saxony, Germany). *J. Petrol.*, 38: 307-336.
- WILLNER A.P., KROHE A. and MARESCH W.V., 2000. Interrelated P-T-t paths in the Variscan Erzgebirge dome (Saxony, Germany): Constraints on the rapid exhumation of high-

- pressure rocks from the root zone of a collisional orogen. *Int. Geol. Rev.*, 42: 64-85.
- WILLNER A.P., SEBAZUNGU E., GERYA T.V., MARESCH W.V. and KROHE A., 2002. Numerical modelling of PT-paths related to rapid exhumation of high-pressure rocks from the crustal root in the Variscan Erzgebirge Dome (Saxony/Germany). *J. Geodyn.*, 33: 281-314.
- ZACK T. and LUVIZOTTOW G.L., 2006. Application of rutile thermometry to eclogites. *Mineral. Petrol.*, 88: 69-85.

Eclogites from the Czech Part of the Erzgebirge

Shah Wali FARYAD¹, J. KONOPÁSEK² and H. KLÁPOVÁ¹

¹ Institute of Petrology and Structural Geology, Charles University in Prague, Albertov 2, 128 43 Prague, Czech Republic

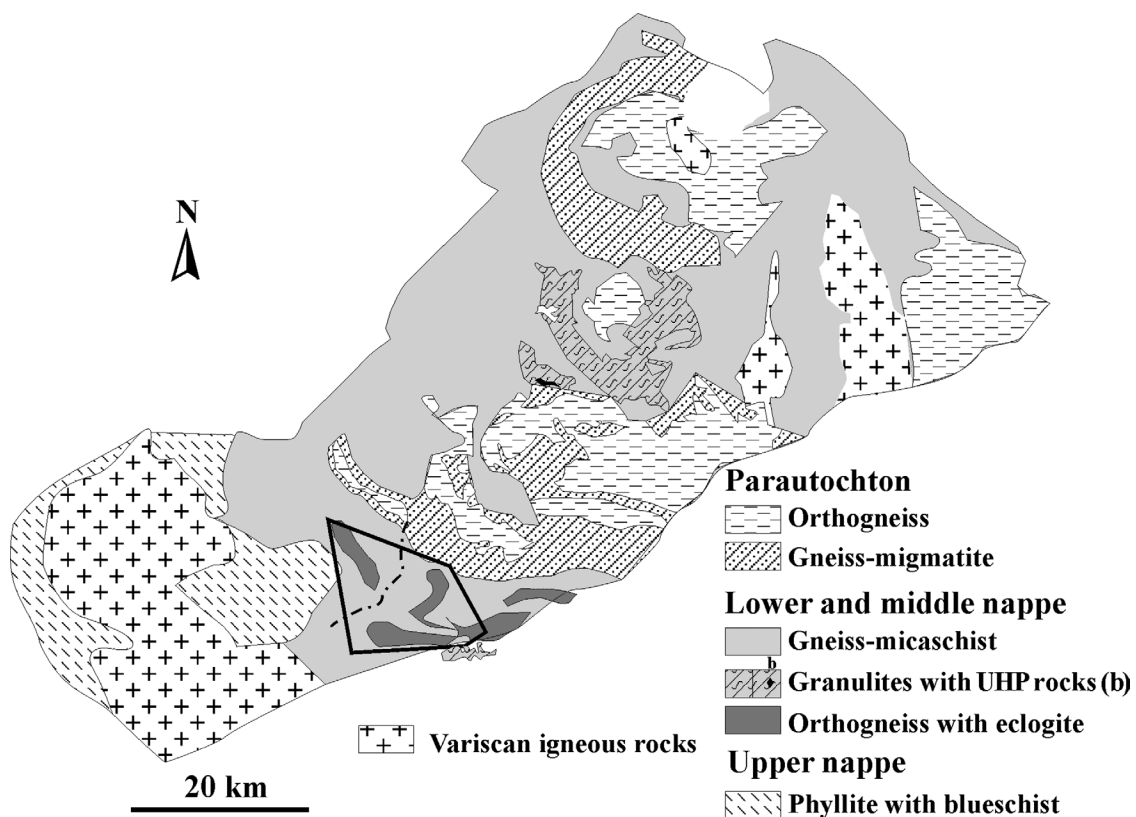
² Czech Geological Survey, Klárov 3, 118 21 Praha 1, Czech Republic

The Krušné Hory complex is formed by upper Proterozoic basement (the Saxothuringian parautochthon) and an overlying nappe stack (lower, middle, and upper nappes) with decreasing grade of metamorphism from bottom to top (Willner et al., 1997; Cháb et al., 2008). The parautochthon is exposed in several dome-like structures and consists of gneisses and migmatites with lenses of amphibolites. The St. Kateřina dome, in the Czech part of the Erzgebirge (Mlčoch and Schulmann, 1992), is formed by orthogneisses derived from an early Ordovician granite (Košler et al. 2004). They show medium-pressure amphibolite facies conditions with no signs of eclogite facies metamorphism (Konopásek, 1998).

The lower nappe is formed by gneisses with HP-UHP rocks (Schmädicke et al., 1992; Mingram, 1998; Rötzler et al., 1998; Willner et al., 1997; Gross 2008). In addition to coesite- and microdiamond-bearing gneisses, they contain lenses and boudins of eclogites and garnet and spinel peridotites. Age dating on zircon yielded 480 Ma for the igneous protholith of orthogneisses and 340 Ma for their metamorphism (Kröner and Willner, 1998; Massonne, 2007). Ages between 333 and 360 Ma for the thermal peak of metamorphism for HT eclogites and garnet peridotite were obtained from Sm-Nd mineral and whole-rock isochrons (Schmädicke et al., 1995).

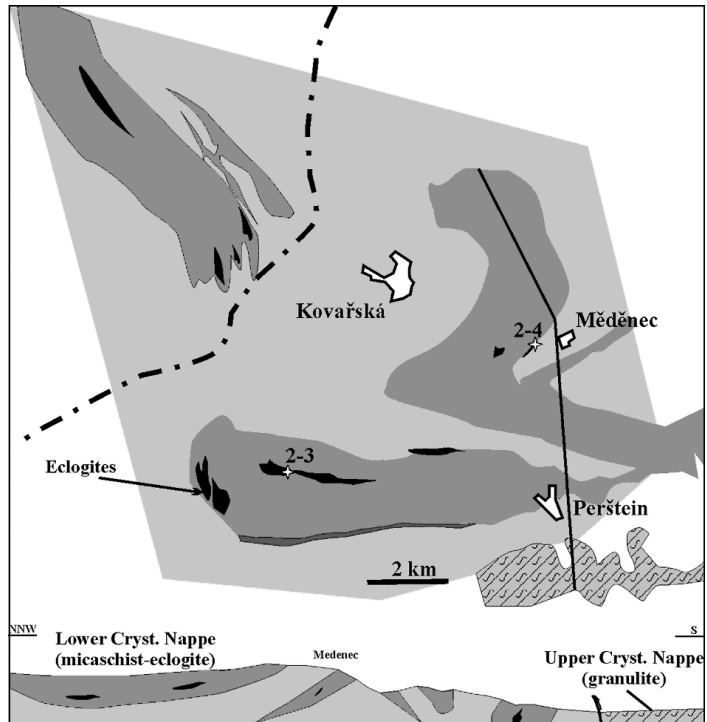
The middle nappe (Fig. 1) is represented by micaschists, gneisses, and lower Ordovician metarhyolite and metagranite (Mingram, 1998; Rötzler et al., 1998; Tichomirova et al., 2001). It contains lenses of eclogites, quartzites, and calc-silicate rocks. In the Czech part, orthogneisses with lenses of eclogites, quartzites and some calc-silicate rocks are present at the top of the middle nappe, above the micaschists. An early Ordovician protolith age for the orthogneisses was obtained by Košler et al. (2004). The micaschists also show HP-MT conditions (Konopásek, 1998; 2001).

The upper nappe is formed by lower-grade metasediments with volcanic material of Ordovician-Silurian age that are intruded by Variscan granite. The phyllitic rocks, which may contain garnet, are characterized by the presence of retrogressed blueschists, greenschists, quartzites, marbles, and calc-silicates. Relics of blueschist facies phases include crossite with epidote and albite (Holub and Souček, 1984).



■ Fig. 1. Simplified geological map of the Krušné Hory Mountains (Erzgebirge), after Cháb et al. (2008).

Alternatively, Konopásek et al. (2001) propose that metamorphic grade increases from bottom to top in the nappe stack. Based on the position of granulite at the Ohra River on the Czech side, they propose that the high-grade rocks overlie the medium grade (lower crystalline nappe, Fig. 2), and the blueschist facies phyllites are interpreted as part of the parautochthonous unit.



■ **Fig. 2.** Geological map of the central part of the Krušné hory Mts.; eclogite occurrences shown in black (Klápová et al. 1998; Konopásek et al. 2001). Numbers 2-3 and 2-4 are locations of excursion stops.

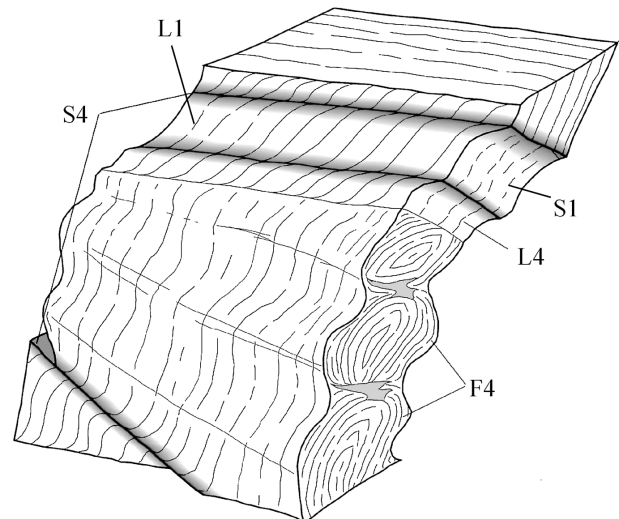
Stop 2-3 (Day 2). Eclogite, Meluzína

Coordinate N50°23'25.3" E13°00'21.9"

The Meluzína hill is a huge natural exposure of eclogite that forms an E–W elongated lens several kilometres in length and up to 250 m thick (Fig. 2). The strongly foliated, eclogite facies fabrics were formed by two deformation events, D1 and D2, which are both defined as syn-eclogitic (Klápová et al., 1998). In spite of two post-eclogitic deformations, D3 and D4, the eclogite is fresh and exhibits a well-developed foliation, S1, containing stretching and mineral lineations, L1 (Fig. 3). S1 is formed by the planar arrangement of platy minerals such as paragonite, phengite, and omphacite. A mineralogical layering characterised by alternations of garnet-rich and garnet-poor/omphacite-rich bands is also present. The late set (D3 and D4) of structures was developed under brittle-ductile conditions. These structures are represented mainly by asymmetrical intrafoliation boudinage, shear bands, and brittle cracks, which are filled by Qtz with Rt and Amp.

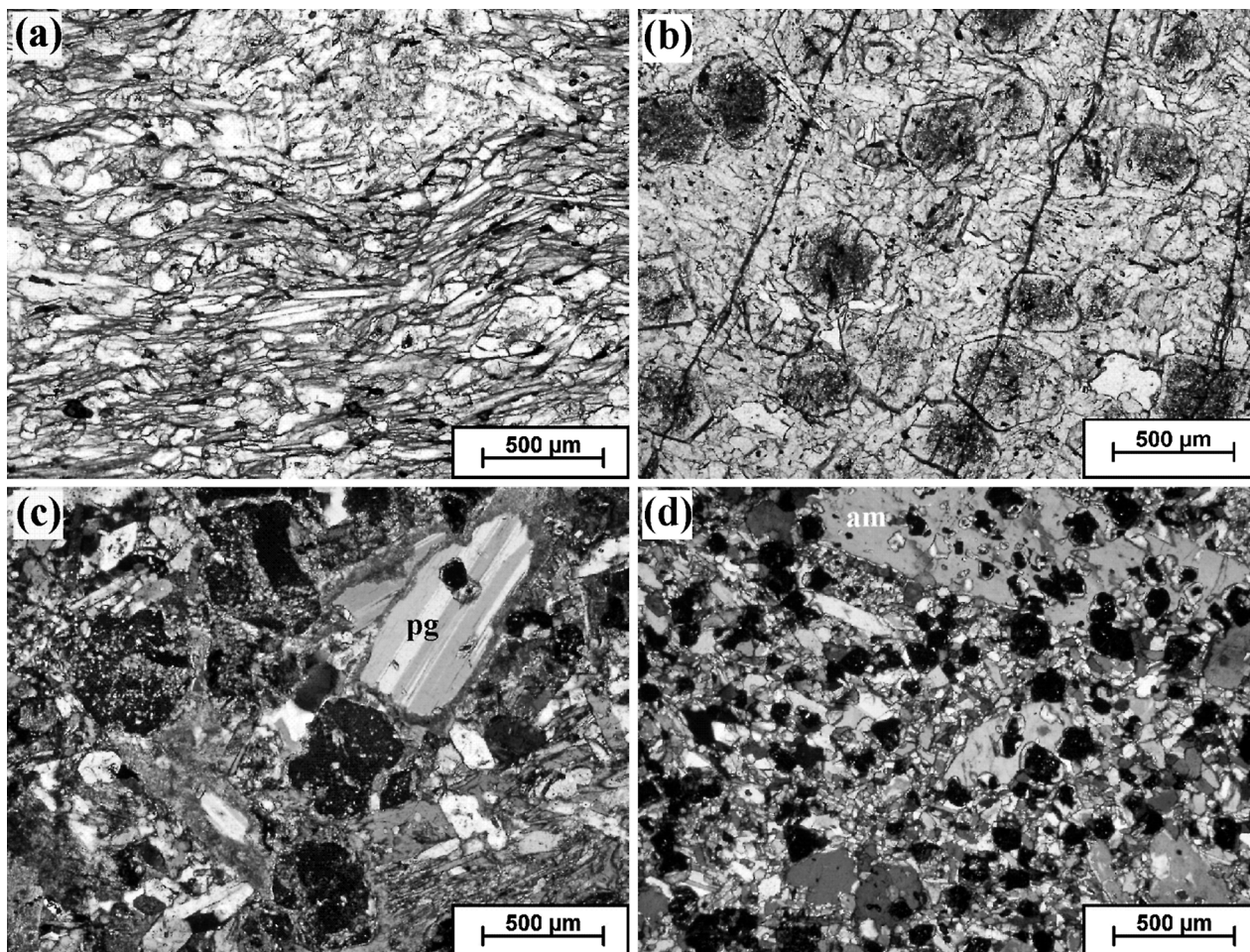
The eclogites have MORB composition (Klápová, 1990). U-Pb SHRIMP dating of 490 ± 14 Ma on zircon and single-zircon U-Pb dating of 342.5 ± 1.6 Ma are taken to be the ages of protolith and high-pressure metamorphism, respectively (von Quadt and Gebauer, 1998).

Based on their textures and mineral compositions, the Krušné hory eclogites can be subdivided into three types. The most frequent, dark-coloured, fine-grained type (type 1) has a layered structure, in which garnet-omphacite layers alternate with amphibole-rich layers. The garnet-omphacite layers may contain quartz, rarely also amphibole, paragonite, phengite, and epidote. Light-coloured, more coarse-grained eclogite (type 2) contains white lenses or discontinuous bands of epidote, sev-

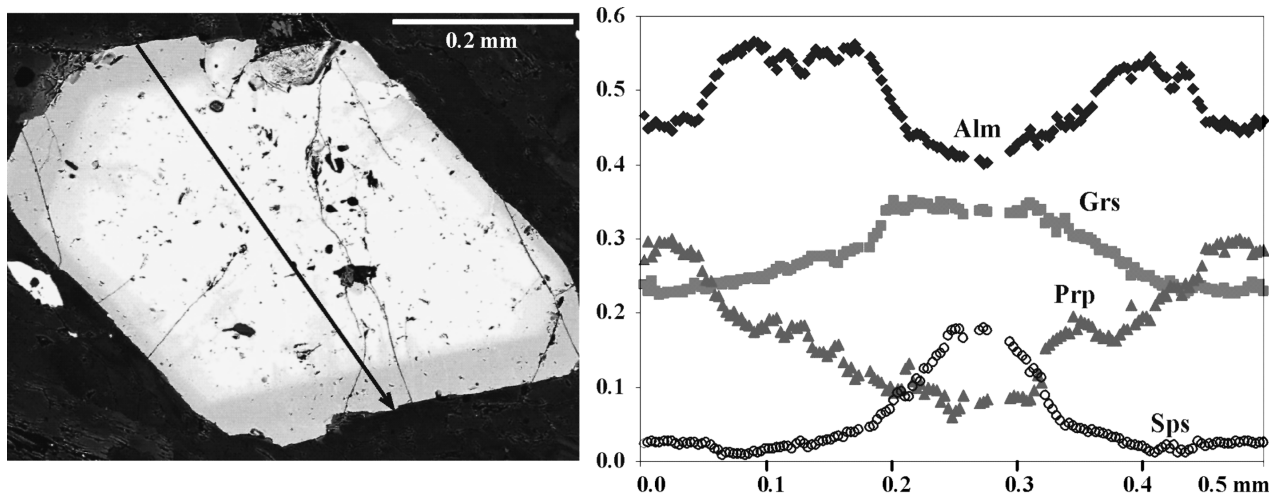


■ **Fig. 3.** Three-dimensional sketch of planar and linear structures in mafic eclogites at the Meluzína locality, central Erzgebirge (Klápová et al. 1998).

eral millimetres thick. It may also contain talc. Both types (1) and (2) show strong foliation, and there is a gradual transition between these two types. The last type (3) is unfoliated eclogite with a regular distribution of garnet and omphacite. It may contain eclogite facies carbonate minerals (Klápová, 1990).



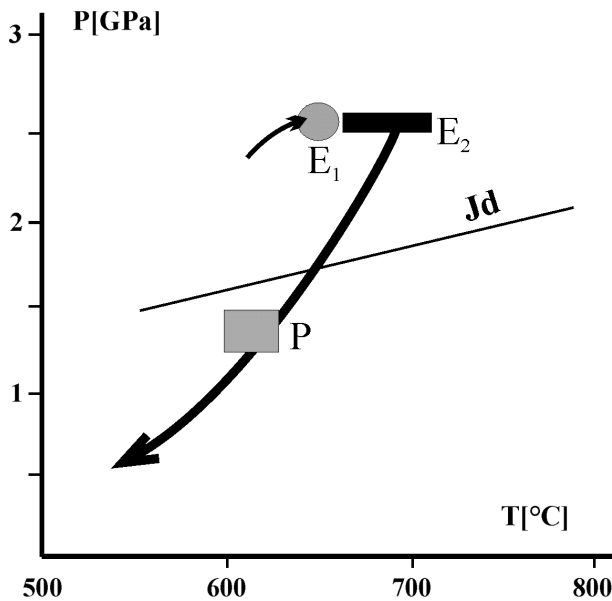
■ Fig. 4. Photomicrographs of textural varieties of eclogite from Meluzina hill (Krušné Hory complex). a and b- garnet in finegrained matrix with omphacite, paragonite and zoisite. c- paragonite rimmed by symplectites of albite + chlorite. d- barroisitic amphibole overgrowing eclogite facies minerals.



■ Fig. 5. Profile (rim to rim) of garnet showing compositional zoning in eclogite.

Omphacite comprises 30 to 50 vol% of eclogite and generally forms elongated crystals that follow foliation of the rock (Fig. 4a). Jadeite content mostly varies from 35 to 52 %. Gar-

net amounts to between 15 and 50 vol% and forms idioblastic crystals up to 2.5 mm in diameter. Garnet grains exhibit clouded, inclusion-rich cores and wide, euhedral, inclusion-free rims



■ **Fig. 6.** Estimated PT conditions for Variscan eclogite (E) in the Krušné Hory Complex (E₂ after Kláková et al. 1998). P indicates PT conditions of Pre-Variscan metamorphic event obtained for the parautochthonous metapelitic rocks (Konopásek 1998).

Stop 2-4 (Day 2). Eclogite, Měděnec

Coordinate N50°25'10.7" E13°06'38.8"

At the locality near Měděnec Village (Fig. 2), we will examine eclogite with a discrete zone that contains atoll garnet formed under eclogite facies conditions. Atoll garnets occur in several localities, but their relations to eclogites lacking atoll garnet are not always clear (Faryad et al., 2010). The presence of atoll garnet is not restricted to a specific rock type but occurs in a variety of metabasites, including quartz-rich types, which probably represent a mixture of mafic rocks and sediments. The eclogite consists of omphacite, garnet, quartz, and small amounts of rutile, amphibole, and albite ± phengite. When different size varieties are compared, it is found that atoll garnets occur mostly in the fine-grained varieties (see Fig. 7a). The atoll garnets consist of a garnet annulus surrounding quartz and/or amphibole. If the atolls are occupied by quartz, their interfaces are sharp and regular (Fig. 7b) and correlate with crystallographic planes of garnet. On the other hand, where amphibole overgrows the atoll, boundaries with the garnet ring are irregular.

Backscattered electron images and compositional profiles (Figs. 8) from whole garnet grains demonstrate that garnet cores (garnet I) and rims (garnet II) have different compositions. The core I, with idiomorphic outlines, has a higher Ca content and lower Fe content compared with its rim (II (Fig. 8a1). Garnet I shows prograde zoning with a decrease of Mn towards the rim. Figure 8b shows a whole garnet with a dark, Ca-rich core and a peninsula connected to the rim. The peninsula and the rim have similar image contrast and, hence, similar compositions (Fig. 8b1).

(Fig. 4b). They show prograde compositional zoning with an increase of Mg/Fe from cores to rims (Fig. 5). Paragonite is partly replaced by a symplectite of albite and chlorite (Fig. 4c). Amphibole ranges from 5 to 20 vol%, and it overgrows the eclogite facies foliation and minerals (Fig. 4d). Chemically, amphibole corresponds to barroisite and winchite. Epidote forms colourless, subhedral to euhedral, prismatic, frequently corroded crystals up to 5 mm in size. Its modal content varies between 5 and 10% in the light eclogite type.

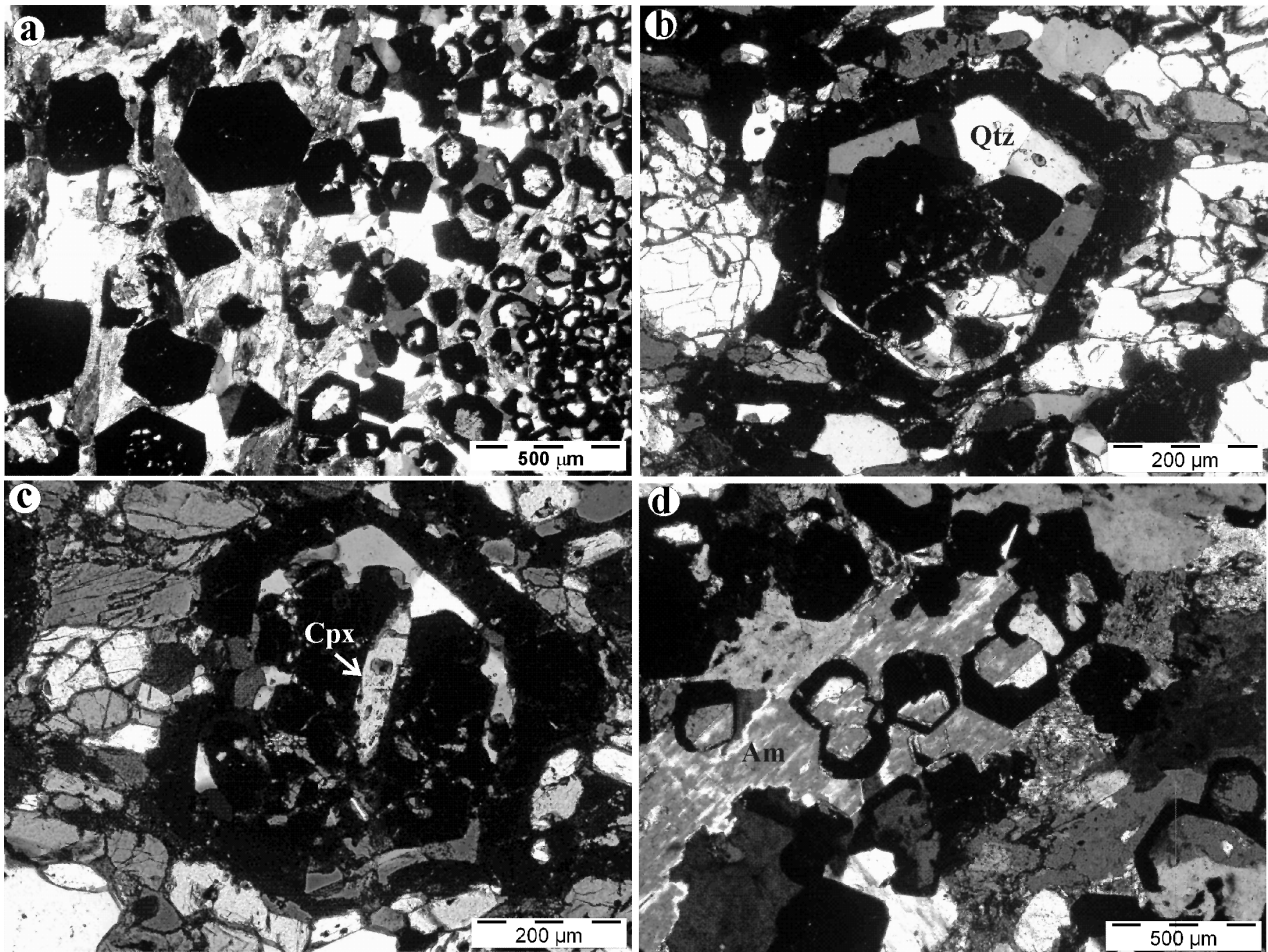
Metamorphic PT conditions

Temperatures and pressures estimated using the garnet-clinopyroxene Fe-Mg exchange thermometer (Ellis and Green, 1979; Ravna, 2000) and garnet-omphacite-phengite barometer (Ravna and Terry, 2004) are 600–650 °C and 2.5–2.6 GPa. Similar pressures were also obtained for eclogites by Kláková et al. (1998) and for micaschists by Konopásek (2001).

Figure 9a shows that the dark, low-Fe zone of garnet has microveins with a similar image contrast to that of the outermost rim of the garnet. These microveins connect garnet core I with the rim, but the core garnet shows a strong compositional gradient at the points of contact between sub-grains with Fe content. Compositional zoning of sub-grains and microveins in garnet I change by substitution of Fe and Mg, while Ca remains almost constant in garnet. Compared with the narrow white veins in the dark rim, sub-grains in the core are separated by wide grey zones and channels with larger Mg contents.

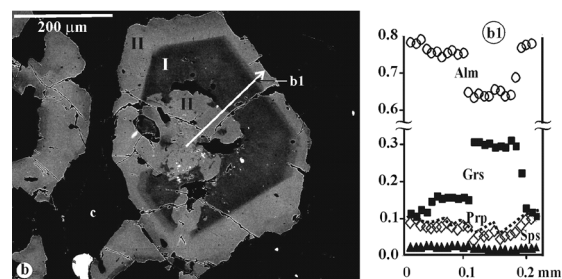
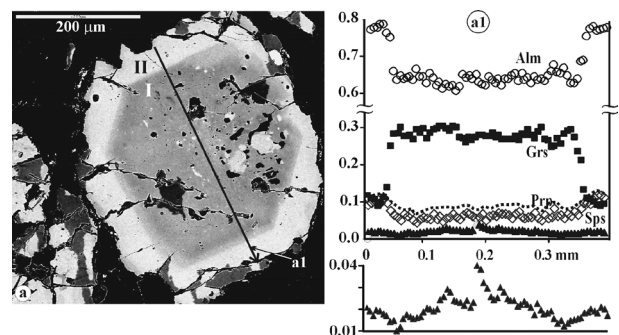
Formation of the atoll garnet is interpreted as resulting from fluid infiltration and element exchange between the garnet core and matrix, a process that was facilitated by temperature increase during eclogite facies metamorphism up to 600 °C/ 2.4 GPa (Fig. 10). In addition to fluid access, the primary textures, mainly grain size, were also effective for the atoll garnet formation. Small grain fractions with thin rims were easily infiltrated by fluid, which used the short distance for element exchange between core and matrix. The core garnet was gradually dissolved and replaced by new garnet having the same crystallographic orientation as the rim or relicts in the core.

If we assume equilibrium of the garnet rim with matrix omphacite, these results suggest that garnet growth continued after the peak of metamorphism, at least in a rock of effectively constant bulk composition. The fact that substantial growth of garnet II happened at a late stage is presumably related to the modification of the local reactive bulk compositions caused by



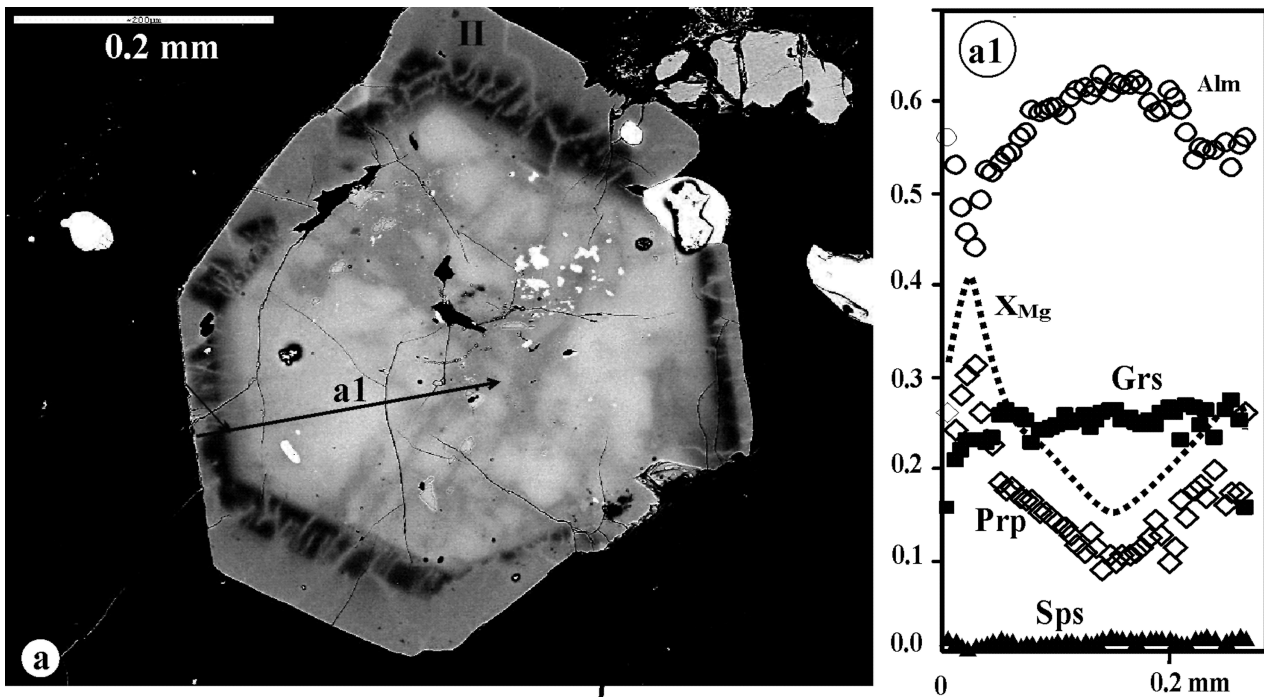
■ **Fig. 7.** Photomicrographs (crossed polarizers) of atoll garnet from eclogite with phengite and amphibole. (a) Contact between two layers with coarse-grained whole and fine-grained atoll garnets; the layers are parallel to foliation in the rock. (b) Present atoll rims with island cores separated by quartz, reflecting crystallographic control of garnet. (c) indicates an omphacite inclusion in the atoll core. (d) Amphibole crystal surrounding the atoll garnets has the same optical orientation as amphibole inside the atoll garnet.

■ **Fig. 8.** BSE images and compositional profiles from quartz eclogite (Faryad et al. 2010). Images (a) and (b) show whole garnets with idiomorphic cores (dark, garnet I) along with compositional profiles (a1 and b1). The dotted lines above the pyrope profiles in a1 and b1 indicate $X_{Mg} = Mg/(Mg+Fe)$ ratios in garnet. Note that there is a peninsula in the cores of (b) that has similar image contrast and compositions to that of the garnet rim II. The y axis in the compositional profiles represents the fractional garnet end-member compositions.

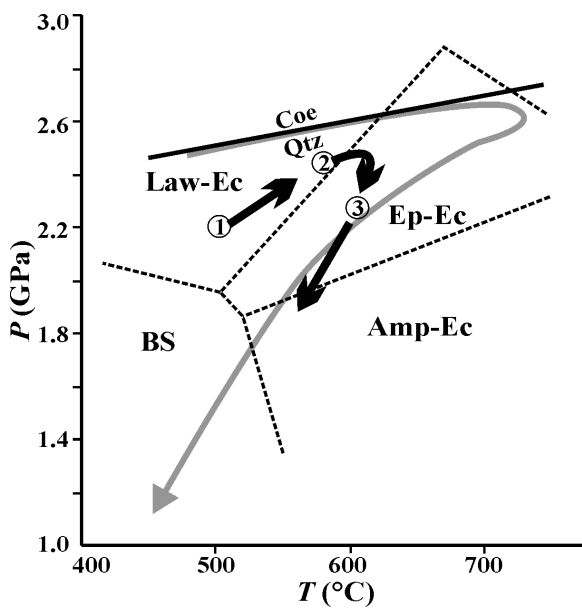


the fluid-assisted enlargement of diffusion domains to include previously inaccessible garnet cores.

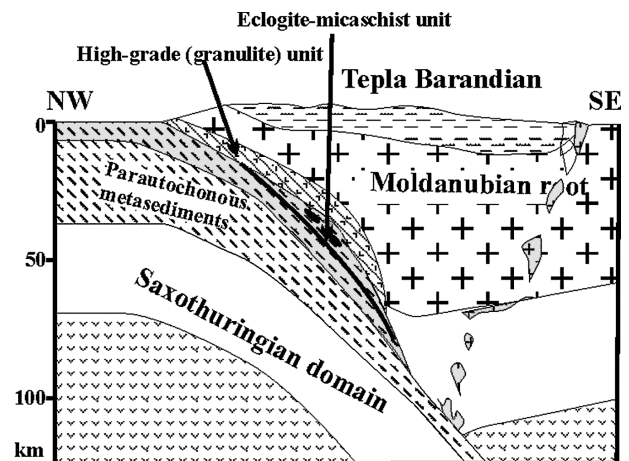
The common occurrence of Na-Ca amphibole of barroisite composition in the matrix with inclusions of omphacite and garnet in eclogites is good evidence for both pressure and temperature decrease during exhumation of the rocks. The retrograde P-T path crossing the amphibole eclogite/blueschist facies boundary was probably one of the reasons for preservation of eclogite facies minerals and textures in the Krušné Hory eclogite.



■ Fig. 9. BSE image and compositional profiles of garnet showing microveins, possibly related to fluid infiltration along narrow channels (veins) at? from? the rim of the garnet (a). The y axis in the compositional profiles (a₁) represents the fractional garnet end-member compositions.



■ Fig. 10. Inferred P-T conditions of atoll garnet in eclogites from the Krušné Hory Complex (Faryad et al. 2010), based on garnet/clinopyroxene thermometry (Ravna 2000; Ai 1994). Maximum pressure conditions are based on data (garnet-omphacite-phengite thermobarometry) from Klápová et al. (1998) and Massonne and Kopp (2005). The P-T path (grey line) is after Massonne and Kopp (2005). Numbers 1–3 correspond to the core (I, 1), the thin zone between the core and rim (2), and the rim or ring (II, 3) of atoll garnet formation (see Fig. 8). Metamorphic facies fields are after Okamoto and Maruyama (1999): BS, blueschist; Law-Ec, lawsonite eclogite; Ep-Ec, epidote eclogite; Amp-Ec, amphibole eclogite.



■ Fig. 11. Tectonic model and nappe succession of the HP/UHP unit in the Saxothuringian zone after O'Brien 1990; Konopásek and Schulmann 2005. The high-grade units are overthrust by low-grade units.

Tectonic interpretation of the Krušné Hory eclogite

It is generally agreed that Krušné Hory HP/UHP rocks formed during subduction of the Saxothuringian oceanic basin and adjacent crustal units beneath Tepla-Barrandia (Bohemia) and Moldanubia (Fig. 11). A Chemenda et al. (1995)-type model has been widely invoked for exhumation of these rocks. Regarding the present position of granulites and UHP rocks in the Erzge-

birge, this high-grade unit is interpreted as occurring at the bottom of the nappe succession (O'Brien, 2000; Willner et al., 2004 etc.), but an opposite arrangement with an increase of metamorphic conditions from bottom to top has been proposed by Konopásek and Schulman (2005).

References

- AI Y., 1994. A revision of the garnet-clinopyroxene Fe²⁺-Mg exchange geothermometer. *Contribution to Mineralogy and Petrology*, 115: 467–473.
- CHÁB J., BREITER K., FATKA O., HLADIL J., KLAVIDA J., ŠIMUNEK Z., ŠTORCH P., VAŠÍČEK Z., ZAJÍC J. and ZAPLETAL J., 2008. Overview of crystalline basement and its Carboniferous and Permian cover sequence of the Bohemian Massif (in Czech). Czech Geological Survey. 283 p.
- CHEMENDA A.I., MATTAUER M. and MALAVIEILLE J., 1995. A mechanism for syn-collisional rock exhumation and associated normal faulting: Results from physical modeling [J]. *Earth Planet. Sci. Lett.*, 132: 225–232.
- ELLIS D.J. and GREEN D.H., 1979. An experimental study of the effect of Ca upon garnet-clinopyroxene Fe-Mg exchange equilibria. *Contribution to Mineralogy and Petrology*, 71: 13–22.
- FARYAD S.W., NAHODILOVÁ R. and DOLEJŠ D., 2010. Incipient eclogite facies metamorphism in the Moldanubian granulites revealed by mineral inclusions in garnet. *Lithos*, 114: 54–69.
- FARYAD S.W., KLÁPOVÁ H. and NOSÁL L., 2010. Mechanism of formation of atoll garnet during high-pressure metamorphism. *Mineralogical Magazine*, 74: 111–126.
- GROSS J., BURCHARD M., SCHERTL H.-P. and MARESCH W.V., 2008. Common high-pressure metamorphic history of eclogite lenses and surrounding metasediments: a case study of calc-silicate reaction zones (Erzgebirge, Germany). *European Journal of Mineralogy*, 20: 757–775.
- HOLUB F.V. and SOUČEK J., 1984. Blueschist-greenschist metamorphism of metabasites in the western Krušné Hory (Erzgebirge) Mts. *Zbl. Geol. Paläont., Teil I*: 815–826.
- KLÁPOVÁ H., 1990. Eclogites of the Bohemian part of the Saxothuringicum. *Rozpravy Československé Akademie Věd, Řada Matematických a Přírodních Věd*, 100: Sešit 5.
- KLÁPOVÁ H., KONOPÁSEK J. and SCHULMANN K., 1998. Eclogites from the Czech part of the Erzgebirge: multi-stage metamorphic and structural evolution. *Journal of the Geological Society London*, 155: 567–583.
- KONOPÁSEK J., 1998. Formation and destabilization of the high pressure assemblage garnet-phengite-paragonite (Krušné Hory Mountains, Bohemian Massif): The significance of the Tschermak substitution in the metamorphism of pelitic rocks. *Lithos*, 42: 269–284.
- KONOPÁSEK J., 2001. Eclogitic micaschists in the central part of the Krušné Hory Mountains (Bohemian Massif). *European Journal of Mineralogy*, 13: 89–100.
- KONOPÁSEK J. and SCHULMANN K., 2005. Contrasting Early Carboniferous field geotherms: evidence for accretion of a thickened orogenic root and subducted Saxothuringian crust (Central European Variscides). *Journal of the Geological Society London*, 162: 463–470.
- KONOPÁSEK J., SCHULMANN K. and LEXA O., 2001. Structural evolution of the central part of the Krušné hory (Erzgebirge) Mountains in the Czech Republic – evidence for changing stress regime during Variscan compression. *Journal of Structural Geology*, 23: 1373–1392.
- KOŠLER J., BOWES D.R., KONOPÁSEK J. and MÍKOVÁ J., 2004. Laser ablation ICPMS dating of zircons in Erzgebirge orthogneisses: evidence for Early Cambrian and Early Ordovician granitic plutonism in the western Bohemian Massif. *European Journal of Mineralogy*, 16: 15–22.
- KRÖNER A. and WILLNER A.P., 1998. Time of formation and peak of Variscan HP-HT metamorphism of quartz-feldspar rocks in the central Erzgebirge, Saxony, Germany. *Contributions to Mineralogy and Petrology*, 132: 1–20.
- MASSONNE H.-J. and KOPP J., 2005. A Low-variance mineral assemblage with talc and phengite in an eclogite from the Saxonian Erzgebirge, Central Europe, and its P-T evolution. *Journal of Petrology*, 46: 355–375.
- MINGRAM B., 1998. The Erzgebirge, Germany, a subducted part of northern Gondwana: geochemical evidence for repetition of early Palaeozoic metasedimentary sequences in metamorphic thrust units. *Geological Magazine*, 135: 785–801.
- MLČOCH B. and SCHULMANN K., 1992. Superposition of Variscan ductile shear deformation on pre-Variscan mantled gneiss structure (Catherine dome, Erzgebirge, Bohemian Massif). *Geologische Rundschau*, 81: 501–513.
- VON QUADT A. and GEBAUER D., 1998. Evolution of eclogitic rocks in the Erzgebirge: a conventional SHRIMP U-Pb zircon and Sm-Nd study. *Acta Universitatis Carolinae Geologica*, 42: 324–325.
- O'BRIEN P.J., 2000. The fundamental Variscan problem: high-temperature metamorphism at different depths and high-pressure metamorphism at different temperatures. In: W. FRANKE, V. HAAK, O. ONCKEN, D. TANNER (Editors), *Orogenic Processes: Quantification and Modelling in the Variscan Belt. Geol. Soc. London Spec. Publ.*, 179: 369–386.
- OKAMOTO K. and MARUYAMA S., 1999. The high-pressure stability limits of lawsonite in the MORB+H₂O system. *American Mineralogist*, 84: 362–373.
- RAVNA E.K., 2000. The garnet-clinopyroxene Fe²⁺-Mg geothermometer: an updated calibration. *Journal of Metamorphic Geology*, 18: 211–219.
- RAVNA E.J.K. and TERRY M.P., 2004. Geothermobarometry of UHP and HP eclogites and schists – an evaluation of equilibria among garnet-clinopyroxene-kyanite-phengite-coesite/quartz. *J. Metamorph. Geol.*, 22: 579–592.
- RÖTZLER K., SCHUMACHER R., MARESCH W.V. and WILLNER A.P., 1998. Characterisation and geodynamic implications of contrasting metamorphic evolution in juxtaposed high-pressure units of the western Erzgebirge. *European Journal of Mineralogy*, 10: 261–280.
- SCHMÄDICKE E., OKRUSCH M. and SCHMIDT W., 1992. Eclogite-facies rocks in the Saxonian Erzgebirge, Germany: high pressure metamorphism under contrasting P-T con-

- ditions. *Contributions to Mineralogy and Petrology*, 110: 226-241.
- TICHOMIROVA M., BERGER H.J., KOCH E.A., BELYATSKI B.V., GÖTZE J., KEMPE U, NASDALA L. and SCHALTEGGER U., 2001. Zircon ages of high-grade gneisses in the eastern Erzgebirge (Central European Variscides)—constraints on origin of the rocks and Precambrian to Ordovician magmatic events in the Variscan fold belt. *Lithos*, 56: 303–332
- WILLNER A.P., RÖTZLER K. and MARESCH W.V., 1997. Pressure-temperature and fluid evolution of quartzofeldspathic metamorphic rocks with a relic high-pressure, granulite-facies history from the Central Erzgebirge (Saxony, Germany). *Journal of Petrology*, 38: 307-336.